

2023

Determining the effect of HMGN1 overexpression in Down syndrome through the comparison of epigenetic marks at H3K27 and PRC2 target gene expression

<https://hdl.handle.net/2144/48180>

"Downloaded from OpenBU. Boston University's institutional repository."

BOSTON UNIVERSITY

ARAM V. CHOBANIAN & EDWARD AVEDISIAN SCHOOL OF MEDICINE

Thesis

**DETERMINING THE EFFECT OF HMGN1 OVEREXPRESSION
IN DOWN SYNDROME THROUGH THE COMPARISON OF EPIGENETIC
MARKS AT H3K27 AND PRC2 TARGET GENE EXPRESSION**

by

SEAN FARLEY

B.S., University of Vermont, 2013

Submitted in partial fulfillment of the
requirements for the degree of
Master of Science

2023

Approved by

First reader

Ella Zeldich, Ph.D.
Assistant Professor of Anatomy and Neurobiology

Second reader

Jean-Pierre Roussarie, Ph.D.
Assistant Professor of Anatomy and Neurobiology

ACKNOWLEDGEMENTS

I would like to first acknowledge all the people who have assisted me in getting here. First and foremost, I would like to thank my parents for their generosity in both love and support over the years. My grandparents for all the dinners and conversations that did more for my head and heart than they know. I would also like to thank Dr. JP Roussarie for lending both his knowledge and lab space to our lentiviral project, and providing such valuable feedback as a reader; Emily Yang, for her immeasurable patience and assistance with growing lentivirus and running ELISAs; Dr. Jonathan Cherry and Morgane Butler for the generous sharing of both their lab space and expertise; Natalie Campbell for her willingness to always answer my questions and occasionally feed my cells. And lastly, I would like to thank Dr. Ella Zeldich for her endless patience, guidance, and willingness to not give up on me - I truly would not be here now without her support.

**DETERMINING THE EFFECT OF HMGNI OVEREXPRESSION IN DOWN
SYNDROME THROUGH THE COMPARISON OF EPIGENETIC MARKS AT
H3K27 AND PRC2 TARGET GENE EXPRESSION**

SEAN FARLEY

ABSTRACT

Down syndrome (DS) is caused by the triplication of chromosome 21, but science is still investigating the precise mechanisms by which this results in the various phenotypes, such as anatomical abnormalities, intellectual deficits, and early development of Alzheimer's disease (AD). The global changes in transcriptional activity and the altered expression of genes not transcribed from chromosome 21 point to changes to the epigenetic landscape. One of the candidate genes for this global gene dysregulation is High Mobility Group Nucleosome Binding Domain 1 (*HMGNI*) which is triplicated in DS.

While investigating DS-associated B-cell acute lymphoblastic leukemia (B-ALL), researchers found the triplication of *HMGNI* alone led to many of the same transcriptional and phenotypic changes that marked DS-associated B-cells from a mouse model with all 31 genes orthologous to human chromosome 21 genes triplicated. Amongst the pathways most affected by triplication, enrichment was greatest for targets of the Polycomb Repressive Complex 2 (PRC2) and sites of the transcriptionally repressive mark it catalyzes, H3K27me3. *HMGNI* instead, promotes transcriptional activation and its overexpression leads to a global increase in RNA transcript levels. Therefore, overexpression of *HMGNI* in DS may cause an increase in transcriptional activity and

prevent the silencing of genes normally silenced by PRC2, with downstream effects on neurogenesis and gliogenesis, abnormal cellular migration, and deviant developmental timing that result in known DS phenotypes.

With this hypothesis, we first wanted to quantify the levels of acetylation versus methylation at H3K27 in trisomy 21 induced pluripotent stem (iPS) cell-derived cellular models: neural progenitor cells (NPCs) and cortical organoids and to determine if there are measurable differences between the genotypes. We found a decrease in H3K27me3 in 130-day-old organoids, but not in NPCs. No changes were detected in the levels of H3K27ac. With the high comorbidity between DS and AD, and changes to the epigenome found in both diseases, we wondered whether there were specific alterations at H3K27 in DS-AD. To determine this, we performed an analysis of human postmortem brain tissue from individuals with DS-AD, AD, and control and quantified H3K27me3 and H3K27ac marks. Our data indicated that there are marginally significant changes in H3K27me3 that are unique to DS-AD as compared to control and AD samples. Encouraged by this data, we next measured gene expression levels of specific PRC2 target genes increased in trisomy. Our goal was to identify the causative relationship between the increased expression of *HMGN1* in trisomy and upregulation of specific PRC2 target genes with known brain-related functions. We found that enhanced expression of particular PRC2 target genes in trisomic cells could be normalized with the short-hairpin RNA (shRNA)-induced knockdown of *HMGN1* expression in trisomic NPCs.

This implicates HMGN1 overexpression in DS in the dysregulation and overexpression of particular genes involved in morphogenesis, neurogenesis, neuronal migration, apoptosis, and cell viability through the antagonism of the PRC2 activity. We provided novel evidence for a possible mechanism for the cellular, molecular, and transcriptomic changes originating from the triplication of *HMGN1* that can potentially lead to DS-related phenotypes such as intellectual disability and AD-related pathology. Furthermore, our findings suggest a possible therapeutic avenue to mitigate these phenotypes by regulating *HMGN1* expression. Taken together, our work is the first to causatively connect HMGN1-induced epigenetic changes to DS-related brain cell phenotypes and to point out to a potential approach for correcting them.

TABLE OF CONTENTS

ACKNOWLEDGMENTS	iv
ABSTRACT.....	v
TABLE OF CONTENTS.....	viii
LIST OF FIGURES	xi
LIST OF ABBREVIATIONS.....	xii
INTRODUCTION	1
Down syndrome	1
HMGN1	5
PRC2	9
HMGN1 and DS	14
HMGN1 in central nervous system (CNS) development	17
HMGN1, PRC2, and DS	20
H3K27ac and H3K27me3 in post-mortem DS, AD, and DS-AD human frontal cortex tissue	23
HMGN1, PRC2, and DS brain hypothesis	26
Using iPS cell-derived models (NPCs and organoids) to study HMGN1, H3K27ac, and H3K27me3 in DS	28
MATERIALS AND METHODS.....	32
Generation of Neural Progenitor Cells	32
Generation of cortical organoids	33

Preserving and Slicing Organoids	35
Immunohistochemistry for NPCs	35
Immunohistochemistry for Organoids	36
Immunohistochemistry for human brain samples	37
Imaging and Quantifying Mean Fluorescence Intensity.....	38
Lentivirus Production	40
Lentivirus Collection and Concentration	41
Enzyme-linked Immunosorbent Assay (ELISA)	41
Viral Transduction	42
FACS Sorting	43
Cells-to-CT and qPCR	43
RESULTS	46
DISCUSSION	63
REFERENCES	73
CURRICULUM VITAE	98

LIST OF TABLES

	Figure Title	Page
1	PRC2 and Development	11
2	HMGN1 and DS	15
3	HMGN1 and CNS Development	19
4	Catalog numbers for ThermoFisher Scientific/Taq-Man assays used in qRT-PCR experiments	45

LIST OF FIGURES

Figure Title	Page
1 HMGN1 binding to the nucleosome	7
2 Gliogenic shift in DS	21
3 Proposed consequences of HMGN1 overexpression and PRC2 antagonism in DS	27
4 Analysis of H3K27ac and H3K27me3 in NPCs	47
5 Analysis of H3K27ac and H3K27me3 in 130-day-old organoids	49
6 Comparing levels of H3K27me3 and H3K27ac in human brain tissue from individuals with DS-AD and AD	51
7 ELISA results and determining level of HMGN1 knock-down with various shRNA constructs	55
8 Results of qRT-PCR experiments to determine relative gene expression levels of select PRC2 target genes and genes differentially expressed in DS in euploid NPCs and NPCs transfected with the HMGN1 shRNA constructs ‘scramble’ (DS-control) and ‘B’ (DS-shRNA-HMGN1)	59
9 Results of qRT-PCR experiment after FACS sorting	62

LIST OF ABBREVIATIONS

5HT:	Serotonin
APP:	Amyloid precursor protein
ATAC-seq:	Transposase-accessible chromatin sequencing
B-ALL:	B-cell acute lymphoblastic leukemia
bHLH:	Basic helix-loop-helix
BrdU:	Bromodeoxyuridine
BRWD1:	Bromodomain and WD repeat domain containing 1
CHCHD2:	Coiled-Coil-helix-coiled-coil-helix Domain Containing 2
ChIP:	Chromatin immunoprecipitation
CHL1:	Cell-adhesion molecule 1
CHUD:	Chromatin unfolding domain
CNPase:	2',3'-Cyclic-nucleotide 3'-phosphodiesterase
CP:	Cortical plate
CRLF2:	Cytokine receptor-like factor 2
DA:	Dopamine
DG:	Dentate gyrus
DKO:	Double-knock-out
DNMT3L:	DNA (cytosine-5)-methyltransferase 3-like
DS:	Down syndrome
DSCAM:	DS cell adhesion molecule
DYRK1A:	Dual specificity tyrosine-phosphorylation-regulated-kinase 1A
EB:	Embryoid body
EED:	Embryonic ectoderm development
ESC:	Embryonic stem cell

ETS2:	ETS proto-oncogene 2
EZH2:	Enhancer of zeste
GEO:	Gene expression omnibus
HAT:	Histone acetyltransferase
HDAC:	Histone deacetylase
HES1:	Hairy and enhancer of split 1
HMG:	High mobility group
HMGN1:	High mobility group binding domain 1
HMT:	Histone methyltransferase
ID2:	Inhibitor of DNA binding 2
Igfbp3:	Insulin-like growth factor-binding protein 3
iPSC:	Induced pluripotent stem cell
IQ:	Intelligence quotient
IUE:	Intra-utero electroporation
JAK-STAT:	Janus tyrosine kinase-signal transducer and activator of transcription
MAPT:	Microtubule-associated protein tau
MBP:	Myelin basic protein
MeCP2:	Methyl CpG-binding protein 2
MEF:	Mouse embryonic fibroblast
MGE:	Medial ganglionic eminence
Mmu16:	Mouse chromosome 16
MNase:	Micrococcal nuclease
MSN:	Medium spiny neuron
NBD:	Nuclear-binding domain
NSC:	Neural stem cell
Olig2:	Oligodendrocyte transcription factor 2

OPC:	Oligodendrocyte precursor cell
PAK1:	P21 activated kinase 1
PCSK1N:	Proprotein convertase subtilisin/kexin type 1 inhibitor
Pdgfr- α :	Platelet-derived growth factor receptor alpha
PEG10:	Paternally expressed 10
PFC:	Prefrontal cortex
PLP:	Proteolipid protein
PolII:	RNA polymerase II
PRC2:	Polycomb repressive complex 2
PSEN1:	Presenilin-1
Pvalb:	Parvalbumin
RUNX1:	Runt-related transcription factor 1
SHH:	Sonic hedgehog
shRNA:	Short-hairpin RNA
SON:	SON RNA and DNA binding protein
Sst:	Somatostatin
SUZ-12:	Suppressor of zeste
SVZ:	Subventricular zone
TC-rMNase-seq:	Time-course digestion with reduced MNase levels followed by high-throughput sequencing
TSS:	Transcription start site
XIST:	X-inactive specific transcript

INTRODUCTION

Disclaimer: Figures and portions of the text in this chapter were originally published as: Farley, S, Grishok, A, & Zeldich, E (2022) Shaking up the silence: consequences of HMGNI antagonizing PRC2 in the Down syndrome brain.

Down Syndrome

Despite occurring in approximately 1 in 700 live births and being one of the leading causes of intellectual disability, the specific mechanisms through which the triplication of chromosome 21 leads to the collection of phenotypes classified as Down syndrome (DS) and how individual genes located on chromosome 21 contribute remains debated (Centers for Disease Control and Prevention (CDC), 2006; Lejeune et al., 1959) . The most well-known feature of the disorder is intellectual disability, with intelligence quotient (IQ) scores for individuals with DS ranging from 10 to 70 (Gueant, 2005). Those with DS have deficits in executive functioning, verbal working memory, language processing, and expressive use of the language (Baburamani et al., 2019; Lanfranchi et al., 2010; Lott & Dierssen, 2010; Startin et al., 2016; Vicari et al., 2005). These disparities in cognitive processing may result from underlying neurobiological differences found in individuals with the disorder, including reduced brain volume (Pinter, Brown, et al., 2001; Pinter, Eliez, et al., 2001), hypocellularity (Guidi et al., 2007), aberrant proliferation of neural progenitor cells and deficient neurogenesis (Guidi et al., 2011), inappropriate cellular migration and late cortical lamination (Utagawa et al., 2022), as well as alterations in

arborization of dendrites and the formation of synapses (L. E. Becker et al., 1986; Petit et al., 1984; Takashima et al., 1989). There is also an abnormal shift from neurogenesis to gliogenesis that occurs, which leads to an increase in astrocyte numbers at expense of neurons and oligodendrocyte production that contributes to decreased neuronal numbers and delayed and abnormal myelination (Golden & Hyman, 1994; Guidi et al., 2007; Petit et al., 1984; Pinter, Eliez, et al., 2001).

Spatiotemporal changes in gene expression are likely at the root of these differences found in DS, with alterations in the transcriptome of DS brain tissue apparent as early as 14 gestational weeks (Olmos-Serrano et al., 2016), and changes to the epigenetic landscape may underlie this global transcriptomic dysregulation. This is supported by findings of changes in gene expression in genes that are not transcribed from chromosome 21 (Olmos-Serrano et al., 2016; Palmer et al., 2021). A study comparing gene expression between DS and non-DS individuals in the dorsal frontal cortex (DFC) and cerebellar cortex (CBC) specifically found that the majority of genes identified as differentially expressed (DEX) between DS and non-DS tissue in the DFC and CBC were not located on human chromosome 21 (HSA21). A median of 4.4% and 3.0% DEX genes were found on non-HSA21 genes in the DFC and CBC, respectively, though HSA21 had the greatest percentage of DEX genes out of all the chromosomes. Interestingly, in the DFC there was an increase in the number of DEX genes as individuals aged, and gene ontology analysis revealed they were potentially involved in nerve impulse transmission, synaptic transmission, cell morphogenesis, cell signaling, and myelination. The genes on HSA21 were found to be upregulated the earliest, with genes located on other chromosomes

becoming more dysregulated with age. This supports what the authors term a “cascade hypothesis” where initial changes in the expression level of genes found on HSA21 occur first and then the effect spreads and genes on other chromosomes become increasingly dysregulated. Although there are likely many different mechanisms influencing the spatiotemporal changes in gene expression, our hypothesis supports alterations to the epigenome playing a significant role. =

Further support is provided by the finding that DEX genes can be either upregulated or downregulated (Palmer et al., 2021), indicating that factors influencing gene expression are involved beyond a simple triplication of HSA21 genes. Indeed, if gene dosage was the primary cause of DS there would be an expected 1.5 fold increase in triplicated gene expression, but instead only 22% are increased in a gene-dosage manner (Aït Yahya-Graison et al., 2007). Differences between expected and actual gene expression levels are also seen in the Ts65Dn mouse model of DS where only 37% percent of the gene orthologs of HSA21 were overexpressed (Kahlem et al., 2004; Lyle et al., 2004). Phenotypic variability between individuals with DS also presents a challenge for gene-dosage alone to be responsible for the presentation of the disorder and implies a more complex set of interactions that can be better explained by epigenetic changes.

A number of genes implicated in epigenetic regulation are located in a region of chromosome 21 containing the q22.2 band and originally referred to as the “Down syndrome critical region” (DSCR). This area was previously thought to be the minimum portion of chromosome 21 whose triplication was required for the most well-known DS phenotypes, such as the intellectual disability, which is why it was considered “critical”

(Korenberg et al., 1990; Sinet et al., 1994). Subsequent studies of segmental trisomy, where particular portions are triplicated instead of the entire chromosome 21, have shown that there is not a single critical region and indicate that complex genetic and epigenetic interactions result in the various phenotypes (Cetin et al., 2012; Korbel et al., 2009; Korenberg et al., 1994; Ronan et al., 2007). The genes implicated in epigenetic regulation include: the chromatin regulators *High Mobility Group Nucleosome Binding Domain 1 (HMGN1)*, *Bromodomain and WD repeat domain containing 1 (BRWD1)* [31–33], *DNA (cytosine-5)-methyltransferase 3-like (DNMT3L)* (Chédin et al., 2002; Laufer et al., 2021), and *SON RNA and DNA binding protein (SON)* (Ahn et al., 2008, 2011; Berdichevskii et al., 1988; Furukawa et al., 2012; Huen et al., 2010; Mattioni et al., 1992); the transcription factors *ETS proto-oncogene 2 (ETS2)* (Graves & Petersen, 1998; Heru Sumarsono et al., 1996; J. Tymms & Kola, 1994; Jayaraman et al., 1999; Seth et al., 1989; Sevilla et al., 1999; Sun et al., 2006; Watson et al., 1997; E. J. Wolvetang, 2003), *Runt-related transcription factor 1 (RUNX1)* (Bowers et al., 2010; Harada et al., 2004; Kagoshima et al., 1993; Kitabayashi, 1998; Lacaud, 2002; North et al., 2004; Oakford et al., 2010; Reed-Inderbitzin et al., 2006; Schnittger et al., 2011) ; and the kinase *Dual specificity tyrosine phosphorylation-regulated-kinase 1A (DYRK1A)*, which has been shown to interact with chromatin remodeling complexes to alter the regulation of genes involved in dendritic growth in DS (W. Becker & Joost, 1998; Lepagnol-Bestel et al., 2009; S. Li et al., 2018; Shen et al., 2008; Yang et al., 2001),.

DNMT3L overexpression resulted in DNA hypermethylation of certain genes involved in neurodevelopment and could suppress the expression of genes necessary for

normal development (Laufer et al., 2021)). *SON* is a splicing co-factor regulating cell cycle progression through the control of splicing events. Its expression is increased in areas of proliferation and development (McKee et al., 2005). *DYRK1A* interacts with the switch/sucrose non-fermentable (SWI/SNF) chromatin remodeling complex (Lepagnol-Bestel et al., 2009), and its overexpression also results in a decrease in RE1-Silencing Transcription Factor (REST) which can lead to premature differentiation of cells and disrupt developmental timing (Canzonetta et al., 2008). Similarly to *DYRK1A*, *BRWD1* also interacts with the SWI/SNF complex and is highly expressed during development, suggesting overexpression in DS could have ramifications for transcriptional activity and developmental timing (Huang et al., 2003). Additionally, *RUNXI* helps recruit SWI/SNF complexes to certain gene promoters and triplication in DS could alter the expression level of downstream gene targets (Bakshi et al., 2010). ETS affects acetylation through interactions with the HAT p300 and could impact neurodevelopment through altering levels of transcriptional activity (Sun et al., 2006). Although there is support for all of these genes potentially leading to alterations in transcriptional activity and developmental timing, the current project is focused on one gene, *HMGNI*. There is evidence for this nucleosome remodeler causing global transcriptomic dysregulation in DS, leading to many downstream developmental aberrations.

HMGNI

This gene encodes for a protein of the same name which is a member of the High Mobility Group Nucleosome Binding proteins, a group of five proteins that bind to

nucleosomes and are involved in chromatin remodeling (Catez et al., 2004; Goodwin et al., 1975). It consists of an N-terminus with a 30-amino acid nucleosome binding domain (NBD) which is flanked by nuclear location signals (NLS1 and NLS2), and a C-terminus which constitutes the chromatin-unfolding domain (CHUD) (Trieschmann et al., 1998; Ueda et al., 2006). HMGN1 binds to the major groove of DNA without specificity for the underlying DNA sequence (Alfonso et al., 1994; Mardian et al., 1980; Trieschmann et al., 1995). It binds near the nucleosome's dyad axis, or the central axis that splits the structure into two identical halves (Cutter & Hayes, 2015). Instead, it has a set of 8 amino acid residues that are in the NBD and conserved in all members of the HMGN family which allow it to bind to the nucleosome (Ueda et al., 2008). It is only able to bind during interphase since two of these serine residues, at position 20 and 24, in the NBD are phosphorylated during mitosis which interferes with their ability to recognize and bind to the nucleosome (Cherukuri et al., 2008; Prymakowska-Bosak et al., 2001, 2002).

The binding of HMGN1 facilitates the decompaction of chromatin, promoting access of the linker DNA, or the stretch of DNA between nucleosomes (Routh et al., 2008), to transcription factors and associating it with transcriptional activity (Paranjape et al., 1995; Prymakowska-Bosak et al., 2002). Please refer to Figure 1 to see a representation of HMGN1 binding to the nucleosome.

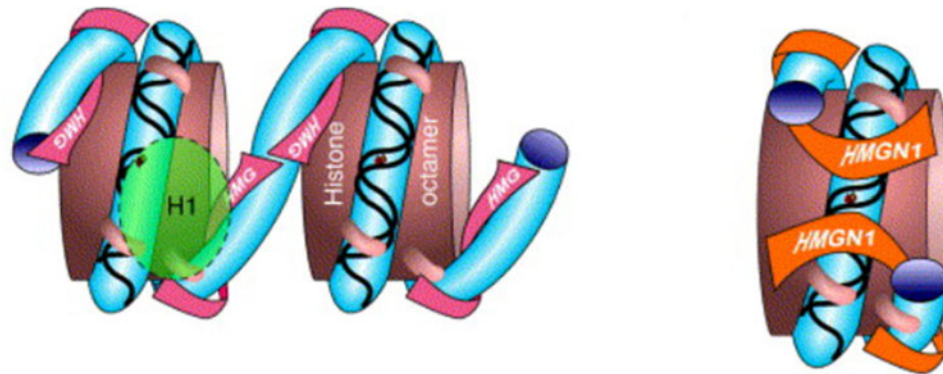


Figure 1: HMGN1 binding to the nucleosome. Schematic representation adapted from the review article “Chromatin unfolding and activation by HMGN chromosomal proteins” (Bustin 2001).

The mechanism through which HMGN1 is thought to exert this loosening influence is the restoration of the electrostatic repulsion of nucleosomal DNA (Clark & Kimura, 1990). HMGN1 has also been shown to colocalize with the epigenetic mark, H3K27ac, a histone modification that consists of an acetyl group bound to the lysine 27 residue on the histone H3 tail (S. Zhang et al., 2022). A study using ChIP-seq analysis demonstrated that HMGN1 localizes specifically with this mark, and not with other marks also associated with increased transcriptional activity, like H3K9ac (S. Zhang et al., 2022). This study also used double-knockout mice for HMGN1 and HMGN2, since both proteins bind to acetylated nucleosomes and can compensate for each other, to reveal that the loss of these proteins results in a reduction of H3K27ac marks (S. Zhang et al., 2022). HMGN1 is also abundant in areas known as super enhancers and enriched in H3K4me1 and H3K27ac. These areas have been identified in the mouse, in multiple cell types including embryonic stem cells (ESCs), mouse embryonic fibroblasts (MEFs), and resting B cells (He et al., 2018). ChIP-

seq data reveals that HMGN1 is located primarily in the transcriptionally active ‘A’ compartment of chromatin and in areas that contain transcription regulatory features, such as the H3K27ac mark, further implicating its involvement in transcriptional regulation (He et al., 2022). H3K27ac can alter the chromatin structure since its acetyl group reduces the positive charge of the histone tail and lowers the electrostatic attraction to the negatively charged DNA (Shaytan et al., 2016). Importantly, HMGN1 also promotes acetylation at H3K27 through enhancement of the histone acetyltransferase (HAT) P300/CBP-associated factor’s (PCAF) activity (Ueda et al., 2006).

The presence of HMGN1 on nucleosomes also results in increased transcriptional capabilities due to its antagonistic relationship with linker histone H1, as they compete for overlapping nucleosomal binding sites (Catez et al., 2002, 2004; Deng et al., 2013). Linker histone H1 binds at the meeting point of linker DNA and the histone core octamer, bringing the strands of DNA closer together and leading to a more compact chromatin conformation, though this ability is impaired by histone acetylation (Ridsdale et al., 1990). Linker histone H1 is implicated in the recruitment of the Polycomb Repressive Complex 2 (PRC2), which will be discussed in more detail in the following section. The PRC2 complex is responsible for the propagation of the H3K27me3 mark, with studies demonstrating that depleting cells of H1 reduces the level of H3K27me3 by two-fold (Fan et al., 2005), but re-incorporating H1 into oligonucleosomes can partially restore levels of histone H3 methylation (Martin et al., 2006). H3K27me3 is associated with transcriptional repression. Therefore, it raises the question of whether the increased levels of of HMGN1 in DS increase the competition with linker histone H1 for nucleosomal binding sites and reduce

its ability to recruit PRC2, which is supported by the depletion of H3K27me3 in areas of HMGN1 binding (Cuddapah et al., 2011). For example, loss of HMGN1 around certain genes, like *Olig1* and *Olig2*, in double knock-out studies reveals an increase in the binding of the PRC2 subunit responsible for the deposition of the H3K27me mark, Enhancer of Zeste 2 (EZH2), and subsequently, an increase in H3K27me3 levels (Deng et al., 2017). The overexpression of HMGN1 could induce a shift in the balance of these competing proteins and lead to a reduction in the transcriptionally repressive H3K27me3 mark (Toskas et al., 2022). The subsequent de-repression of these intended targets of PRC2 could contribute to the abnormal neurological development seen in DS.

PRC2

The PRC2 complex serves as a histone methyltransferase (HMT), with the SET domain of the EZH2 subunit depositing mono-, di-, and tri- methyl groups at H3K27 (Kuzmichev et al., 2002). When linker histone H1 proteins were experimentally depleted in spleen, thymus, and bone marrow tissue in mice there was a reduction in H3K27me3 levels, and found H1 proteins stimulate PRC2 activity (Willcockson et al., 2021). A positive feedback loop also exists whereby Embryonic ectoderm development (EED) subunit's aromatic cage recognizes the H3K27me3 mark and selectively binds to it, and studies have found that the recognition of this mark is necessary for PRC2's activity (Margueron et al., 2009; Xu et al., 2010).. It has been shown that the PRC2 complex can engage with two neighboring nucleosomes, recognizing the H3K27me3 mark one and

depositing methyl groups on the other, thereby effectively propagating the mark (Poepsel et al., 2018).

PRC2 is essential for appropriate neurological development and alterations can lead to changes in the timing of neurogenesis (J. Liu et al., 2017; P.-P. Liu et al., 2019; Pereira et al., 2010), inappropriate neuronal orientation and cortical radial migration (DiMeglio et al., 2013; Zhao et al., 2015), difficulties in maintaining a neuronal identity (Buontempo et al., 2022; X. Feng et al., 2016; Toskas et al., 2022; vonSchimmelmann et al., 2016), and aberrant glial cell development and fate determination (Deng et al., 2017; Douvaras et al., 2016; Sher et al., 2008; W. Wang et al., 2020) as summarized in Table 1.

Developmental effect	Related findings	References
Proper timing of neurogenesis	EZH2-KO in mice leads to a premature exhaustion of the pool of neural progenitor cells, decreased neuronal density at the cortical plate and precocious astrocyte generation.	Pereira et al., (2010)
	EED-KO mice experience impaired neurogenesis, growth retardation, and death. EED ablation leads to abnormal neuronal differentiation during the hippocampal dentate gyrus formation.	Liu et al., (2019)
	miR-203 is repressed by EZH2 in neural progenitor cells and negatively regulates proliferation. EZH2-KO results in the reduction of neural progenitor proliferation.	Liu et al., (2017)
Appropriate neuronal orientation and cortical radial migration	EZH2 inhibition results in abnormal neuronal orientation, reduced neuronal numbers at the cortical plate and ectopic expression of Reelin.	Zhao et al., (2015)
	EZH2-mediated repression of <i>Netrin1</i> is necessary for appropriate migration of pontine neurons in the cortico-ponto-cerebellar pathway in mice. EZH2-KO results in ectopic <i>Netrin1</i> induction and aberrant neuronal migration.	Di Meglio et al., (2013)
Maintenance of neuronal identity	Deletion of EED disrupts the acquisition and maintenance of neuronal identity and functionality in differentiated dopaminergic and serotonergic neurons.	Toskas et al., (2022)
	Conditional knock-out of EZH2 results in reduced proliferation of granule precursor cells, decrease in the Purkinje cell population, and increase in GABAergic interneurons in the mouse cerebellum.	Feng et al., (2016)
	Conditional KO of EZH2 results in loss of H3K27me3 marks in differentiating neurons, and causes changes to molecular networks that govern glutamatergic neuron differentiation, leading to a disruption in the balance of inhibitory/excitatory neurons during development	Buontempo et al., (2022)

	Combined EZH1 and EZH2 KO leads to a loss of H3K27me3 marks in MSNs in the striatum, down-regulation of lineage-specific and function-specific MSN genes and upregulation of the death-promoting genes.	Von Schimmelmann et al., (2017)
Glial cell development and fate determination	Pharmacological inhibition of EZH2 leads to increased expression of <i>Olig1</i> and <i>Olig2</i> . Increased depositions of H3K27me3 marks is detected in the genomic loci of <i>Olig1</i> and <i>Olig2</i> in HMGN-KO ESCs.	Deng et al., (2017)
	KO of EZH2 or EED do not affect the generation of OPC but inhibit their differentiation into mature, myelinating oligodendrocytes. PRC2 is necessary for repression of the Notch pathway.	Wang et al., (2020)
	EZH2 regulates NSC differentiation into glial cells in mice, with high expression levels of EZH2 associated with increased oligodendrocyte production and decreased production of astrocytes while low levels of EZH2 correlate with a reduction in oligodendrocyte generation and increased numbers of astrocytes.	Sher et al., (2008)
	Increased levels of <i>EZH2</i> and <i>EED</i> mRNAs are detected during the early stage of OPC lineage commitment and development in mouse and human ESCs and human iPSCs.	Douvaras et al., (2016)

Table 1: PRC2 and Development. Table summarizing findings on the role of PRC2 in development. Adopted from the review article “Shaking up the Silence: consequences of HMGN1 antagonizing PRC2 in the Down syndrome brain” by Farley et al. (Farley et al., 2022)

EZH2 knock-out studies in mice (Pereira et al., 2010) reveal thinner cortical plates and a reduction in neurons because of the premature depletion of the pool of cortical progenitor cells due to an initially rapid process of neurogenesis (both direct and indirect) that limits subsequent renewal. Similarly, deletion of the EED subunit in mice resulted in a decreased hippocampal dentate gyrus (DG) volume (P.-P. Liu et al., 2019). Decreased brain volume and hypocellularity are known features of DS, with deficits in hippocampal

volume particularly notable due to the disease's hallmark symptom of intellectual disability (Aylward et al., 1999; Golden & Hyman, 1994; Guidi et al., 2007; Pinter, Eliez, et al., 2001; Winter et al., 2000) EZH2 is also necessary for proper neuronal migration and knock-down with shRNA leads to irregular neuronal orientation during radial migration, which results in a decrease in the number of neurons reaching the upper cortical plate (Zhao et al., 2015). The silencing of certain genes, such as Reelin, by the PRC2 complex, is thought to be necessary for proper cortical lamination, and this process can be experimentally altered by reducing EZH2 expression (Zhao et al., 2015).

Maintaining appropriate neuronal and glial identities is also contingent upon silencing by the PRC2 complex and its H3K27me3 mark. For example, post-mitotic midbrain dopaminergic (mDA) and hindbrain serotonergic (5HT) neurons in mice that lacked the EED subunit of PRC2 lost their cell-type specific transcriptomic signatures, and the repression of either non-mDA and non-5HT genes (Toskas et al., 2022). A precocious shift from neurogenesis to gliogenesis is observed with changes in PRC2 expression, with GFAP-expressing cells appearing earlier in the cortical plate of EZH2 knock-out mice than controls (Pereira et al., 2010). Overexpression of EZH2 also leads to an acceleration in the switch from neurogenesis to gliogenesis in mice and induces early oligodendrocyte development (Sher et al., 2008). Conversely, a reduction in its expression in the same cell type leads to an increase in astrogenesis at the expense of oligodendrocyte development (Sher et al., 2008).

Importantly, PRC2 also represses death-promoting genes and genes responsible for neurodegeneration in both forebrain medium spiny neurons (MSNs) and cerebellar

Purkinje cells (PC), indicating this role is widespread and impacts various parts of the brain (vonSchimmelmänn et al., 2016). Taken together, it is clear that PRC2 is needed for the proper timing of neurodevelopment, as well as the acquisition and maintenance of specific identities.

HMGNI and DS

A connection between *HMGNI* and DS was initially made in the context of studying acute B-cell lymphoblastic leukemia (B-ALL). DS individuals carry a 20-fold risk of developing B-ALL, known as DS-associated ALL (DS-ALL) (Lane et al., 2014; Mullighan et al., 2009; Rabin & Whitlock, 2009), particularly versions in which there is a rearrangement of cytokine receptor-like factor 2 (CRLF2) that results in activation of the Janus kinase/signal transducers (JAK/STAT) pathway. Researchers utilized the Ts1Rhr mouse model of DS, which carries a triplication of part of mouse chromosome 16 (Mmu16) that is orthologous to the DS critical region on human chromosome 21 (chr.21q22) that contains *HMGNI* (Belichenko et al., 2009). Reliably developing DS-ALL, the transcriptome of B-cells in these mice was compared with several human DS B-cell datasets using network enrichment analysis and found to contain an enrichment of PRC2 target genes and sites containing the H3K27me3 mark. In MEFs, the change in expression level of genes normally marked by H3K27me3 was significant enough to allow for discrimination between DS-ALL and B-ALL B-cells. The reduction in H3K27me3 marks in Ts1Rhr B-cells resulted in the activation of bivalently marked genes, which were highly enriched in this cell population. These findings indicated that the mouse ortholog of

chr.21q22 could reduce levels of H3K27me3, but even more surprising is that the researchers found triplicating *HMGNI* alone *in vivo* was sufficient to recapitulate many of the changes to the transcriptome and phenotype of B-cells with all 31 orthologous genes triplicated, suggesting a particularly strong impact of this one gene. Further support for this conclusion was provided by the finding that *HMGNI* overexpression in Ts1Rhr B-cells led to a global amplification in gene expression, and enrichment of H3K27ac was found in the genes with the greatest increase in expression levels (Mowery et al., 2018). Remarkably, the levels of *HMGNI* are consistently increased in DS brain tissue as well as in different animal and cellular models of DS as we summarized in Table 2. This further supports the potential significance of *HMGNI* as a global transcriptomic effector.

DS Phenotype	Title	Related Findings	References
Overexpression of HMGNI	Chromosomal protein HMG-14 gene maps to the Down syndrome region of human chromosome 21 and is overexpressed in mouse trisomy 16	Ts16 mouse model of DS has 1.5 times more <i>HMGNI</i> protein and mRNA than WT and supports the gene dosage effect of <i>HMGNI</i> triplication	Pash et al. (1990)
	Chromosomal protein HMG-14 is overexpressed in Down syndrome	Fibroblasts from DS individuals express <i>HMGNI</i> at levels 1.6 higher than non-DS individuals	Pash et al. (1991)
	Functional transcriptome analysis of the postnatal brain of the Ts1Cje mouse model for Down syndrome reveals	<i>HMGNI</i> is upregulated in the Ts1Cje mouse model of DS	Ling et al. (2014)

	global disruption of interferon-related molecular networks		
	Transcriptional disruptions in Down syndrome: a case study in the Ts1Cje mouse cerebellum during post-natal development	<i>HMGN1</i> was overexpressed in the cerebellum of the Ts1Cje mouse model of DS during post-natal development	Potier et al. (2006)
	Bioinformatics analysis of biomarkers and transcriptional factor motifs in Down syndrome	Raw gene expression data from DS rat brain tissue, Ts1Cje cerebellum tissue, and adult human DS tissue analyzed using Gene Expression Omnibus and showed overexpression of <i>HMGN1</i>	Kong et al. (2014)
	Down syndrome developmental brain transcriptome reveals defective oligodendrocyte differentiation and myelination	Raw gene expression data analyzed in humans with DS using Gene Expression Omnibus and found <i>HMGN1</i> overexpressed in the hippocampus, cerebellar cortex, and areas of the pre-frontal cortex, and primary visual cortex	Rodriguez-Ortiz et al. (2000)
Intellectual disability	Genetic contributions to variation in general cognitive function: a meta-analysis of genome-wide association studies in the CHARGE consortium	A genome-wide association study of general cognitive function in adults found <i>HMGN1</i> as the single gene-based significant association in the study	Davies et al. (2015)
Cancer	Triplication of a 21q22 region contributes to B cell	<i>HMGN1</i> suppresses H3K27me3 and	Lane et al. (2014)

	transformation through HMGN1 overexpression and loss of histone H3 Lys27 trimethylation	promotes B cell proliferation in B-ALL	
	Trisomy of a down syndrome critical region globally amplifies transcription via HMGN1 overexpression	<i>HMGN1</i> globally amplifies transcription	Mowery et al. (2018)
	HMGN1 plays a significant role in CRLF2-driven Down Syndrome leukemia and provides a potential therapeutic target in this high-risk cohort	<i>HMGN1</i> is involved in signaling pathways in CRLF2-driven DS leukemia	Page et al. (2022)
Behavioral changes	The chromatin-binding protein HMGN1 regulates the expression of methyl CpG-binding protein 2 (MECP2) and affects the behavior of mice	<i>HMGN1</i> downregulates <i>MeCP2</i> and its aberrant expression produces behavioral changes in mice consistent with ASD and DS phenotypes	Abuhatzira et al. (2011)

Table 2: HMGN1 and DS. Table summarizing the findings connecting HMGN1 to various DS phenotypes. Adopted from the review article “Shaking up the Silence: consequences of HMGN1 antagonizing PRC2 in the Down syndrome brain” by Farley et al. (Farley et al., 2022)

HMGN1 in CNS development

HMGN1 has been implicated in neural development through its effect on chromatin compaction. Studies using mice and *X. laevis* embryos have both demonstrated the early and important role *HMGN1* plays, with depletion leading to profound developmental

abnormalities or delays in development (Körner et al., 2003; Mohamed et al., 2001). Through binding to lineage specific regulatory sites, HMGN1 is involved with the maintenance of cell-type specific identity, and its loss increases the rapidity with which MEFs are reprogrammed into iPSCs (He et al., 2018). Reduction in the number of *Nestin*-positive neural progenitor cells in the SVZ of mouse brain is found in HMGN1 knock-out mice, indicating a role in the regulation of this group of cells in early development (Deng et al., 2013).

HMGNI has been causatively linked to the shift from neurogenesis to gliogenesis, with the forced expression of this protein in human NPCs leading to the generation of astrocytes instead of neurons, and knockdown producing fewer astrocytes (Nagao et al., 2014).

One of the most interesting recent findings on *HMGNI* is that its experimental manipulation can lead to observable behavior changes in mice (Abuhatzira et al., 2011). *HMGNI* is a negative regulator of the gene *MeCP2*, with transcriptional analysis revealing a 30% reduction in *MeCP2* transcript levels in DS. Similar results were found in MEFs that also overexpressed *HMGNI* (Abuhatzira et al., 2011). Behavioral tests were conducted with mice either over-or-under expressing *HMGNI*, in addition to controls, and the manipulation of levels resulted in changes in their preference for novel social interaction and novel object recognition consistent with autistic-like phenotypes (Korbel et al., 2009) and cognitive deficits associated with DS (Pinto et al., 2020). The behavioral alterations were attributed to the global effect of *HMGNI* on the accessibility of chromatin and suggested for the first time the connection between HMGN1 dysregulation and the changes

in behavior. We have summarized the existing data related to the possible effects of HMGN1 in neurodevelopment in Table 3.

Title	Major Findings	References
Developmental role of HMGN proteins in <i>Xenopus laevis</i>	Altered <i>HMGN1</i> levels lead to malformations in <i>Xenopus laevis</i> development at the post-blastula stage	Körner et al. (2003)
High-mobility group proteins 14 and 17 maintain the timing of early embryonic development in the mouse	HMGN1 protein is necessary for the appropriate timing of embryo development in mice; depletion leads to developmental delays	Mohamed et al. (2001)
Binding of HMGN proteins to cell specific enhancers stabilizes cell identity	Loss of HMGN1 protein accelerates reprogramming of MEFs into iPSCs	He et al. (2018)
High mobility group nucleosome-binding family proteins promote astrocyte differentiation of neural precursor cells	<i>HMGN1</i> expression promotes astrocyte differentiation	Nagao et al. (2014)
HMGN1 modulates nucleosome occupancy and DNase I hypersensitivity at the CpG island promoters of embryonic stem cells	Loss of <i>HMGN1</i> reduces the number of Nestin-positive NPCs in SVZ in mouse brain	Deng et al. (2013)

Interplay between H1 and HMGN epigenetically regulates OLIG1 and 2 expression and oligodendrocyte differentiation	Loss of <i>HMGN1</i> reduces <i>OLIG1</i> and <i>OLIG2</i> expression and impairs normal oligodendrocyte differentiation Loss of HMGN1 decreases the amount of MBP and proteolipid protein (PLP) in the spinal cord of mice	Deng et al. (2017)
---	--	--------------------

Table 3: HMGN1 and CNS Development. Table summarizing the findings between HMGN1 and development of the CNS. Adopted from the review article “Shaking up the Silence: consequences of HMGN1 antagonizing PRC2 in the Down syndrome brain” by Farley et al. (Farley et al., 2022).

HMGN1, PRC2 and DS

Taken together, *HMGN1* overexpression in DS and the possible antagonism of PRC2 activity support a major role of *HMGN1* in the DS brain pathology. In our recently published review, we discussed how different transcriptomic and phenotypic aberrations in DS might be explained by the hypothesis that increased levels of *HMGN1* in DS disrupt the activity of PRC2 and increase the transcription of PRC-2 target genes (Farley et al., 2022). To avoid redundancy, I provide an example here of the DS-related gliogenic shift and the connection to the cross-talk between HMGN1 and PRC2, as we illustrated in Fig. 1. Neuroepithelial cells normally progress to radial glial cells (RGCs) that give rise to outer RGCs, apical RGC, and intermediate progenitor cells. These cells are able to produce initially different types of neurons and subsequently, give rise to glial cells like

oligodendrocytes and astrocytes. However, this process is altered in DS, resulting in an accelerated progression to gliogenesis.

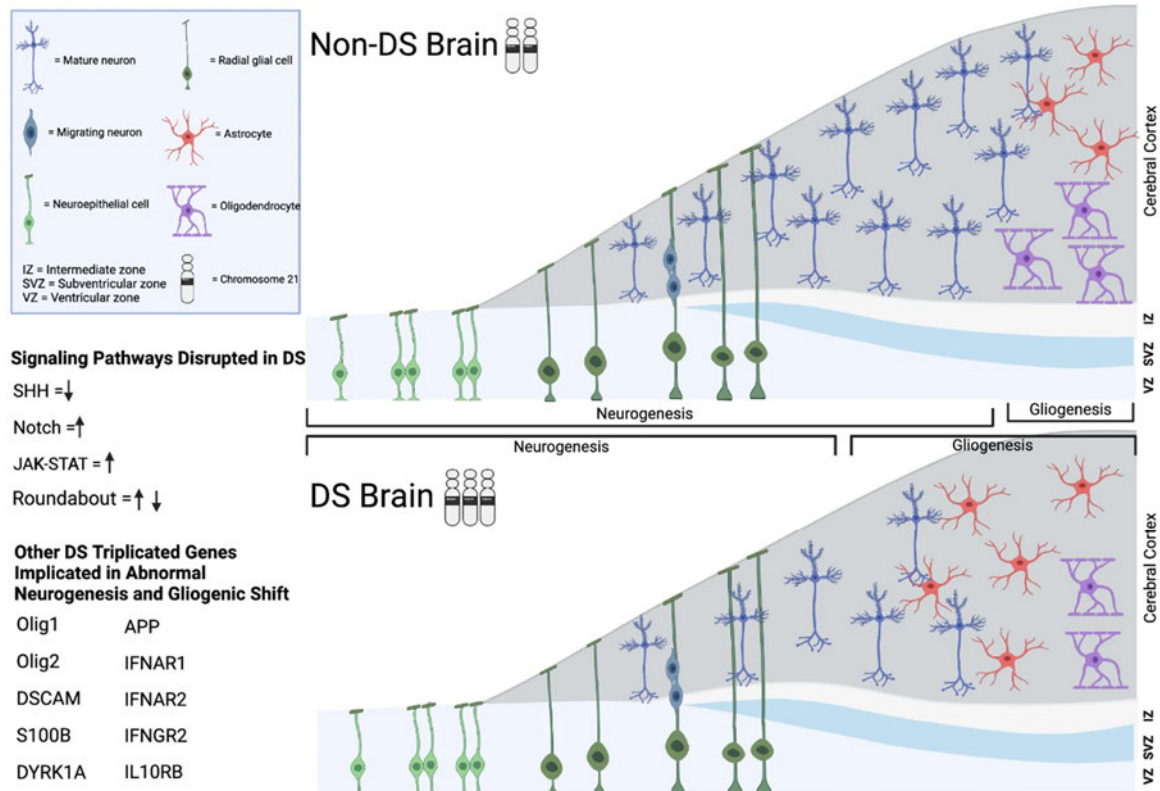


Figure 2: Gliogenic shift in DS. Illustration of the proposed changes in the balance of neurons, oligodendrocytes, and astrocytes that results from the premature shift from neurogenesis to gliogenesis in DS, and changes in astrocyte versus oligodendrocyte production. Adapted from the review article “Shaking up the Silence: consequences of HMG1 antagonizing PRC2 in the Down syndrome brain” by Farley et al. (Farley et al., 2022).

The significant difference in the expression of oligodendrocyte-specific genes in DS and deficits in myelinating oligodendrocytes have been shown previously (Ábrahám et al., 2012; Bhattacharyya et al., 2009; Klein et al., 2022; Olmos-Serrano et al., 2016; Seol et al., 2023; K. E. Wisniewski & Schmidt-Sidor, 1989) and hypothesized to play a role in the intellectual deficits in DS. The decreased levels of myelinating oligodendrocytes in DS have been partially attributed to a shift in the balance between the production of glial cells, with increased production of astrocytes at expense of neurons and oligodendrocytes

(Reiche et al., 2019). One explanation for this shift could be the extra copy of the *amyloid precursor protein (APP)* gene on HSA21 since increased astrogenesis has been observed in NPCs exposed to increased levels of *APP* (Sugaya, 2008). Overexpression of *APP* in trisomy can also lead to increased levels of the APP intracellular domain (AICD), which can upregulate the expression of the Patched1 (*Ptch1*) receptor and has been shown to attenuate SHH signaling in trisomic NPCs. SHH signaling is crucial for the appropriate expression levels of transcription factors involved in oligodendrocyte differentiation, so a decrease in the effectiveness of this signaling pathway could result in aberrant oligodendrocyte development (Klein et al., 2022). The *Ptch1* promoter in this experiment was also found to be hyperacetylated on H3, and *HMGNI* is known to increase levels of H3 acetylation (Ueda et al., 2006). The overexpression of *HMGNI* could also influence this process by amplifying the effect of *APP* even more than would be expected through triplication alone. *HMGNI* could also be involved in decreased levels of myelinating oligodendrocytes through the antagonism of the PRC2 complex since deficits have been found when either the EZH2 or EED subunits of PRC2 are depleted (W. Wang et al., 2020).

Changes in transcriptional activity due to the antagonizing action of *HMGNI* on PRC2 may also explain why many signaling pathways whose control is attributed to genes besides *HMGNI* could be related to this gene. For example, genes such as *ROBO2*, *ROBO4*, and *SLIT2* are responsible for influencing neuronal migration and axon development are targeted by EZH2 and SUZ-12 (Kamminga et al., 2006; Lee et al., 2006; Nuytten et al., 2008). It is through this mechanism that developmental phenotypes attributed to other genes may be influenced by the overexpression of *HMGNI* in DS.

H3K27ac and H3K27me3 in post-mortem DS, AD, and DS-AD human frontal cortex tissue

Alzheimer's disease (AD) is a neurodegenerative disease marked by the accumulation of amyloid-beta (A β) plaques (Götz et al., 2001; Lewis et al., 2001), hyperphosphorylated tau, neurofibrillary tangles (NFTs) (Arnold et al., 1991), and an increase in neuron death (Gómez-Isla et al., 1997). The initial cleavage of the transmembrane protein APP is carried out by either α or β secretase, but only cleavage with β -secretase with a subsequent cleavage by γ -secretase results in A β peptides that can aggregate into plaques. These peptides consist of either 40 or 42 amino acids, deemed A β 40 or A β 42 respectively (Gouras et al., 2000), with the extra amino acids in A β 42 make it more likely to accumulate into plaques than A β 40 (Goate et al., 1991; Gouras et al., 2000). The accumulation of A β plaques and different isoforms of the A β peptide, such as oligomers, can lead to an increase in hyperphosphorylated tau and accelerated development of NFTs (Götz et al., 2001; Lewis et al., 2001). One of tau's normal functions is to stabilize and maintain the integrity of microtubules but loses this capability when it is hyperphosphorylated, contributing to neurodegeneration (Gómez-Isla et al., 1997).

AD pathology is common in DS, with most individuals developing amyloid beta (A β) plaques, hyperphosphorylated tau, NFTs, signs of oxidative stress, neuroinflammation, and neurodegeneration by the fourth decade of life (Griffin et al., 1989; Mann & Esiri, 1989; Perluigi & Butterfield, 2012; Royston et al., 1999; Schupf et al., 1998;

Wilcock & Griffin, 2013), Brains from individuals with DS have greater levels of soluble A β 42 as early as 21 gestational weeks, with none being detected in age-matched controls (Teller et al., 1996). After age 40 they also have progressive accumulation of both insoluble A β 40 and A β 42 (K. E. Wisniewski et al., 1985).

Deposits were initially found in the parahippocampus and inferior temporal gyrus, with the CA1 and subiculum regions of the hippocampus and the dentate gyrus developing deposits with increasing age (Leverenz & Raskind, 1998).

The high prevalence of AD pathology in DS has historically been attributed to the triplication of APP that is transcribed from HSA21 (Rumble et al., 1989). Another HSA21 gene, the transcription factor, *ETS2*, activates the *APP* promoter and can also influence its overexpression in DS and lead to increased levels of A β production (E. W. Wolvetang et al., 2003, p. 21). Deleting the extra copy of *APP in vitro* was shown to reduce A β production and adjust the altered A β 42 to A β 40 ratio found in AD, but did not have an effect on tau pathology or NFTs (Ovchinnikov et al., 2018). Studies have demonstrated that the DS brain is particularly vulnerable to complement activation and subsequent inflammation and that this environment can increase the rate of A β accumulation and reduce its ability to be cleared (Head et al., 2001; Stoltzner et al., 2000, 2000). Strikingly, despite the near universality of AD pathology in individuals with DS, a small minority never develop symptoms of dementia (K. Wisniewski et al., 1978; K. E. Wisniewski et al., 1985), increasing the complexity of the relationship between pathology and presentation.

Epigenetic changes induced by the overexpression of *HMGNI* may provide some insight into the variability in developing dementia and the underlying mechanisms linking

AD and DS. Studies looking at changes to post-translational histone modifications in AD have shown mixed results, but generally support the idea of epigenetic dysregulation in the disease (Lithner et al., 2013; Marzi et al., 2018; Persico et al., 2022; Rao et al., 2012; K. Zhang et al., 2012). Alterations in H3K27ac levels have been found in the entorhinal cortex of post-mortem AD tissue (Marzi et al., 2018). Of particular interest, researchers have found that H3K27ac levels are altered around genes important for the pathology of the disease, such as *APP*, *microtubule-associated protein tau (MAPT)*, *presenilin-1 (PSEN1)*, and *PSEN2* (Cruchaga et al., 2012; De Strooper et al., 1998; Goate et al., 1991; Scheuner et al., 1996). Increased acetylation of histone H3 was found in pyramidal neurons from individuals with AD and correlated with the level of pathology (Narayan et al., 2015). Another study revealed an increase in H3K27ac marks in the lateral temporal lobe of individuals with AD (Nativio et al., 2020). This was tied to disease-specific pathways that were positively correlated with the level of neurodegeneration due to A β 42 (Nativio et al., 2020). Alterations in post-translational histone modifications have been independently associated with AD and DS, but to our knowledge, no studies have been conducted that look at these markers in the context of DS-AD.

Increased *HMGNI* expression has been found in *post-mortem* human tissue from individuals with DS, including areas of prefrontal cortex. Olmos-Serrano et al., (Olmos-Serrano et al., 2016) found *HMGNI* mRNA expression to be increased in the dorsal prefrontal cortex in human DS post-mortem tissue across various developmental periods (Olmos-Serrano et al., 2016), and Rodriguez-Ortiz et al. (Rodríguez-Ortiz et al., 2021) used raw gene expression data available from the Gene Expression Omnibus (GEO) of the

National Center for Biotechnology Information (NCBI) to determine expression levels of *HMGNI* in areas associated with cognition in individuals with DS and also found overexpression in the prefrontal cortex. If HMGNI is overexpressed in these areas it could mean an alteration in transcriptional activity in areas associated with cognition and potentially connect the overexpression of this particular gene to changes in intellect in individuals with DS.. Quantifying the levels of H3K27ac and H3K27me3 in post-mortem DS-AD tissue may provide support for the dysregulation of HMGNI in DS and a link between changes to the epigenetic landscape due to overexpression of *HMGNI* and AD pathology.

HMGNI, PRC2, and DS brain hypothesis

So far, I have discussed the evidence focused on the hypothesis that the triplication and subsequent overexpression of *HMGNI* in DS leads to global alterations in transcriptional activity by antagonizing the action of PRC2 and results in the derepression of PRC2 target genes. This antagonistic relationship potentially contributes to the neurodevelopment abnormalities described above as well as other DS-related phenotype including AD pathology. For a summary of this hypothesis please refer to Figure 2.

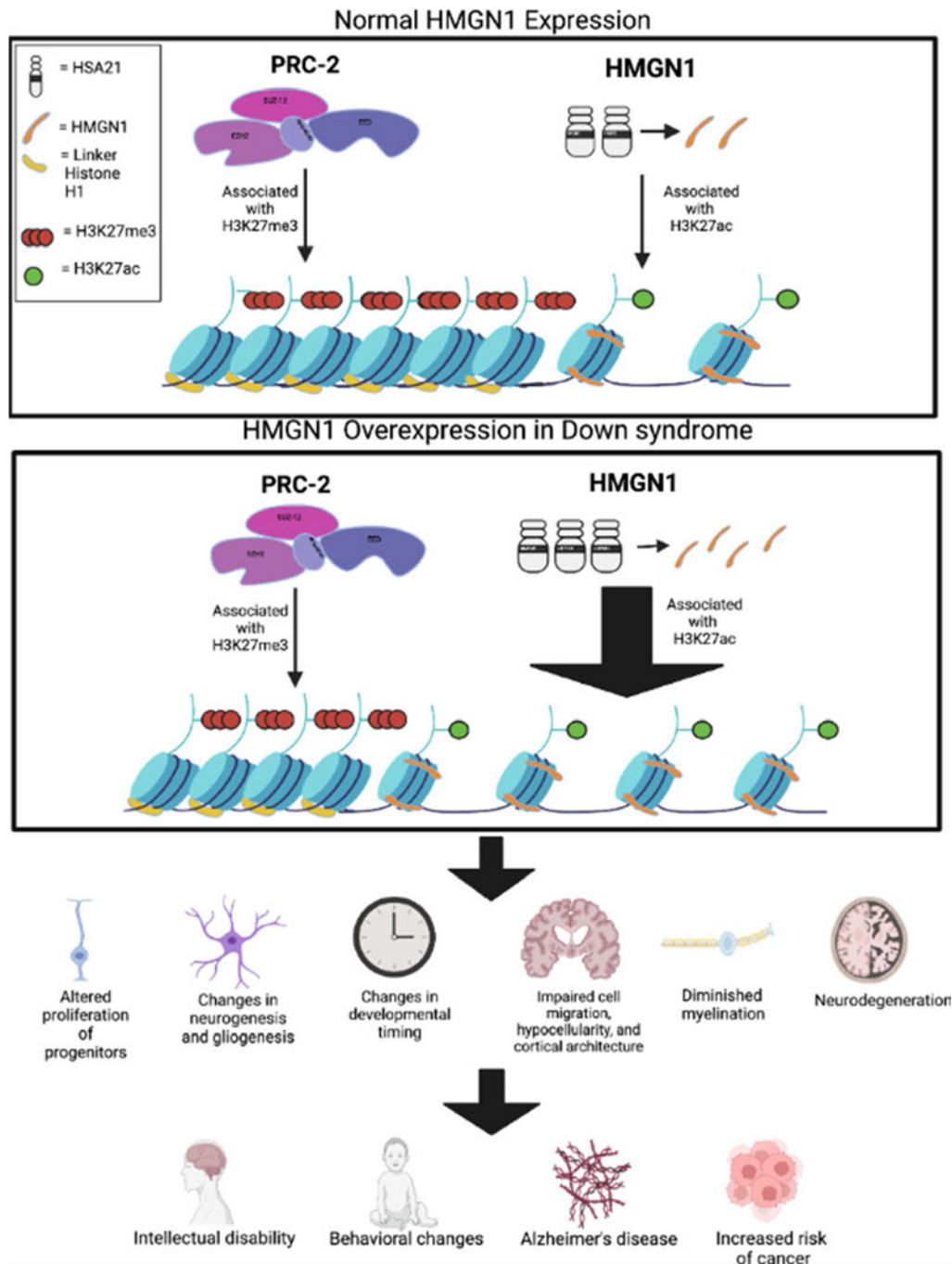


Figure 3: Proposed consequences of HMGN1 overexpression and PRC2 antagonism in DS. Illustration of the possible mechanism of PRC2 antagonism by PRC2 in DS. Increased levels of HMGN1 are available to bind to nucleosomes, resulting in a more less compacted chromatin structure available for transcription. This leads to changes at the cellular level that then contribute to DS phenotypes. Adopted from the review article “Shaking up the Silence: consequences of HMGN1 antagonizing PRC2 in the Down syndrome brain” by Farley et al. (Farley et al., 2022).

Using iPSC cell-derived models (NPCs and organoids) to study HMGN1, H3K27ac, and H3K27me3 in DS

The ability to reprogram human cells into iPSCs using factors discovered by the Yamanaka lab (Takahashi et al., 2007; Takahashi & Yamanaka, 2006) has had a profound effect on the study of human development and disorders by providing a human-derived model of pluripotency that avoids much of the controversy surrounding ESCs but recapitulates many of their features, including self-renewal capabilities and the ability to differentiate into cells from all three germ layers (Takahashi & Yamanaka, 2006). The reprogramming was initially achieved using somatic cells (Takahashi et al., 2007; Takahashi & Yamanaka, 2006), such as human fibroblasts, hematopoietic cells, and amniotic fluid cells have also been reprogrammed (Aasen et al., 2008; Anchan et al., 2011; Loh et al., 2009; Lu et al., 2013; Park et al., 2008; Pipino et al., 2014; Yu et al., 2007). The use of iPSCs has proven especially valuable because it allows for the creation of isogenic cell lines that can serve as their own control. In trisomy, these cell lines are created from cells that are initially donated by the same individual with DS but lose their extra copy of chromosome 21 through random mutations during reprogramming or due to mosaicism, in which not all of the individual's cells contain an extra copy of HSA21 (Maclean et al., 2012; Weick et al., 2013). Isogenic lines are particularly useful for studying a complex disorder like DS because any differences in gene expression or epigenetic changes can be directly attributed to an extra copy of chromosome 21 since there will be no differences due to variability between individual donors.

The use of iPSCs as a model for DS was helped by the development of a protocol to create 2-D neuronal culture using SMAD inhibition and then direct them toward different neural lineages (Chambers et al., 2009). By day 11, the iPSC-derived NPCs were expressing the neural marker PAX6, and using various manipulations the researchers were then able to induce the cells to differentiate into various neural cell types validated by IHC and select markers. Using this protocol researchers were able to further generate glutamatergic cortical neurons and recreate an accurate temporal representation of neuronal development of all six layers of cortex (Shi, Kirwan, & Livesey, 2012; Shi, Kirwan, Smith, MacLean, et al., 2012; Shi, Kirwan, Smith, Robinson, et al., 2012). Glutamatergic cortical projection neurons created from iPSCs derived from DS patients also exhibit AD pathology (Shi, Kirwan, Smith, MacLean, et al., 2012), and contain marks of increased oxidative stress and reduced synaptic activity consistent with DS (Weick et al., 2013).

With DS iPSC-derived neurons recapitulating some of the known features in DS, studying their precursors may provide insight into the mechanisms leading to these changes. NPCs can be a useful model for studying the early changes in neurogenesis in DS since trisomic NPCs expanded in culture replicate many of the differences observed during cortical development in trisomy 21. These include a decrease in proliferation (Contestabile et al., 2007; Jiang et al., 2013), temporal changes in neurogenesis (Bhattacharyya et al., 2009), and changes in the number of GABAergic interneurons produced (Bhattacharyya et al., 2009). With epigenetic changes the suspected cause of many transcriptomic changes that ultimately lead to DS phenotypes, it is essential to firmly establish the epigenetic differences found in DS. A recent study conducted by Meharena et al. (Meharena et al.,

2022) found an increase in levels of H3K27ac and a decrease in H3K27me3 in trisomic NPCs, supporting our hypothesis that *HMGNI* overexpression in DS leads to increased levels of acetylation at H3K27 but disrupts PRC2's ability to deposit methyl groups at the same site, ultimately leading to derepression of genes that would otherwise be silenced through H3K27me3. Importantly, their finding that changes to chromatin accessibility occur only in NPCs but not iPSCs supports the delayed emergence of differences in neurodevelopment between DS and non-DS brains. An assay for transposase-accessible chromatin (ATAC-seq) also found an increase in chromatin accessibility in the trisomic NPCs of an isogenic pair, as well as an overall increase in nascent RNA transcripts, supporting an increase in transcriptional activity due to an additional HSA21 that is in line with *HMGNI*'s proposed role in increasing chromatin accessibility.

The use of organoids in neurobiology research has increased dramatically over the past few years as they are able to generate different neuronal and glial cells types and recapitulate some of their interactions to produce a more realistic model of the human brain than 2D or mouse models (Amiri et al., 2018; Eiraku et al., 2008; Lancaster et al., 2013; Paşca et al., 2015; Song et al., 2019). The transcriptomic and epigenetic landscape of organoids has been mapped and corresponds well to the known dynamics of the human embryonic brain at mid-gestation (Amiri et al., 2018), legitimizing their use for studying epigenetic markers like H3K27ac and H3K27me3. They also capture the neurogenesis, developing ventricular zone-like structures that give rise to both deep and superficial neurons (Paşca et al., 2015). Importantly, the switch from neurogenesis to gliogenesis is also modeled (Paşca et al., 2015). Organoids generated from trisomic iPSCs mimic the

neurodevelopmental changes found in the disorder, including decreased neuronal proliferation that results in smaller organoids (Z. Li et al., n.d.; Tang et al., 2021), the overproduction of inhibitory neurons (Tang et al., 2021), and AD-like pathology (Alić et al., 2021). With these developmental similarities, organoids provide a valuable model for studying whether early disruptions to proper neurodevelopment are possibly due to changes in transcriptional activity resulting from the overexpression of *HMGNI*.

In this project, we assessed whether there are measurable differences in the levels of acetylation and trimethylation at H3K27 in two different isogenic cellular models that recapitulate aspects of early neural development, as well as in post-mortem DS brain tissue. Since our hypothesis is that increased expression of *HMGNI* in DS results in chromatin changes that increase transcriptional activity, it was important to first quantify the levels of these markers. Additionally, we experimentally knocked down *HMGNI* expression to non-DS levels and measured the expression level of non-HSA21 genes, overexpressed in trisomy and known to be PRC2 target genes. By doing this, we attempted to establish a causative link between overexpression of *HMGNI* in trisomy and aberrant expression of PRC-2 targets genes to provide support for the proposed mechanism of *HMGNI* antagonizing PRC2 in DS.

MATERIALS AND METHODS

Generation of Neural Progenitor Cells:

Neural progenitor cells (NPCs) were created from human induced pluripotent stem cells (iPSCs) that were originally derived from fibroblasts acquired from an individual with trisomy 21. These were used to create trisomic (WC-24-02-DS-M) and isogenic euploid control (WC-24-02-DS-B) iPSC lines that were identical except for the extra copy of human chromosome 21. These lines were provided and validated by the Bhattacharyya lab at the University of Wisconsin-Madison.

NPCs were generated by a Ph.D. student in the lab following the embryoid body protocol provided by StemCell Technologies (protocol number: 10000005588). NPCs were thawed and then cultured and passaged on Matrigel® (Fisher Scientific #354277) using NPC medium, which contained Neurobasal (50%Gibco #12348-017) and DMEM/F-12 (Gibco #11320-033), mixed 1:1 ratio; GlutaMax (1:100, Invitrogen #35050061), Beta-Mercaptoethanol (1mM; Gibco #21985-023), N2 supplement (1:200, Gibco #17502-048), B-27 supplement (1:100, Invitrogen #12587), NEAA (1:100; Gibco #11140-50, 100U/mL); Penicillin/Streptomycin (1:100; Life Technologies #15140122), β -fibroblast growth factor (10ng/mL, R&D Systems #233-FB-25/CF), and epidermal growth factor (10ng/mL, R&D Systems # 236-EG-200). For thawing, a cryovial containing 1mL of frozen NPCs was thawed and added to 4mL of warm DMEM/F-12 already in a 50mL conical tube and centrifuged at 300g for 5 minutes. The pellet was resuspended in 1mL of NPC medium and added to a new well coated with Matrigel® (Fisher Scientific #354277).

When cells were 80-90% confluent they were passaged and seeded for the experiment. This was done by washing once with DMEM/F-12 before adding 1mL Accutase™ (StemCell Technologies #07920) and placing the plate in a 37°C incubator for 5 minutes. One ml of DMEM/F-12 was added to the well after 5 minutes to neutralize the Accutase and the solution was pipetted up-and-down gently to dissociate the cells before collecting and adding them to a 50mL conical tube. An additional 3mL of DMEM/F-12 was added to equal a total of 5mL of solution, and the tube was then placed in a centrifuge for 5 minutes at 300g. The supernatant was aspirated and the cells were resuspended in another 1mL of NPC medium. For maintenance, 1×10^6 cells per 1 well of a 6 well Matrigel -coated plate were used with NPC medium changes every other day. For the experiments, the number of live cells were counted using a hemocytometer to plate the cells at a density of 0.25×10^6 per 1 well of a 24 well plate on Matrigel -coated coverslips in 0.5ml of NPC media. The plates were placed back in a 37°C incubator, and the cells were fixed with 4% PFA after 24 hours.

Generation of cortical organoids

Cortical organoids were generated by another student in the lab following the protocol below. To create a single cell suspension for passaging, iPS cells were washed with PBS before adding Accutase to the well for 5 minutes. The cells were then centrifuged for 5 minutes at 200rpm before being resuspended in 2mL of mTeSR™ Plus (StemCell #100-0276) with 50µM Rock inhibitor (Tocris BioSciences 1254) added (referred as starter media). A hemocytometer was used to count the cells to ensure they were resuspended at

a concentration of 15,000 cells per well. Using the protocol described in Madhavan et al., 2018, these iPSCs were used to generate organoids. To begin, 15,000 iPSCs in 150 μ L starter media per well were plated in low-adherence V-bottom wells in a 96-well plate. Daily media changes were performed for 6 days using TeSR5/6 (StemCell Technologies) medium with 2.5 μ M Dorsomorphin (Sigma #P5499) and 10 μ M SB-431542 (Sigma S4317) added. Organoid medium was used beginning on day 7 and contained Neurobasal-A (Invitrogen #10888022) with B-27 supplement (1:50) (Invitrogen #12587), GlutaMax 12 (1:100) (Invitrogen #35050061), and 100U/mL Penicillin/Streptomycin (1:100) added. Through day 25, 20ng/mL fibroblast growth factor 2 (R&D Systems #233-FB-25/CF) and 20ng/mL epidermal growth factor (R&D Systems # 236-EG-200) were also added to the medium, and half changes of the media were performed daily. Between days 16 and 20, each organoid was transferred to a single well in ultra-low attachment 24 well plates. To induce neural differentiation, 20ng/mL brain derived neurotrophic factor (BDNF) (AF-450-02) and 20ng/mL neurotrophic factor 3 (NT3) (450-03) were both added to the organoid medium on day 27. From this point forward, 1% Geltrex (A1569601) was also added to the organoid medium. Daily half media changes were performed from day 27 to day 39. Half media changes were performed every other day from day 41 to day 51, and during this period no molecules were added to supplement the organoid medium. Supplements were added again on day 51, starting with 10ng/mL platelet-derived growth factor AA (PDGF) (R&D Systems #221-AA) and 10ng/mL insulin-like growth factor (IGF) (R&D Systems #291-GF-200), and media changes were performed every 2 days. The organoid medium was supplemented with 40ng/mL 3,3',5-triiodothyronine (T3) (Sigma

T6397) on day 61, and 2 day changes were continued until day 71. From day 71 through 130, the organoid medium was not supplemented with any small molecules and half media changes were performed every other day.

Preserving and Slicing Organoids

After 130 days the organoids were fixed overnight in 4% paraformaldehyde (PFA) before being washed 3 times in PBS. They were then placed in 30% sucrose for cryoprotection and embedded in the same concentration of sucrose with optimal cutting temperature (OCT) embedding medium at a ratio of 60:40, frozen and stored at -80°C. The organoids were then sectioned in 12µm increments and mounted on slides that are stored at -80°C.

Immunohistochemistry for NPCs

NPCs were washed three times with PBS and then incubated in a blocking solution containing 5% donkey serum in 0.1% Triton-X in PBS for one hour at room temperature. Primary antibodies diluted in the same blocking solution were then added to the wells and allowed to incubate overnight at 4°C. Three 10-minute washes were performed the next day, with the first two washes using PBST and the last one using only PBS. They were then placed in the dark and allowed to incubate in the secondary antibodies diluted in blocking solution, for 1 hour at room temperature with gentle agitation. Three 10-minute washes were again performed, with the first two washes using PBST and the last one using only PBS. The round cover slips were then carefully removed from the well plate and placed

cell-side down onto a slide containing Vectashield with DAPI (Invitrogen #2273701) and stored at 4°C.

The following primary antibodies were used: anti-H3K27me3 (1:200) (Abcam #ab6002) and anti-H3K27ac (1:2000) (Abcam #177178). The secondary antibodies used were donkey anti-mouse 488 (Invitrogen #A21202) and donkey anti-rabbit 546 (Invitrogen #A10040) and were both conjugated with Alexa fluor and used at a concentration of 1:500.

Immunohistochemistry for Organoids

Slides with organoids were first allowed to thaw for 20 minutes and then the organoids were outlined with a hydrophobic pen before being placed in blocking solution containing 5% donkey serum in 0.1% Triton-X in PBS for one hour at room temperature. Primary antibodies diluted in the same blocking solution were then added to the wells and allowed to incubate overnight at 4°C. Three 10-minute washes were performed the next day, with the first two washes using PBST and the last one using only PBS. They were then allowed to incubate in the secondary antibodies for 1 hour at room temperature with light blocking and gentle agitation. Three 10-minute washes were again performed, with the first two washes using PBST and the last one using only PBS. Vectashield with DAPI (Invitrogen #2273701) was added to each slide before placing a coverslip and storing at 4°C.

The following primary antibodies were used: anti-H3K27me3 (1:200) (Abcam #ab6002) and anti-H3K27ac (1:2000) (Abcam #177178). The secondary antibodies used

were donkey anti-mouse 488 (Invitrogen #A21202) and donkey anti-rabbit 546 (Invitrogen #A10040) and were both conjugated with Alexa fluor and used at a concentration of 1:500.

Immunohistochemistry for human brain samples

Samples of frontal cortex tissue were obtained from 11 human donors with either DS, AD, DS-AD, or control subjects and generously donated by UC-Irvine as part of the Down Syndrome BioBank Consortium and Dr. Charlotte Granholm-Bentley from the University of Colorado – Denver and Anschutz Medical School. Both formalin-fixed paraffin-embedded (FFPE) and frozen samples were obtained and analyzed. To prepare the FFPE slides for IHC and analysis they were first baked at 57°C for 30 minutes before being undergoing a dewaxing protocol provided by the Center for Traumatic Encephalopathy at Boston University. The slides were placed in Xylene for three 10 minute washes, then they were transferred to 100% isopropyl alcohol for two 2 minute washes, then onto a 30 minute wash in methanol before being rinsed for 2 minutes in 95% isopropyl alcohol, and finally they were rinsed for 5 minutes in deionized water. To perform antigen retrieval the slides were microwaved at 98°C and 750 watts for 20 minutes while in 10x AR 6 solution (Akoya Biosciences, AR600250ML). The slides were washed once in PBST for two minutes and then outlined using a hydrophobic pen before incubating in blocking solution containing 3% donkey serum in 0.4% Triton-X in PBS for 30 minutes followed by incubation with primary antibodies diluted in buffer containing 1% donkey serum in 0.4% Triton-X in PBS for one hour at room temperature. They were then washed 3x for two minutes each with TBST and gentle agitation followed by incubation in the secondary antibody diluted in 1%

donkey serum in 0.4% Triton-X in PBS for 30 minutes at room temperature. The slides were again washed 3x for two minutes each with TBST and gentle agitation followed by incubation in the Opal dye suspended in 5mL of 1x amplification diluent solution (1:500, Akoya Biosciences FP1609) for 10 minutes. Then the slides were washed 3x for two minutes each with TBST before adding 400 μ L of DAPI working solution per slide, which consists of two drops of DAPI solution (Akoya #NEL811001KT) in 1mL of TBST. Lastly, ProLong Gold Antifade Mountant (Invitrogen #P36930) was used to mount glass coverslips on the slides.

The following primary antibodies were used: mouse anti-H3K27me3 (1:100, Abcam #ab6002) and rabbit anti-H3K27ac (1:100, Abcam #177178). Secondary antibodies were conjugated with horseradish peroxidase (HRP) and used at a concentration of 1:500 (Jackson Immunoresearch #715-035-151 and # 711-035-152). Opal fluorophore 520 and 650 were both used at a concentration of 1:150 and suspended in 1% donkey serum in 0.4% Triton-X in PBS. For nuclear staining, spectral DAPI solution was added to TBST (Akoya Biosciences FP1490).

Imaging and Quantifying Mean Fluorescence Intensity

Image analysis was performed on two different types of slides: those containing NPCs and those with organoids. For the organoid slides, each contained between two and four organoids. Three images were taken of edge sections of each organoid using a Zeiss LSM 710 confocal microscope (Carl Zeiss, GER) with a 40x objective lens, 1.5x zoom, 8-bit pixel depth, and 0.21 μ m pixel size. Z-stack images were collected for each section at

1024x1024 resolution. Quantification of mean fluorescence intensity (MFI) was done by splitting each image into individual channels, subtracting the background level of fluorescence, and thresholding using the 'Otsu' auto-thresholding option. The z-stack images were analyzed using the particle analysis option after thresholding, with $0.25\mu\text{m}^2$ selected as the minimum particle size. After testing minimum particle size options from 0.025 to 2, $0.25\mu\text{m}^2$ was determined to most accurately capture the regions of interest and was thus selected as the minimum value.

Three areas were imaged and used to determine the MFI for each organoid. Outliers were identified using an interquartile range (IQR) test where any data points that are more than 1.5 IQR above Q3 or below Q1 are considered outliers and can be removed. The observations were averaged to determine the MFI for each individual organoid. Then, the MFI mean value of the euploid control was calculated as 100% and served for the normalization of the trisomic samples. The data from 3 independent differentiation experiments were quantified through the same pipeline and the values for euploid and trisomic samples were averaged. An F-test was run to find whether variances were equal or unequal, and then an unpaired students t-test was performed in Microsoft Excel to determine significance, with a p-value of <0.05 as the cutoff value.

A similar method was used for slides containing NPCs. Glass coverslips onto which either NPCs had been grown were mounted on glass slides, with each slide containing 2 or 3 of these glass coverslips with the same type of cells (i.e. either trisomic or euploid). Images were taken of 3 different areas of each coverslip, generally one from the top right, one from the bottom center, and one from the top left, to get as representative a sample as

possible. Images were processed and quantified the same way as we did for the organoids.

The data from three independent differentiation experiments was quantified.

Lentivirus Production

The day before transfection HEK-293 cells were seeded at a density of 6×10^6 cells (Takara #632180) per 10cm dish in 15mL DMEM/F-12 (ThermoFisher 11320-033) with 10% FBS (Takara #631106) and 1mM Sodium Pyruvate (Life Technologies #11360-070). Cells were approximately 70% confluent one day after seeding. The transfection solution was made in sterile 1.5mL microcentrifuge tubes, with a single tube used for a single 10-cm dish of HEK-293 cells. Four different lentiviral plasmids (A, B, C, and D) containing different HMGN1 shRNA constructs and a GFP reporter (OriGene #TL319506) were used for the transfections of the assigned cultures and tested to determine which was most effective at reducing the expression of HMGN1 to euploid levels (see 'qPCR' section). There was also a plasmid with scrambled HGMN1 shRNA which was included as a control. The following was added to the microcentrifuge tube: 2 μ g of the transfer plasmid, 3.33 μ g of pMDLg/pRRE plasmid, 3.33 μ g of pRSV/REV plasmid, 2.22 μ g of pMD2.G, 222 μ L of Opti-MEM and 39 μ L of PEI solution. The transfection solution was incubated at room temperature for 5-10 minutes and then added dropwise across the 10-cm dish before placing the dish in a 37°C 5% CO₂ humidified incubator for 8-16 hours before the viral medium was replaced with fresh complete medium (DMEM/F-12, 10% FBS, 1mM sodium pyruvate).

Lentivirus Collection and Concentration

On the third day after transfection the supernatants were collected in 50mL centrifuge tubes and spun at 1200g for 5 minutes at 4°C. Each supernatant was filtered using a 0.22µM PES steriflip tube (Fisher Scientific 12565269). The volume of each viral preparation was measured and Lenti-X concentrator (Takara #631232) was added as 1/3 of this volume. This solution was then incubated for 30 minutes at 4°C before being centrifuged at 1500g for 45 minutes at 4°C. The supernatant was discarded and the remaining pellet was resuspended in 1mL of cold sterile DPBS before being aliquoted and stored at -80°C.

Enzyme-linked Immunosorbent Assay (ELISA)

The ELISA kit (Takara Bio #632200) was used according to the manufacturer's instructions. A 200pg/mL stock solution was created by diluting 20µL of the p24 Control (10ng/mL) into 980 µL of fresh complete tissue medium consisting of DMEM/F-12 (Gibco #11320-033) and 10% FBS (Takara #631106) for a 1:50 dilution. Using this as diluent, four additional standard dilutions of 100, 50, 25, and 12.5pg/mL were created. 200µL of each standard curve dilution, supernatant sample, and culture medium was dispensed into correctly labeled duplicate wells and incubated at 37°C for 60 minutes. The contents of each well were aspirated, and the plate was washed five times using 350µL of wash buffer per well. Then each well was filled with 100µL of Streptavidin-HRP conjugate and incubated at room temperature for 30 minutes before being aspirated and washing the plate five times again using wash buffer. After washing, a multi-channel pipet was used to

dispense 100uL of Substrate solution into each well. The plate was then protected from light and allowed to incubate at 18-22°C for 30 minutes. After this time, 100µL of the included Stop Solution-was added to each well to stop the reaction. A microtiter plate reader previously blanked using a negative control well was used to read the absorbance values at 450nm and determine the virus titer. A standard curve was constructed using the standards with known protein concentration, and this was then used to determine the p24 concentration of the virus preparations. The concentration was converted from ng p24/mL to IFU/mL using the ratio of p24/IFU calculated with a control virus with a known IFU/mL. .. The calculated viral titer was 4.2×10^9 IFU/mL was used.

Viral Transduction

The viral preparation was thawed and spun down at 500g for 5 minutes before use. The medium was aspirated from each well and NPC medium was mixed with the viral solution (40-80 µL) to achieve a total volume of 1mL in each well. The plate was then centrifuged at 1000g for 45 minutes before being placed in a 37°C incubator for 6 hours. After 6 hours the virus-containing medium was aspirated and replaced with NPC medium. The antibiotic puromycin (Gibco #A1113802) was initially introduced two days as transduction as a selector for cells that did not integrate the plasmid at a concentration of 3µg/mL, as resistance was conferred via an anti-biotic resistant construct integrated into the plasmid. However, even introducing puromycin at a concentration as low as 0.15 µg/mL was found to be cytotoxic to the cells. The expression of GFP was used to determine the extent of cells transduced with the lentiviral plasmid beginning 48 hours after

transduction. This was initially checked using a fluorescence microscope, but the GFP-positive cells were eventually separated out by FACS sorting done by the Flow Cytometry Core Lab at Boston University.

FACS Sorting

To separate out NPCs that had successfully integrated the plasmid introduced via lentivirus we had FACS sorting performed by the Flow Cytometry Core Lab at Boston University. A live-dead stain was performed as well as one to separate out cells marked by GFP, a positive indicator of successful uptake. About a million cells were available for sorting per condition. The cells were transferred from the well-plate to 50mL conical tubes and placed in FACS sorting buffer consisting of PBS with 1% bovine serum albumin (AmericanBio AB1249) and Calcein blue (5mM, Life Technologies 65-0855-39). The cells were then sorted based on the expression of GFP using the MoFlo Astrios EQ Cell Sorter system (Beckman Coulter B52102) before being placed back in 50mL conical tubes in their original NPC medium described above.

Cells-to-CT and qPCR

Cells-to-CT and qPCR were done similarly for the cells that did not go through the FACS sorting (mixed population of cells) and the cells that were collected after the sorting. Thirty thousand cells were seeded per well in 96 well plates and allowed to attach overnight. To determine the expression level of HMGN1 and select PRC2 target genes the TaqMan Gene Expression Cells-to-CT™ kit (Life Technologies #4399002) was used to

extract mRNA from NPCs transduced with lentivirus carrying each of the four different plasmids containing HMGN1 shRNA in order to produce cDNA. A Bio-Rad C1000 thermocycler (BioRad) was used for reverse transcription reaction to generate cDNA from this extracted mRNA with the reverse transcription enzyme mix provided in the kit. Two μL of cDNA generated using was used per one well of 96 well plate for qRT-PCR reaction that was performed using the BioRad CFX96 Real-Time System, with the final analysis done using BioRad CFX Maestro. The data was analyzed using delta delta CT, normalized to the house keeping genes *GAPDH* and *UBC*. At least 4 biological replicates were used for each condition (plasmids A, B, C, scramble, and euploid control) and the mean expression levels for each condition were determined, with the expression levels normalized to that of the euploid control. To compare differences between trisomic and euploid, and trisomic with HMGN1 shRNA and euploid, two-tailed unpaired student's t-tests were performed, with a p-value < 0.05 set as the mark of significance.

Gene Target	ThermoFisher Catalog Number
<i>PCSK1N</i>	Hs00560041_m1
<i>PEG10</i>	Hs00248288_s1
<i>ID2</i>	Hs04187239_m1
<i>HES1</i>	Hs00172878_m1
<i>IGFBP3</i>	Hs00181211_m1
<i>HMGNI</i>	Hs05024785_sH
<i>CHCHD2</i>	Hs00853326_g1
<i>APP</i>	Hs00169098_m1
<i>SHH</i>	Hs00179843_m1
<i>XIST</i>	Hs01079824_m1
<i>CHL1</i>	Hs00544069_m1

Table 4: Catalog numbers for ThermoFisher Scientific/Taq-Man assays used in qRT-PCR experiments. All probes were labeled with FAM dye except for UBC which was labeled with VIC.

RESULTS

Quantifying and comparing levels of H3K27ac and H3K27me3 in NPCs

Based on the potential effect of HMGN1 triplication on the cell fate acquisition and identity, we investigated first the differences in the H3K27 marks in euploid and trisomic NPCs generated from one isogenic line. To determine the levels of H3K27ac and H3K27me3 in both trisomic and euploid NPCs, IHC was performed before images were taken using a confocal microscope (**Fig. 4A**). The expression level of each marker was quantified using MFI and then analyzed for comparison between euploid and trisomic NPCs. For a more comprehensive analysis, Z-stack images which contain between 12-22 “optical slices”, or individual images that are taken at increasing z positions and then “stacked” together, were used. H3K27me3 (**Fig. 4B**) and H3K27ac (**Fig. 4C**) levels were first quantified for each of the three independent NPC differentiation experiments, with the average MFI determined for each well of NPCs in both the euploid and trisomic conditions. The MFI of the trisomic wells was normalized to the euploid control in each of the experiments, with the data from all three experiments then averaged and analyzed. Unpaired independent student’s t-test were performed to determine if a statistically significant difference existed between the MFI levels of either H3K27ac or H3K27me3 in trisomic NPCs as compared to euploid. When the results from all three experiments were averaged there was no significant difference found between euploid and trisomic for either H3K27me3 (**Fig. 4B**) or H3K27ac (**Fig. 4C**).

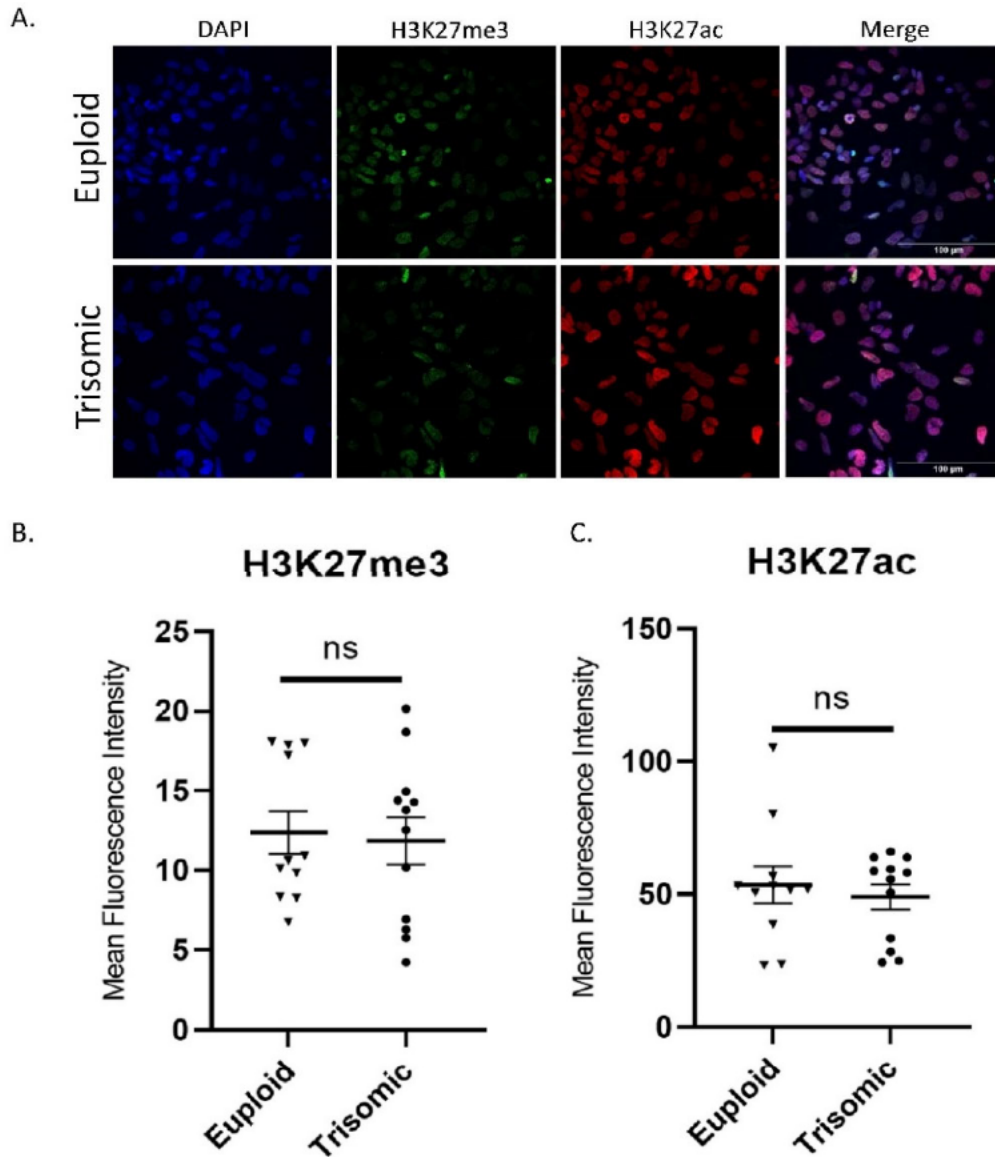


Figure 4. Analysis of H3K27ac and H3K27me3 in NPCs. **A.** Representative images of IHC staining of NPCs taken from Z-stack showing DAPI, H3K27me3, H3K27ac, and channels merged. Scale bar, 100 μ m **B.** Graph showing the average MFI, as a marker of H3K27me3 levels, for euploid and trisomic NPCs. Each triangle (euploid) or dot (trisomic) represents the MFI of one individual well of NPCs used to determine the average (euploid, n=11; trisomic, n=12). The results were analyzed using unpaired student t-test. Error bar represents standard error of the mean (SEM). **C.** Graph showing the average MFI, as a marker of H3K27ac levels, for euploid and trisomic NPCs. Each triangle (euploid) or dot (trisomic) represents the MFI of one individual well of NPCs used to determine the average (euploid, n=11; trisomic, n=12). The results were analyzed using unpaired student t-test. Error bar represents SEM.

Quantifying and comparing H3K27ac and H3K27me3 in 130-day-old organoids

Since no difference was found in NPCs, we next wanted to look at a more mature and complex system that better recapitulates brain development. Therefore, we aimed to determine if there are differences in levels of H3K27ac and H3K27me3 in both trisomic and euploid 130-day old cortical organoids generated from the same isogenic line. In contrast to the NPCs, the organoid model represents more diverse and mature cell types including different types of progenitors, neurons, astrocytes, and oligodendrocytes. This was carried out in an almost identical manner to the previously described experiment using NPCs, with IHC performed first and then images of the organoids taken with a confocal microscope (**Fig. 5A**). The expression level of each marker was quantified by analyzing the z-stack images to determine the MFI for each of the three different areas of each organoid that were imaged and then averaging these results to determine the MFI for each individual organoid. The H3K27me3 (**Fig. 5B**) and H3K27ac (**Fig. 5C**) levels of each trisomic organoid were normalized to the euploid control from the same experiment, the data was averaged and unpaired independent student's t-test was run to determine statistical significance. There was a statistically significant decrease in H3K27me3 in the trisomic organoids (**Fig. 5B**), but no statistical significance was found when comparing H3K27ac (**Fig. 5C**).

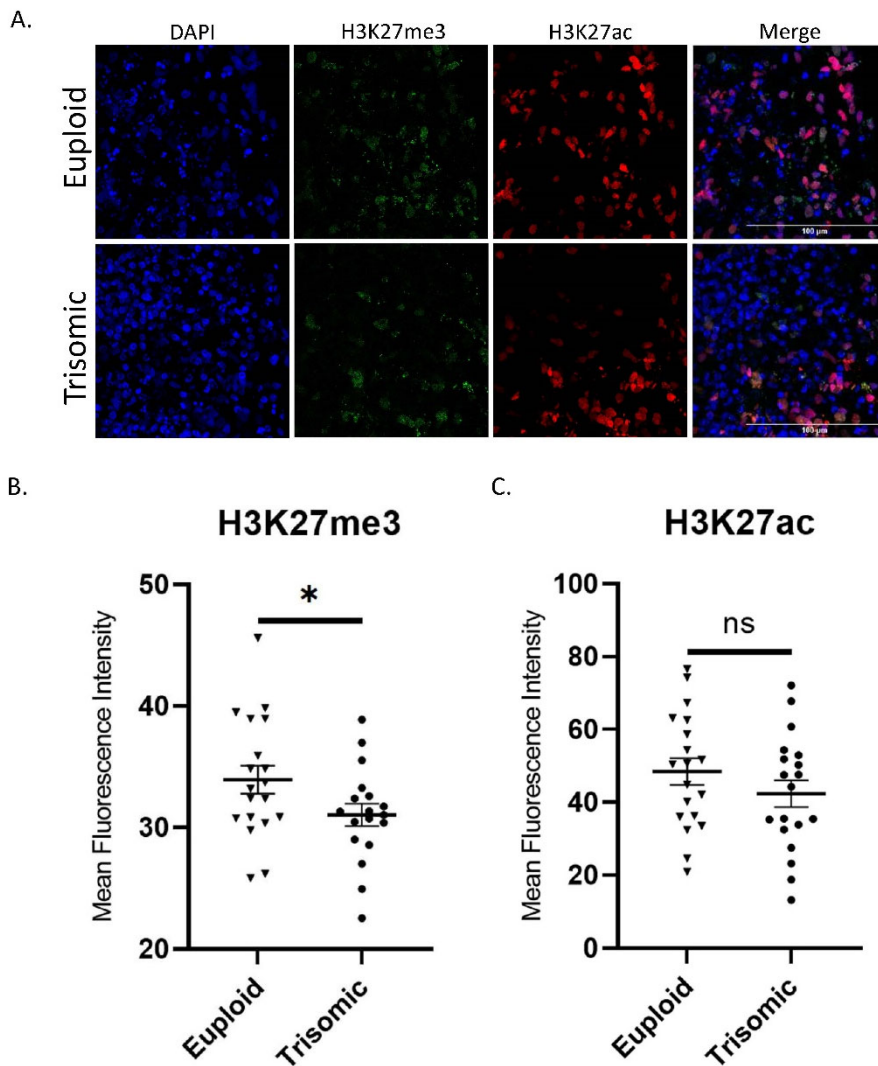


Figure 5. Analysis of H3K27ac and H3K27me3 in 130-day-old organoids. A. Representative images of IHC staining of organoids taken from Z-stack showing DAPI, H3K27me3, H3K27ac, and channels merged. Scale bar, 100μm B. Graph showing the average MFI, as a marker of H3K27me3 levels, for euploid and trisomic organoids. Each triangle (euploid) or dot (trisomic) represents the MFI of one individual organoid used to determine the average (euploid, n=19; trisomic, n=18). The results were analyzed using unpaired student t-test. Error bar represents SEM. * $p < 0.05$. One trisomic organoid was identified as an outlier based on the quartile outlier test and removed from the analysis. C. Graph showing the average MFI, as a marker of H3K27ac levels, for euploid and trisomic organoids. Each triangle (euploid) or dot (trisomic) represents the MFI of one individual organoid used to determine the average (euploid, n=19; trisomic, n=19). The results were analyzed using unpaired student t-test. Error bar represents SEM.

Quantifying and comparing H3K27ac and H3K27me3 in brain tissue from individuals with DS, DS-AD, or AD

Since studies have identified changes in both histone acetylation and methylation levels in AD (278-281), we were curious as to whether there were specific changes in H3K27ac and H3K27me3 in AD and DS-AD. However, despite a well-documented comorbidity between DS and AD pathology no studies were performed on the assessment of H3K27 in DS-AD and the comparison to the AD brain. Thus, we aimed to quantify the levels of H3K27me3 (**Fig. 6A**) and H3K27ac (**Fig. 6B**) in human frontal cortex tissue from individuals with DS-AD and AD and age-matched controls. The paraffin-embedded slides were provided by Dr. Ann-Charlotte Granholm-Bentley in conjunction with the UC Irvine Brain Bank as part of the Down Syndrome Biobank Consortium. The 5 μ m sections were stained using IHC and then imaged using a confocal microscope. The control cases were imaged first in order to calibrate the settings, and these settings were reused to image the AD and DS-AD cases in order to maintain consistency. The MFI was quantified and averaged for each experimental group, with independent student t-tests run to compare each experimental group against the control group. Remarkably, when we compared the H3K27me3 pattern between the three groups, H3K27me3 of DS-AD group showed a reduction in this mark that almost reached statistical significance, compared to both control and AD the p-values were 0.068 and 0.063, respectively. Noticeably, no differences were found between the control and AD cases in the assessment of this mark. There were no statistically significant differences in the level of H3K27ac found in human brain tissue.

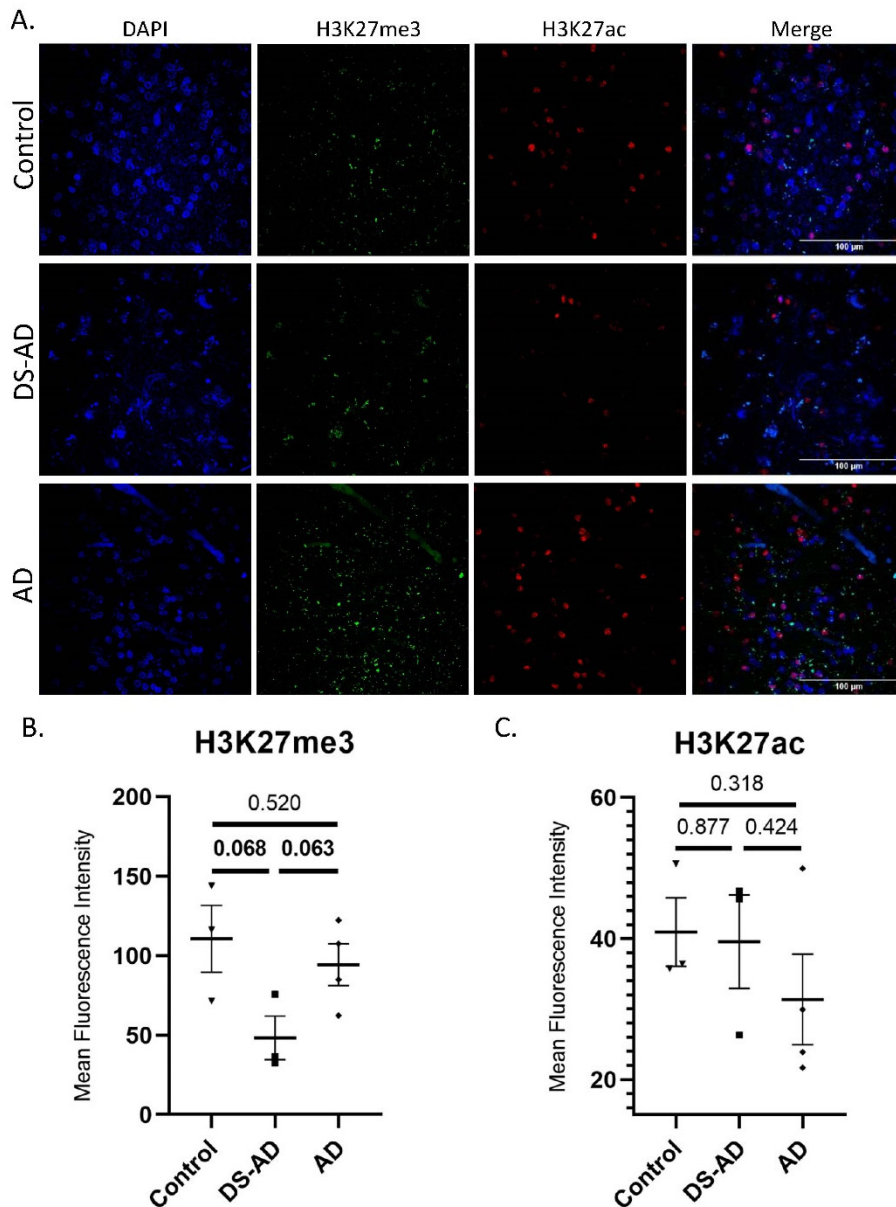


Figure 6: Comparing levels of H3K27me3 and H3K27ac in human brain tissue from individuals with DS-AD and AD. **A.** Representative images showing IHC staining taken from Z-stack for each of the three conditions; DS-AD, AD, and age-matched controls. Scale bar = 100 μ m. **B.** Graph showing the average MFI, as a marker of H3K27me3 levels, in brain tissue samples from individuals with DS-AD, AD, and age-matched controls (control, n=3; DS-AD, n=3; AD, n=4). Each triangle (control), square (DS-AD), or diamond (AD) represents the average MFI of one brain sample taken from one individual, which were then averaged per condition. Student t-tests were then performed to determine the p-value for each intergroup comparison. Error bars represent SEM. **C.** Graph showing the average MFI, as a marker of H3K27ac levels, in brain tissue samples from individuals with DS-AD, AD, and age-matched controls (control, n=3; DS-AD, n=3; AD, n=4). Each triangle (control), square (DS-AD), or diamond (AD) represents the average MFI of one brain tissue sample taken from one individual, which were then averaged per condition. Student t-tests were then performed to determine the p-value for each intergroup comparison. Error bars represent SEM.

Choosing an HMGNI shRNA construct to reduce HMGNI expression in NPCs

In our cortical organoid cellular model, we found a significant global effect of trisomy on H3K27me3 that could potentially be attributed to the increased expression of HMGNI. Although *HMGNI* levels in organoids were not measured, in our previous single-cell RNA-seq in organoids we detected upregulated levels of *HMGNI* across multiple cell clusters (Z. Li et al., n.d.) and we did find a relative expression level of 1.4 in trisomic NPCs when normalized to euploid. Since the organoids were produced from NPCs differentiated using the same protocol, it is expected that *HMGNI* would also be upregulated in this model. In addition, the data obtained from human brain samples suggested similar decreases in H3K27me3, and *HMGNI* is known to be upregulated in prefrontal cortex tissue in human brains (Rodríguez-Ortiz et al., 2021). Since H3K27me3 is a repressive epigenetic mark, if antagonism of PRC2 by *HMGNI* prevents its deposition we would expect to see an upregulation of genes that normally carry this mark (Kamminga et al., 2006; Mikkelsen et al., 2008; Nuytten et al., 2008; Rouillard et al., 2016). The genes looked at were also upregulated in our previous trisomic datasets (Klein et al., 2022; Z. Li et al., n.d.), and therefore we aimed to determine if *HMGNI* might influence the changes in expression level found in certain genes in DS. Since our hypothesis was that overexpression of *HMGNI* in DS leads to its different phenotypes through derepression of PRC2 target genes, normalizing its expression to euploid levels should normalize the expression of these target genes.

To do this we used shRNA to specifically downregulate the expression of *HMGNI* in NPCs through RNA interference. The shRNA construct consists of complementary RNA sequences that are self-complementary and thus generate hairpin-like loop formation, and are also complementary to the mRNA targeted for silencing, in this case, *HMGNI*. The hairpin structure is cleaved and the guide RNA strand is loaded onto a large ribonucleoprotein complex, the RNA-induced silencing complex (RISC) (Paddison et al., 2002). This can bind and degrade mRNA molecules with a complementary sequence which allows for selective targeting and knock-down of specific genes, in this case, *HMGNI*. When delivered using lentiviral vectors, the shRNA expression cassette carried by the virus will be reverse transcribed into DNA and incorporated into the genome of the desired cell, which will then constitutively express the shRNA. This means that the knock-down of the targeted gene will be propagated through subsequent cell divisions and passed down to daughter cells, thus downregulating the target mRNA and the corresponding protein.

Various shRNAs targeting the same mRNA will not all display perfect silencing efficiency. We thus tested four different shRNA constructs targeting *HMGNI*, as well as scrambled shRNA (shRNA-Scr) – the control that does not target *HMGNI*, for their ability to silence *HMGNI*. We produced lentiviral particles for each of them, and measured the viral titers before introducing them into NPCs through lentiviral transduction. An ELISA assay was performed to determine the predicted viral titer for each of the shRNA constructs, including the control ‘scramble’ (**Fig.7A**). Assistance with generating virus in HEK293 cells and the ELISA assay was provided by the Roussarie Lab at Boston University’s Chobanian and Avedisian School of Medicine. All four constructs provided

comparable titers, enabling us to measure the change in the expression level of *HMGNI* resulting from each of the different constructs to select the most appropriate construct to continue with. The goal was to select the construct that would reduce *HMGNI* expression to a level most comparable to euploid control to then determine if the expression of PRC2 target genes that are overexpressed in our trisomic cells were reduced.

We next aimed to determine which construct was most effective at reducing *HMGNI* expression to a level most comparable to euploid. To do this, a qRT-PCR experiment was performed after transduction of NPCs to determine the specific effect of each construct on *HMGNI* expression (**Fig. 7B**), and to compare the level of expression to that of euploid.

Of note, the plasmids carrying *HMGNI* shRNA contained two additional genes that should have allowed for the identification and selection of cells that had successfully incorporated the plasmid into their genome. One additional gene encoded GFP expression, and the other conferred antibiotic resistance. Cells that had taken up the plasmid expressed GFP and GFP expression was monitored as evidence for successful transduction. The introduction of the antibiotic Puromycin to the cell medium would kill any cells that had not successfully integrated the plasmid. However, despite repeatedly decreasing the antibiotic concentration this method of negative selection was discontinued due to toxicity and the death of a high number of cells, including GFP-positive cells which have been successfully transduced. Thus, we used a mixed population of cells where about 70% of cells were transduced. The results of this qPCR experiment revealed the shRNA-B construct to be effective in reducing *HMGNI* expression to levels comparable to euploid.

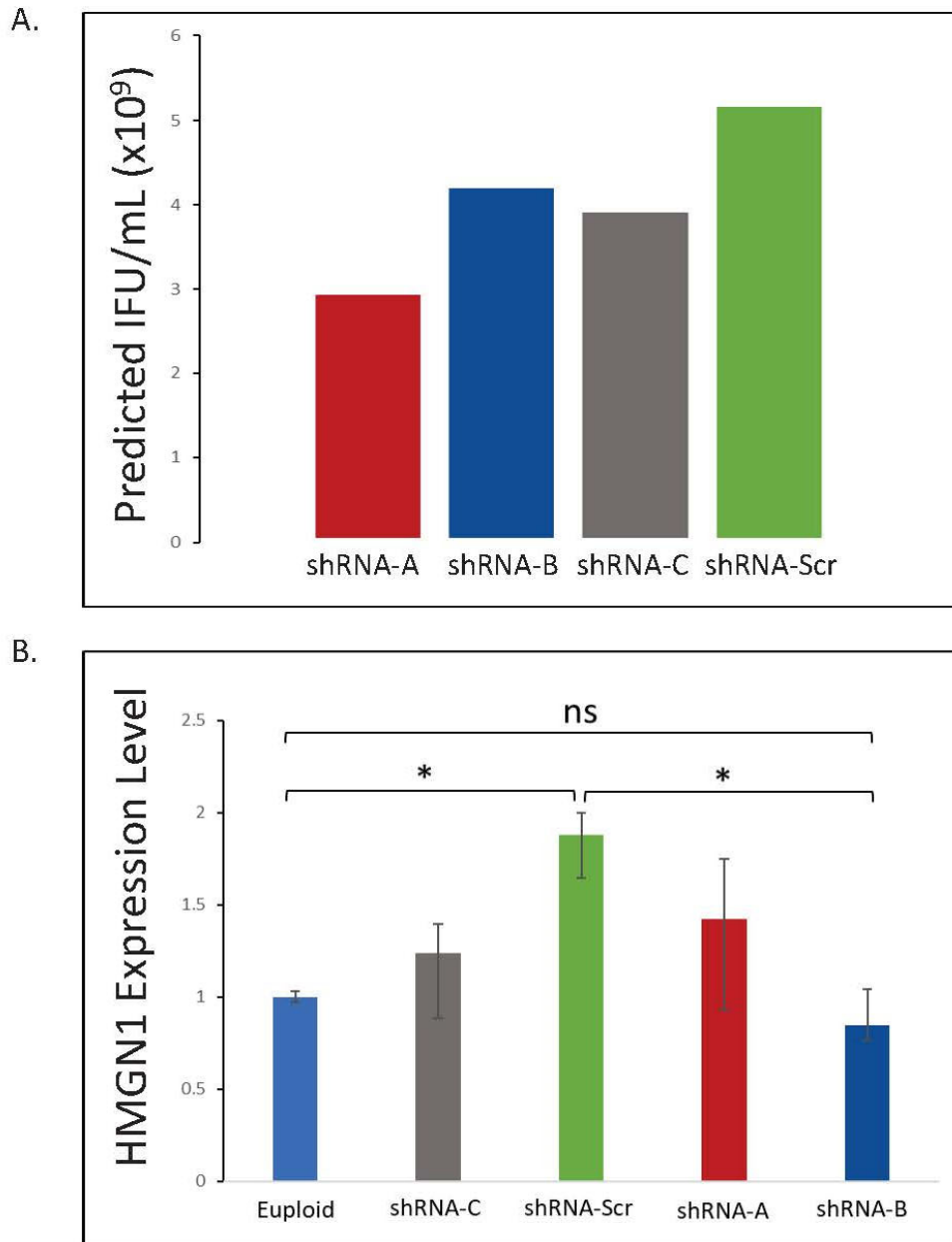


Figure 7: ELISA results and determining level of HMGN1 knock-down with various shRNA constructs. **A.** The results of an ELISA experiment to determine the predicted viral titer produced in HEK293 cells transfected with each of the different *HMGN1* shRNA constructs. **B.** The results of a qRT-PCR experiment to measure the relative expression level of *HMGN1* using cDNA created from mRNA extracted from NPCs transduced with each of the various *HMGN1* shRNA constructs, as well as euploid (control) NPCs. The results were analyzed using $\Delta\Delta CT$ method and GAPDH and UBC were used as house-keeping genes. Error bars represent standard error. * $p < 0.05$.

Using qRT-PCR to determine the effect of HMGNI silencing on the expression levels of select PRC2 target genes in trisomic NPCs. No cell selection was performed.

A qRT-PCR experiment was conducted to determine the relative gene expression levels of various previously demonstrated PRC2 targets (Adams & Cory, 2007; Kamminga et al., 2006; Mikkelsen et al., 2008; Rouillard et al., 2016) and upregulated in trisomic cells in our previous data sets. If we find that these genes are upregulated in trisomy and are downregulated by the *HMGNI* shRNA, it will signify the causative relationship between the gene dosage effect of HMGNI and the upregulation of these genes. To identify whether the expression level of these target genes would be altered after introducing *HMGNI* shRNA, we transduced trisomic NPCs with lentiviral particles carrying *HMGNI* shRNA-B. Similarly as before, cells used in this experiment included both NPCs that had taken up the construct and those that had not, as it was impossible to isolate the NPCs carrying the constructs because of the high toxicity of the antibiotics.

The results of the qRT-PCR experiment revealed differences in expression levels for several genes which have been identified as targets of PRC2 and are differentially expressed in trisomy 21 (Adams & Cory, 2007; Kamminga et al., 2006; Mikkelsen et al., 2008; Rouillard et al., 2016)(**Fig. 8**). The genes tested were Coiled-Coil-helix-coiled-coil-helix Domain Containing 2 (*CHCHD2*), Insulin-like growth factor binding protein 3 (*IGFBP3*), Paternally expressed 10 (*PEG10*), Sonic hedgehog (*SHH*), Proprotein convertase subtilisin/kexin type 1 inhibitor (*PCSKIN*), Cell-adhesion molecule 1 (*CHL1*), and Amyloid Beta precursor protein (*APP*).The protein product of gene *PCSKIN*, is involved in neuropeptide cleavage (Y. Feng et al., 2002; Hoshino et al., 2014) and has been

associated with NFTs and AD pathology (Wada et al., 2004). PCSKIN is involved in axon guidance (F. Wei et al., 2014) and neuronal migration (C. Li et al., 2016). The levels of *PCSKIN* were significantly different between euploid and both shRNA-Scr and shRNA-B. For *PEG10*, overexpression of which has been shown to inhibit neural migration (Pandya et al., 2021), there were significant differences in expression between euploid and both shRNA-Scr and shRNA-B, as well as between shRNA-Scr and shRNA-B. *CHLI* has been implicated in intellectual disability (C. Li et al., 2016) and is therefore important to study in the context of DS. Our results revealed a significant decrease in expression level in the NPCs carrying the shRNA-B construct as compared to shRNA-Scr.

As a powerful morphogen, *SHH* plays a significant role in the development of the ventral neural tube, as well as the production of different cell types (Cai et al., 2005; Fogarty et al., 2005; Kessaris et al., 2006). The levels of *SHH* were below the detection threshold in the euploid cells (CT value above 40 is not detected by our instrument), and thus it was impossible to determine a p-value. The differences in the expression between shRNA-Scr and shRNA-B did not reach statistical significance, (p-value=0.068), but showed a trend towards the decrease in mRNA for *SHH* with the ‘B’ construct as compared to ‘scramble’.

The prevalence of AD pathology in DS is often attributed to the increase in APP production and A β plaques secondary to the triplication of the *APP* gene. The expression levels for both *APP*, an A β paternal protein were significantly different between euploid and both shRNA-Scr and shRNA-B, and between shRNA-Scr and shRNA-B. Similar dynamic was observed for *CHCHD2* that is involved in cell migration (Y. Wei et al., 2015),

maintaining homeostasis in mitochondria (W. Liu et al., 2020), and the differentiation process of neuroectoderm (Che et al., 2018; Zhu et al., 2016). *IGFBP3* was shown to be involved in apoptosis and controlling cellular proliferation (Butt et al., 2000). There were significant differences found between expression levels of euploid and both shRNA-Scr and shRNA-B for *IGFBP3*. Importantly, there was no significant difference in the level of expression of *HMGNI* between euploid and shRNA-B, but there was significantly higher expression in the NPCs carrying the shRNA-Scr construct, indicating a reduction in expression comparable to euploid using shRNA-B.

The genes tested are implicated in various functions including but not limited to cell differentiation, morphogenesis, regulation of apoptosis, cell migration, cell adhesion, axon guidance, and transcriptional regulation. *HMGNI* was also tested to ensure the level of expression was indeed comparable to euploid levels. Taken together, this data implicates *HMGNI* in regulating genes involved in normal neuronal development.

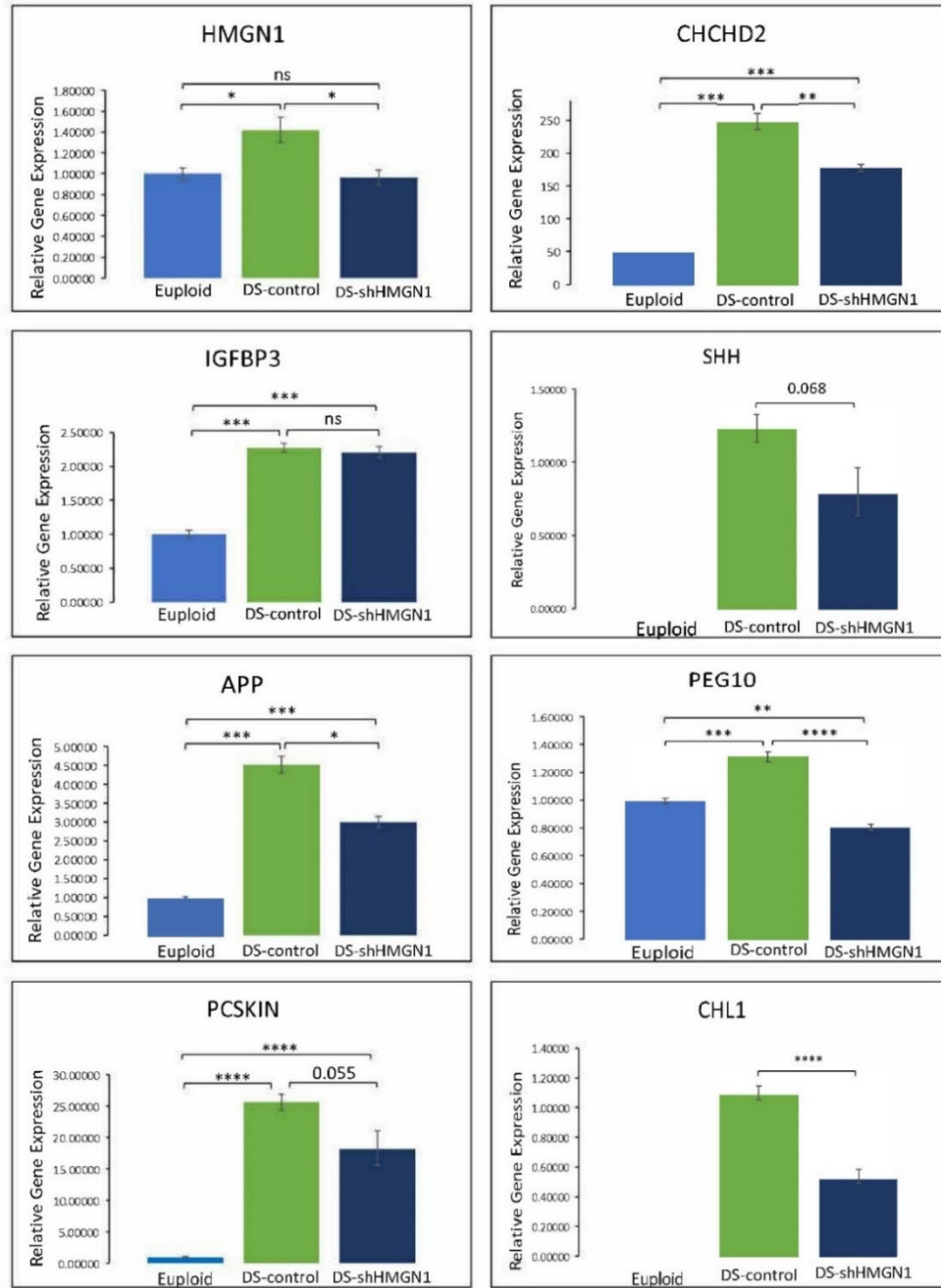


Figure 8: Results of qRT-PCR experiments to determine relative gene expression levels of select PRC2 target genes and genes differentially expressed in DS in euploid NPCs and NPCs transfected with the HMGN1 shRNA constructs 'scramble' (DS-control) and 'B' (DS-shRNA-HMGN1). The results of the qRT-PCR experiment were performed to measure relative expression level of select PRC2 target genes and genes known to be differentially expressed in DS, including *HMGN1*. The results were analyzed using $\Delta\Delta CT$ method and GAPDH and UBC were used as house-keeping genes. Error bars represent standard error. * $p < 0.05$; ** $p < 0.01$; *** $p < 0.001$; **** $p < 0.0001$.

Measuring gene expression levels post-FACS sorting to determine the effect of HMGN1 silencing on the expression levels of select PRC2 target genes in trisomic NPCs.

Another qRT-PCR experiment was run after FACS sorting, during which we were able to isolate the NPCs based on the expression of GFP (**Fig. 9**). Despite a low number of cells after FACS sorting (less than 100,000 per condition), we were able to detect all genes except *CHL1*, which was also not detected in unsorted NPCs. The experimental groups for this experiment included euploid NPCs, trisomic NPCs, those carrying the shRNA-scramble construct, and those carrying the shRNA-B construct. The aim of this experiment was to more accurately measure the impact of the shRNA on gene expression levels as compared to the previously described experiments that still included NPCs that had not integrated the constructs.

Since the isolation of the transduced cells gave a more reliable readout, we expanded our studies and evaluated more PRC2 target genes, including *HES1*, *ID2*, and *XIST*. *HES1* is a downstream target of the Notch signaling pathway and involved in the timing of neurogenesis (Hatakeyama et al., 2004; Nye et al., 1994). Overexpression of *ID2* is implicated in the halting of the process of oligodendrocyte differentiation (S. Wang et al., 2001). *XIST* is a long noncoding RNA involved in the silencing of the inactive X-chromosome (Brown et al., 1992) and has been shown to be highly dysregulated in AD (Fernandez-Martinez et al., 2009). There were also three genes originally evaluated that were not included in further qRT-PCR testing. For HMGN1, this was due to already having determined the normalization of its expression to close to euploid levels and not feeling

testing it further would be of use since we were looking at its effect on other gene's expression levels. For IGFBP3 and SHH, we found that the level of expression was not significantly reduced in the NPCs carrying the HMGN1 shRNA construct. This could mean that HMGN1 overexpression does not necessarily lead to their dysregulation in trisomy, since its correction did not normalize expression. Thus, their misexpression in DS might be not a direct consequence of HMGN1 overexpression.

For both *APP* and *CHCHD2*, there were significant differences in expression level between euploid and trisomic, euploid and shRNA-B, and trisomic and shRNA-B. *HES1* and *ID2* both demonstrated significant differences in expression between euploid and trisomic, and trisomic and shRNA-B. For *PEG10*, there was significance found between the levels of expression for euploid and trisomic, and euploid and shRNA-B. For *CHLI*, there was only a significant difference between the expression in trisomic NPCs and those with shRNA-B. *PCSKIN* had significant differences in expression between euploid and both trisomic and shRNA-B, and also between trisomic and shRNA-B. *XIST* also showed significant differences in expression between euploid and both trisomic and shRNA-B, and between trisomic and shRNA-B.

In summary, we were able to show statistically significant changes in the expression level of these PRC2 target genes after reducing the expression of *HMGN1*, indicating a causative role in the upregulation of expression of these target genes in trisomy 21.

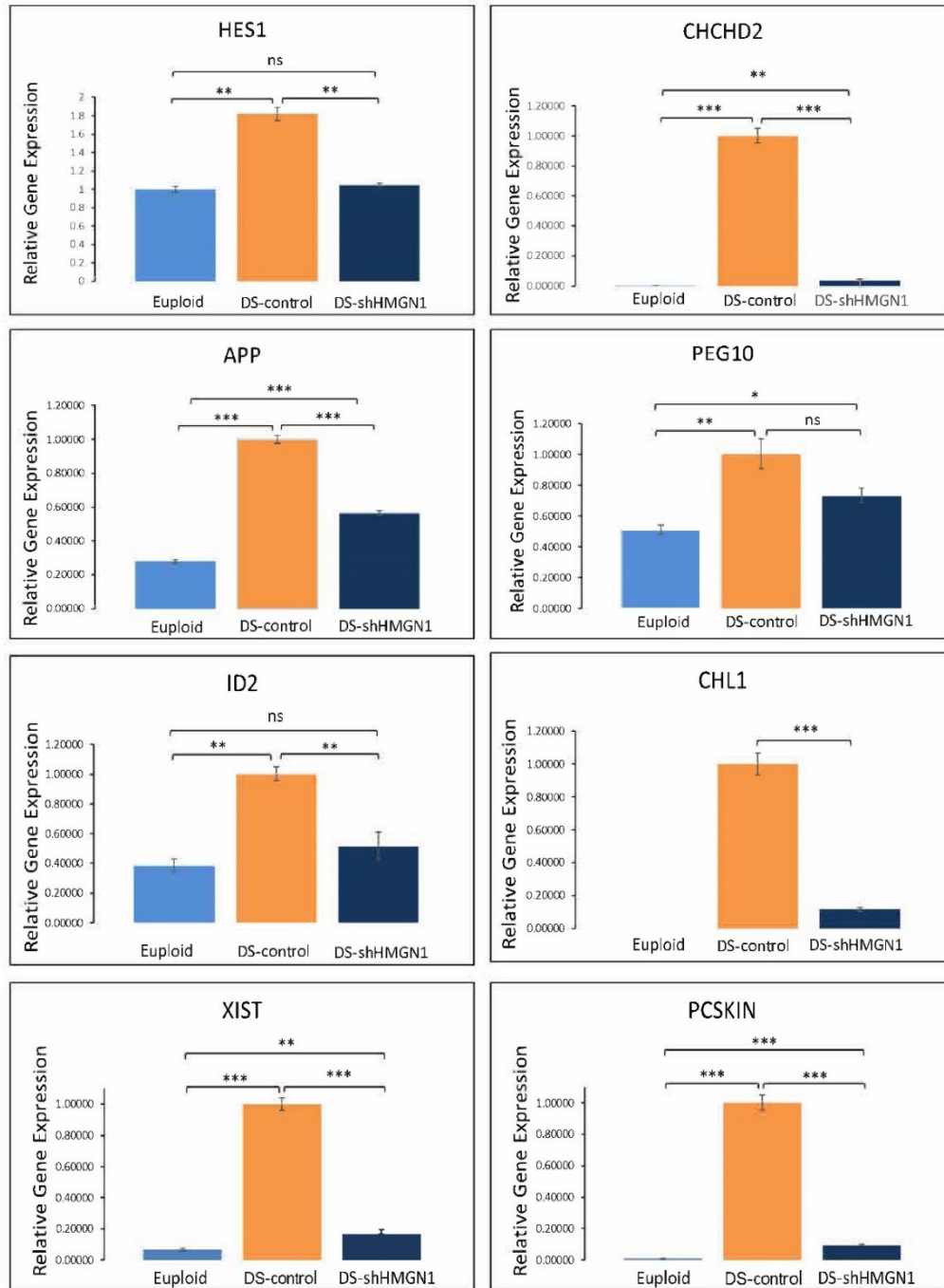


Figure 9: Results of qRT-PCR experiment after FACS sorting. Graphs showing the relative gene expression of select PRC2 target genes and genes known to be differentially expressed in DS after FACS sorting to isolate NPCs that successfully integrated plasmid containing *HMG1* shRNA construct B (DS-shRNAHMG1). The gene expression level was compared between euploid, trisomic (DS-control), and trisomic NPCs carrying the shRNA-B plasmid (DS-shRNAHMG1). The results were analyzed using $\Delta\Delta\text{CT}$ method and GAPDH and UBC were used as house-keeping genes. Error bars represent standard error. * $p < 0.05$; ** $p < 0.01$; *** $p < 0.001$.

DISCUSSION

The aim of this project was to attempt to connect the triplication of *HMGNI* in DS to dysregulation of gene expression levels in trisomic cells. Our working hypothesis was that increased levels of *HMGNI* in trisomy lead to increased levels of H3K27ac and decreased levels of H3K27me3, resulting in the de-repression of PRC2 target genes. We quantified the changes in H3K27 marks in trisomy 21 as a first attempt to link the overexpression of *HMGNI* to the development of DS phenotypes. Our main findings show significantly decreased levels of H3K27me3 in DS-derived cortical organoids and postmortem DS brain samples. Since H3K27me3 and H3K27ac are mutually exclusive we expected to also see an increase in the levels of this epigenetic mark. However, the inability to detect significant changes in H3K27ac may simply indicate that the mechanisms are more complicated and not solely governed by the overexpression of *HMGNI* or absence of H3K27me3 marks. , The correction in expression level for certain genes targeted by PRC2 by normalizing *HMGNI* expression does suggest a role in preventing the silencing action of PRC2 in DS.

We initially attempted to observe global changes induced by *HMGNI* by quantifying levels of H3K27ac and H3K27me3 in 130-day-old organoids, generated from 3 independent differentiation experiments. We observed a statistically significant decrease in H3K27me3, which is consistent with the hypothesis that this mark is decreased in DS due to the antagonism of the PRC2 complex by increased levels of HMGNI at the nucleosomes. Despite HMGNI's known association with H3K27ac we have not found a global increase in the H3K27ac mark, indicating that the relationship between this

epigenetic signature and HMGN1 may be more complex than the proposed antagonistic relationship with H3K27me2 marks. For example, H3K27 residue can be a target for another epigenetic modifier that will lead to interference with the acetylation of this residue after H3K27me3 mark is removed (Pan et al., 2018).

We also did not observe statistically significant differences in H3K27ac or H3K27me3 levels by assessing their expression in trisomic NPCs. This was disappointing since another study by Meharena et al. (Meharena et al., 2022) identified significant differences when comparing these marks in NPCs. Different differentiation protocols were used, but both should have resulted in NPCs of a similar age and stage of development (i.e. both would be PAX6 and SOX1 expressing). However, any variability in developmental stage, even in some of the NPC population, could have led to different results. Differences may also be a function of using different isogenic lines. Perhaps, increasing the sample size and including NPCs differentiated from multiple isogenic lines would produce different results and statistically significant changes. It would be beneficial to repeat the studies in NPC with more isogenic cell lines to determine if individual variation may be the reason for the lack of significant changes in the current study.

Next, we sought to quantify these marks in postmortem brain tissue (frontal cortex), as neither cell model could fully recapitulate the system dynamics at play in the human brain, since even organoids lack cellular heterogeneity present in brain tissue (for example multiple subtypes of neurons and microglia). In addition, the human brain more faithfully recapitulates the accumulation of epigenetic and transcriptomic age-related changes. Previous studies have measured H3K27ac and H3K27me3 in human DS and human AD

brain tissue separately (Nativio et al., 2020; Persico et al., 2022), but the quantification of these marks in human DS-AD brain tissue has not been attempted before.

In post-mortem tissue from the entorhinal cortex of individuals with AD, researchers have found an increase in H3K27me3 signal intensity as compared to controls (Persico et al., 2022). H3K27ac levels have also been quantified in human entorhinal cortex from those with AD, but the results were much more variable, with both hypo- and hyper-acetylation found in different areas. However, the areas with the greatest differential expression of H3K27ac were identified as being near genes known to be involved with AD pathology, such as *APP* (Marzi et al., 2018). These findings, along with the differences in H3K27ac and H3K27me3 found in trisomic NPCs (Meharena et al., 2022), reveal epigenetic changes present in both DS and AD and informed our decision to perform this novel experiment. Despite a small sample size (n=3-4), we identified an almost significant decrease in levels of H3K27me3 between those with DS-AD and both age-matched controls and individuals with only AD, indicating a difference in DS-AD tissue with broad-ranging consequences on gene expression that has not been documented before. With known alterations to the epigenome in both DS and AD, our novel results support a complex system where the changes in each condition may affect each other in dynamic ways that have not been studied before, with the overexpression of *HMGNI* in DS possibly playing a role in this dysregulation. The encouraging results we saw when comparing H3K27me3 in human brain tissue and organoids supported the establishment of a causative connection between *HMGNI* overexpression and differentially expressed PRC2 target

genes in DS cells that were identified in our previous transcriptomic studies in trisomic NPCs and organoids (Klein et al., 2022; Z. Li et al., n.d.).

Using *HMGNI* shRNA, we were indeed able to reduce the expression of a number of genes identified as PRC2 targets, including *CHCHD2*, *IGFBP3*, *SHH*, *XIST*, *HES1*, *ID2*, *CHLI*, *APP*, and *PEG10* (Adams & Cory, 2007; Kamminga et al., 2006; Mikkelsen et al., 2008; Rouillard et al., 2016). These results demonstrate that *HMGNI* is at least partly responsible for the increase found in trisomy. These genes are implicated in morphogenesis, neurogenesis, neuronal migration, cell death and viability and more, making them particularly relevant to the transcriptomic and phenotypic dysregulation seen in DS brain cells.

CHCHD2 is involved in cell migration (Y. Wei et al., 2015), maintaining homeostasis in mitochondria (W. Liu et al., 2020), and the differentiation process of neuroectoderm (Che et al., 2018; Zhu et al., 2016). Alterations in normal cell migration have been noted in both human DS brain tissue and mouse models of DS (Aldridge et al., 2007; Chakrabarti et al., 2007; Guidi et al., 2011), and the upregulation of this gene in trisomy 21 may contribute to the mechanism through which this occurs.

PEG10 has also been shown to play a role in neuronal migration during brain development, with overexpression inhibiting the appropriate neuronal migration to the cortical plate (Pandya et al., 2021). Its importance in neurodevelopment is highlighted by its expression levels peaking during normal fetal development (Miller et al., 2014). In line with this, decreased cortical plate volume has been documented in DS as early as 28 gestational weeks (Tarui et al., 2020). The overexpression of *PEG10* found in trisomic

NPCs could point to a mechanism for the disruption of the process of adequate neuronal migration critical for proper cortical development contributing further to the intellectual disability found in DS.

CHLI is another gene involved in neuronal migration as well as in axon guidance and cell adhesion (F. Wei et al., 2014), and synaptic plasticity (C. Li et al., 2016). It is involved in cognitive functioning, with multiple case studies implicating its duplication in intellectual disability (C. Li et al., 2016). Since this gene is increased in trisomy without being triplicated, and its potential link to cognitive deficits, it was important to look at the impact of *HMGNI* on the expression of *CHLI*, and assess whether its expression may be increased in DS due to the dysregulation of PRC2 activity.

SHH-mediated pathways are important in morphogenesis and spatial patterning of the cells in the neural tube. It has been implicated in the ventralization of the neural tube, and the generation of OPCs and inhibitory neurons (Cai et al., 2005; Fogarty et al., 2005; Kessaris et al., 2006). Considering the well-known deficits in myelinating oligodendrocytes found in DS and the dysregulation of this pathway in trisomy, it was important to include this gene in the study as one of the targets of PRC2 (Kamminga et al., 2006; Mikkelsen et al., 2008). Inhibitory/excitatory neuron imbalance can be also attributed to the abnormal activation of *SHH* and aberrant ventralization patterning. Our previous study showed an abnormal expression of *SHH* target genes in DS-derived iPS lines (Klein et al., 2022). Furthermore, correcting the *SHH* dysregulation in the same isogenic line, used in the current study, led to a correction in the expression of two important transcription factors needed for the differentiation of NPCs into OPCs, *Olig2* and *NKX2.2*. NPCs

induced to adopt a rostral-brain like fate showed a reduced response to *SHH* signaling and changes in the level of *Olig2* and *NKX2.2* expression, but modulation of the response using an SHH agonist normalized the level of expression of both transcription factors, indicating an important role of *SHH* in the development of OPCs. Interestingly, response to *SHH* signaling was location-dependent, with ventrally derived NPCs showing normal levels of response to *SHH* signaling as compared to the rostrally derived NPCs and indicates the need for the ability to selectively correct *SHH* expression.

HES1 is an essential component of the Notch signaling pathway, which is known to be dysregulated in DS (Fischer, 2005). Playing a critical role in the timing of neural stem cell differentiation, changes in *HES1* expression can lead to disorganization of the neural tube and improper timing of neurogenesis in favor of gliogenesis (Hatakeyama et al., 2004; Nye et al., 1994). This upregulation of *HES1* has been previously attributed to the cross-talk of *Notch1* and *APP* (Fischer, 2005), as well as through a different mechanism of regulation involving the SHH pathway (Ingram et al., 2008).

We also identified several genes related to more neurodegenerative phenotypes. *IGFBP3* is known to be involved in anti-proliferative and pro-apoptotic pathways through the modulation of proteins associated with apoptotic processes, such as Bax, Bad, and Bcl-2 (Butt et al., 2000). Evidence for dysregulation of these proteins, including elevated levels of Bax and decreased Bcl-2 levels, have been identified in the DS brain (Seidl et al., 2001). Increased rates of apoptosis have been identified in certain regions of the human DS brain, as well as in animal and cellular models of DS. This includes the cerebral cortex (Seidl et al., 2001; Takashima et al., 1989), hippocampus (Guidi et al., 2007), cerebellum (Seidl et

al., 2001), NPCs derived from DS iPSCs (Hibaoui et al., 2014), and cortical spheroids (Z. Li et al., n.d.). For this reason, identifying the upregulation of *IGFBP3* in trisomy and the subsequent decrease in expression level with the knockdown of *HMGNI* provides a causative mechanism through which increased apoptosis could be induced in DS and lead to hypocellularity.

PCSKIN encodes the protein Proprotein convertase subtilisin/kexin type 1 inhibitor (proSAAS), which is involved in the neuroendocrine signaling pathway and peptide cleavage (Y. Feng et al., 2002; Hoshino et al., 2014). ProSAAS immunoreactivity with NFTs in patients with AD has been established (Wada et al., 2004), though the precise relationship between the two is still unclear. Its mRNA has been found in many types of differentiating neurons and it is widely expressed during development (Morgan et al., 2005). It is possible that the overexpression of *PCSKIN* in trisomy may play a role in the tauopathy and AD pathology common in DS.

ID2 is implicated in the inhibition of oligodendrocyte differentiation. Its overexpression is known to prevent the differentiation of OPCs into oligodendrocytes, while its absence can lead to the premature differentiation of OPCs (S. Wang et al., 2001). It is normally located in the nucleus but translocates to the cytoplasm before the process of differentiation begins. While not necessary for this process to occur, it appears that *ID2* slows and controls the rate of differentiation. The finding of *ID2* overexpression in trisomic NPCs provides another possible mechanism for the decreased levels of oligodendrocytes in DS and the imbalance between these glial cells and astrocytes.

XIST is expressed solely by the inactive X-chromosome and codes for a long noncoding RNA responsible for the silencing of this chromosome (Brown et al., 1992). It is known to carry out this function through recruitment of the EED and EZH2 subunits of the PRC2 complex and subsequent methylation of H3K27 (Plath et al., 2003). It is also known to be severely dysregulated in AD and has the highest level of overexpression in late onset AD (LOAD) (Fernández-Martínez et al., 2020). With the frequent comorbidity of AD pathology and DS, regulation of *XIST* expression via *HMGNI* provides additional support for our main hypothesis.

Taken together, these PRC2 target genes are all implicated in some aspects of neurodevelopment, cell-signaling, cell migration, cognition, or neurodegeneration and are also differentially expressed in DS. If *HMGNI* does indeed lead to the derepression of PRC2 target genes, the various DS phenotypes that could result from dysregulation of these pathways might be mediated by a common molecular event – the abnormal upregulation of *HMGNI*. Therefore, altering *HMGNI* levels may provide a therapeutic avenue for correcting the expression level of these genes in DS.

Additionally, we tested the gene *APP* which is known to be located on HSA21 and is often triplicated in DS. The near-universal development of AD pathology in DS is often attributed to this triplication and an increase in APP production and subsequent A β deposition (McCarron et al., 2014). Individuals with DS due to a segmental trisomy of HSA21 that does not include the *APP* gene have been reported to not have the same AD pathology common in DS, lending support to the role of *APP* overexpression in the presentation of the disease (Prasher et al., 1998). Although *APP* is not one of the

prototypical PRC2 target genes, but a study found a 1.9 fold change in *APP* expression after EZH2 knockdown, implicating it as a potential target of PRC2 (Nuytten et al., 2008). Since both *APP* and *HMGNI* are located on HSA21, we were interested in whether *HMGNI* overexpression may exacerbate the overexpression of *APP* even more. Furthermore, if overexpression of *APP* in DS does lead to AD pathology, could altering *HMGNI* expression mitigate some of this pathology? If so, normalization of *HMGNI* expression could prove even more important in correcting *APP* expression in DS. Indeed, our data showed that reducing the expression of *HMGNI* does mitigate the expression of *APP*, providing support for the hypothesis that its overexpression in DS may not be solely due to its triplication, and that by decreasing the expression of *HMGNI* we could decrease the effect of *APP* in DS and possibly resolve some AD-related pathology.

The results we obtained are novel and indicate future research in this area is important. It would also be helpful to carry out future analyses of H3K27ac and H3K27me3 in human brain tissue obtained from more individuals, in order to reach significance in the comparisons between control, DS-AD and AD. Furthermore, DS brain tissue devoid of AD pathology in future studies would add significantly to our understanding of the HMGNI-induced epigenetic modifications in DS. It would also be valuable to carry out further qRT-PCR experiments after *HMGNI* knock-down to causally link its level of expression with PRC2 target gene expression, but instead of lentiviral transduction it would be preferable to use CRISPR/Cas9. This is a more specific and targeted approach to eliminate one of the triplicated alleles and reduced expression levels of HMGNI to that of euploid in order to better understand the influence of its overexpression in DS. We may also avoid the issues

related to excessive cell death that occurred using lentivirus. Additionally, we would be able to cross-validate the data using an alternate approach since off-target effects can occur with both CRISPR/Cas9 and shRNA, but they will be different.

Normalizing HMGN1 expression, it would be interesting to conduct a genome-wide analysis of gene expression. Doing this would provide valuable information on whether all PRC2 target genes are impacted by this gene and reveal any global effects *HMGN1* might have. It would also provide valuable information on the level of influence HMGN1 has versus other genes triplicated in DS. Isolating the effect of HMGN1 on different cell types or determining specific deposition patterns would also be interesting and could help explain how certain DS phenotypes are produced. Results we did obtain that are close to significance are promising and call for further research into the role of *HMGN1* overexpression in DS. Studies focused on the functional outcomes of the correction of the PRC2 target genes (assessment of neuronal migration or apoptotic processes following the correction) should provide more evidence for the biological causality between the transcriptomic changes and DS-related phenotypes.

In sum, we found a significant decrease in H3K27me3 in an organoid-model of trisomy 21 and in human DS-AD tissue, a novel comparison that has not been documented before. We also demonstrated a causative effect of *HMGN1* overexpression on the expression level of various PRC2 target genes, including genes that are already triplicated in DS, such as *APP*. This research provides support for a possible antagonistic role of *HMGN1* in DS that leads to global changes to the epigenome and impacts the silencing of PRC2 target genes.

REFERENCES

- Aasen, T., Raya, A., Barrero, M. J., Garreta, E., Consiglio, A., Gonzalez, F., Vassena, R., Bilić, J., Pekarik, V., Tiscornia, G., Edel, M., Boué, S., & Izpisua Belmonte, J. C. (2008). Efficient and rapid generation of induced pluripotent stem cells from human keratinocytes. *Nature Biotechnology*, 26(11), 1276–1284. <https://doi.org/10.1038/nbt.1503>
- Ábrahám, H., Vincze, A., Veszprémi, B., Kravják, A., Gömöri, É., Kovács, G. G., & Seress, L. (2012). Impaired myelination of the human hippocampal formation in Down syndrome. *International Journal of Developmental Neuroscience*, 30(2), 147–158. <https://doi.org/10.1016/j.ijdevneu.2011.11.005>
- Abuhatzira, L., Shamir, A., Schones, D. E., Schäffer, A. A., & Bustin, M. (2011). The Chromatin-binding Protein HMG1 Regulates the Expression of Methyl CpG-binding Protein 2 (MECP2) and Affects the Behavior of Mice. *Journal of Biological Chemistry*, 286(49), 42051–42062. <https://doi.org/10.1074/jbc.M111.300541>
- Adams, J. M., & Cory, S. (2007). The Bcl-2 apoptotic switch in cancer development and therapy. *Oncogene*, 26(9), 1324–1337. <https://doi.org/10.1038/sj.onc.1210220>
- Ahn, E.-Y., DeKelver, R. C., Lo, M.-C., Nguyen, T. A., Matsuura, S., Boyapati, A., Pandit, S., Fu, X.-D., & Zhang, D.-E. (2011). SON Controls Cell-Cycle Progression by Coordinated Regulation of RNA Splicing. *Molecular Cell*, 42(2), 185–198. <https://doi.org/10.1016/j.molcel.2011.03.014>
- Ahn, E.-Y., Yan, M., Malakhova, O. A., Lo, M.-C., Boyapati, A., Ommen, H. B., Hines, R., Hokland, P., & Zhang, D.-E. (2008). Disruption of the NHR4 domain structure in AML1-ETO abrogates SON binding and promotes leukemogenesis. *Proceedings of the National Academy of Sciences of the United States of America*, 105(44), 17103–17108. <https://doi.org/10.1073/pnas.0802696105>
- Aït Yahya-Graison, E., Aubert, J., Dauphinot, L., Rivals, I., Prieur, M., Golfier, G., Rossier, J., Personnaz, L., Creau, N., Bléhaut, H., Robin, S., Delabar, J. M., & Potier, M.-C. (2007). Classification of human chromosome 21 gene-expression variations in Down syndrome: Impact on disease phenotypes. *American Journal of Human Genetics*, 81(3), 475–491. <https://doi.org/10.1086/520000>
- Aldridge, K., Reeves, R. H., Olson, L. E., & Richtsmeier, J. T. (2007). Differential effects of trisomy on brain shape and volume in related aneuploid mouse models. *American Journal of Medical Genetics. Part A*, 143A(10), 1060–1070. <https://doi.org/10.1002/ajmg.a.31721>
- Alfonso, P. J., Crippa, M. P., Hayes, J. J., & Bustin, M. (1994). The Footprint of Chromosomal Proteins HMG-14 and HMG-17 on Chromatin Subunits. *Journal of Molecular Biology*, 236(1), 189–198. <https://doi.org/10.1006/jmbi.1994.1128>

Alić, I., Goh, P. A., Murray, A., Portelius, E., Gkanatsiou, E., Gough, G., Mok, K. Y., Koschut, D., Brunmeir, R., Yeap, Y. J., O'Brien, N. L., Groet, J., Shao, X., Havlicek, S., Dunn, N. R., Kvaratsberg, H., Brinkmalm, G., Hithersay, R., Startin, C., ... Nižetić, D. (2021). Patient-specific Alzheimer-like pathology in trisomy 21 cerebral organoids reveals BACE2 as a gene dose-sensitive AD suppressor in human brain. *Molecular Psychiatry*, 26(10), 5766–5788. <https://doi.org/10.1038/s41380-020-0806-5>

Amiri, A., Coppola, G., Scuderi, S., Wu, F., Roychowdhury, T., Liu, F., Pochareddy, S., Shin, Y., Safi, A., Song, L., Zhu, Y., Sousa, A. M. M., PsychENCODE Consortium, Gerstein, M., Crawford, G. E., Sestan, N., Abyzov, A., & Vaccarino, F. M. (2018). Transcriptome and epigenome landscape of human cortical development modeled in organoids. *Science (New York, N.Y.)*, 362(6420), eaat6720. <https://doi.org/10.1126/science.aat6720>

Anchan, R. M., Quaas, P., Gerami-Naini, B., Bartake, H., Griffin, A., Zhou, Y., Day, D., Eaton, J. L., George, L. L., Naber, C., Turbe-Doan, A., Park, P. J., Hornstein, M. D., & Maas, R. L. (2011). Amniocytes can serve a dual function as a source of iPS cells and feeder layers. *Human Molecular Genetics*, 20(5), 962–974. <https://doi.org/10.1093/hmg/ddq542>

Arnold, S. E., Hyman, B. T., Flory, J., Damasio, A. R., & Van Hoesen, G. W. (1991). The topographical and neuroanatomical distribution of neurofibrillary tangles and neuritic plaques in the cerebral cortex of patients with Alzheimer's disease. *Cerebral Cortex (New York, N.Y.: 1991)*, 1(1), 103–116. <https://doi.org/10.1093/cercor/1.1.103>

Aylward, E. H., Li, Q., Honeycutt, N. A., Warren, A. C., Pulsifer, M. B., Barta, P. E., Chan, M. D., Smith, P. D., Jerram, M., & Pearlson, G. D. (1999). MRI Volumes of the Hippocampus and Amygdala in Adults With Down's Syndrome With and Without Dementia. *American Journal of Psychiatry*, 156(4), 564–568. <https://doi.org/10.1176/ajp.156.4.564>

Baburamani, A. A., Patkee, P. A., Arichi, T., & Rutherford, M. A. (2019). New approaches to studying early brain development in Down syndrome. *Developmental Medicine & Child Neurology*, 61(8), 867–879. <https://doi.org/10.1111/dmcn.14260>

Bakshi, R., Hassan, M. Q., Pratap, J., Lian, J. B., Montecino, M. A., van Wijnen, A. J., Stein, J. L., Imbalzano, A. N., & Stein, G. S. (2010). The human SWI/SNF complex associates with RUNX1 to control transcription of hematopoietic target genes. *Journal of Cellular Physiology*, 225(2), 569–576. <https://doi.org/10.1002/jcp.22240>

Becker, L. E., Armstrong, D. L., & Chan, F. (1986). Dendritic atrophy in children with Down's syndrome. *Annals of Neurology*, 20(4), 520–526. <https://doi.org/10.1002/ana.410200413>

- Becker, W., & Joost, H.-G. (1998). Structural and Functional Characteristics of Dyrk, a Novel Subfamily of Protein Kinases with Dual Specificity. In *Progress in Nucleic Acid Research and Molecular Biology* (Vol. 62, pp. 1–17). Elsevier.
[https://doi.org/10.1016/S0079-6603\(08\)60503-6](https://doi.org/10.1016/S0079-6603(08)60503-6)
- Belichenko, N. P., Belichenko, P. V., Kleschevnikov, A. M., Salehi, A., Reeves, R. H., & Mobley, W. C. (2009). The “Down Syndrome Critical Region” Is Sufficient in the Mouse Model to Confer Behavioral, Neurophysiological, and Synaptic Phenotypes Characteristic of Down Syndrome. *Journal of Neuroscience*, 29(18), 5938–5948.
<https://doi.org/10.1523/JNEUROSCI.1547-09.2009>
- Berdichevskii, F. B., Chumakov, I. M., & Kiselev, L. L. (1988). [Decoding of the primary structure of the son3 region in human genome: Identification of a new protein with unusual structure and homology with DNA-binding proteins]. *Molekuliarnaia Biologiia*, 22(3), 794–801.
- Bhattacharyya, A., McMillan, E., Chen, S. I., Wallace, K., & Svendsen, C. N. (2009). A critical period in cortical interneuron neurogenesis in down syndrome revealed by human neural progenitor cells. *Developmental Neuroscience*, 31(6), 497–510.
<https://doi.org/10.1159/000236899>
- Bowers, S. R., Calero-Nieto, F. J., Valeaux, S., Fernandez-Fuentes, N., & Cockerill, P. N. (2010). Runx1 binds as a dimeric complex to overlapping Runx1 sites within a palindromic element in the human GM-CSF enhancer. *Nucleic Acids Research*, 38(18), 6124–6134. <https://doi.org/10.1093/nar/gkq356>
- Brown, C. J., Hendrich, B. D., Rupert, J. L., Lafrenière, R. G., Xing, Y., Lawrence, J., & Willard, H. F. (1992). The human XIST gene: Analysis of a 17 kb inactive X-specific RNA that contains conserved repeats and is highly localized within the nucleus. *Cell*, 71(3), 527–542. [https://doi.org/10.1016/0092-8674\(92\)90520-m](https://doi.org/10.1016/0092-8674(92)90520-m)
- Buontempo, S., Laise, P., Hughes, J. M., Trattaro, S., Das, V., Rencurel, C., & Testa, G. (2022). EZH2-Mediated H3K27me3 Targets Transcriptional Circuits of Neuronal Differentiation. *Frontiers in Neuroscience*, 16, 814144.
<https://doi.org/10.3389/fnins.2022.814144>
- Butt, A. J., Firth, S. M., King, M. A., & Baxter, R. C. (2000). Insulin-like growth factor-binding protein-3 modulates expression of Bax and Bcl-2 and potentiates p53-independent radiation-induced apoptosis in human breast cancer cells. *The Journal of Biological Chemistry*, 275(50), 39174–39181. <https://doi.org/10.1074/jbc.M908888199>
- Cai, J., Qi, Y., Hu, X., Tan, M., Liu, Z., Zhang, J., Li, Q., Sander, M., & Qiu, M. (2005). Generation of oligodendrocyte precursor cells from mouse dorsal spinal cord independent of Nkx6 regulation and Shh signaling. *Neuron*, 45(1), 41–53.
<https://doi.org/10.1016/j.neuron.2004.12.028>

Canzonetta, C., Mulligan, C., Deutsch, S., Ruf, S., O'Doherty, A., Lyle, R., Borel, C., Lin-Marq, N., Delom, F., Groet, J., Schnappauf, F., De Vita, S., Averill, S., Priestley, J. V., Martin, J. E., Shipley, J., Denyer, G., Epstein, C. J., Fillat, C., ... Nizetic, D. (2008). DYRK1A-dosage imbalance perturbs NRSF/REST levels, deregulating pluripotency and embryonic stem cell fate in Down syndrome. *American Journal of Human Genetics*, 83(3), 388–400. <https://doi.org/10.1016/j.ajhg.2008.08.012>

Catez, F., Brown, D. T., Misteli, T., & Bustin, M. (2002). Competition between histone H1 and HMGN proteins for chromatin binding sites. *EMBO Reports*, 3(8), 760–766. <https://doi.org/10.1093/embo-reports/kvf156>

Catez, F., Yang, H., Tracey, K. J., Reeves, R., Misteli, T., & Bustin, M. (2004). Network of dynamic interactions between histone H1 and high-mobility-group proteins in chromatin. *Molecular and Cellular Biology*, 24(10), 4321–4328. <https://doi.org/10.1128/MCB.24.10.4321-4328.2004>

Centers for Disease Control and Prevention (CDC). (2006). Improved national prevalence estimates for 18 selected major birth defects—United States, 1999-2001. *MMWR. Morbidity and Mortality Weekly Report*, 54(51), 1301–1305.

Cetin, Z., Yakut, S., Mihci, E., Manguoglu, A. E., Berker, S., Keser, I., & Luleci, G. (2012). A patient with Down syndrome with a de novo derivative chromosome 21. *Gene*, 507(2), 159–164. <https://doi.org/10.1016/j.gene.2012.07.018>

Chakrabarti, L., Galdzicki, Z., & Haydar, T. F. (2007). Defects in Embryonic Neurogenesis and Initial Synapse Formation in the Forebrain of the Ts65Dn Mouse Model of Down Syndrome. *Journal of Neuroscience*, 27(43), 11483–11495. <https://doi.org/10.1523/JNEUROSCI.3406-07.2007>

Chambers, S. M., Fasano, C. A., Papapetrou, E. P., Tomishima, M., Sadelain, M., & Studer, L. (2009). Highly efficient neural conversion of human ES and iPS cells by dual inhibition of SMAD signaling. *Nature Biotechnology*, 27(3), 275–280. <https://doi.org/10.1038/nbt.1529>

Che, X.-Q., Zhao, Q.-H., Huang, Y., Li, X., Ren, R.-J., Chen, S.-D., Guo, Q.-H., & Wang, G. (2018). Mutation Screening of the CHCHD2 Gene for Alzheimer's Disease and Frontotemporal Dementia in Chinese Mainland Population. *Journal of Alzheimer's Disease*, 61(4), 1283–1288. <https://doi.org/10.3233/JAD-170692>

Chédin, F., Lieber, M. R., & Hsieh, C.-L. (2002). The DNA methyltransferase-like protein DNMT3L stimulates de novo methylation by Dnmt3a. *Proceedings of the National Academy of Sciences of the United States of America*, 99(26), 16916–16921. <https://doi.org/10.1073/pnas.262443999>

- Cherukuri, S., Hock, R., Ueda, T., Catez, F., Rochman, M., & Bustin, M. (2008). Cell Cycle-dependent Binding of HMGN Proteins to Chromatin. *Molecular Biology of the Cell*, 19(5), 1816–1824. <https://doi.org/10.1091/mbc.e07-10-1018>
- Clark, D. J., & Kimura, T. (1990). Electrostatic mechanism of chromatin folding. *Journal of Molecular Biology*, 211(4), 883–896. [https://doi.org/10.1016/0022-2836\(90\)90081-V](https://doi.org/10.1016/0022-2836(90)90081-V)
- Contestabile, A., Fila, T., Ceccarelli, C., Bonasoni, P., Bonapace, L., Santini, D., Bartesaghi, R., & Ciani, E. (2007). Cell cycle alteration and decreased cell proliferation in the hippocampal dentate gyrus and in the neocortical germinal matrix of fetuses with down syndrome and in Ts65Dn mice. *Hippocampus*, 17(8), 665–678. <https://doi.org/10.1002/hipo.20308>
- Cruchaga, C., Chakraverty, S., Mayo, K., Vallania, F. L. M., Mitra, R. D., Faber, K., Williamson, J., Bird, T., Diaz-Arrastia, R., Foroud, T. M., Boeve, B. F., Graff-Radford, N. R., St. Jean, P., Lawson, M., Ehm, M. G., Mayeux, R., Goate, A. M., & for the NIA-LOAD/NCRAD Family Study Consortium. (2012). Rare Variants in APP, PSEN1 and PSEN2 Increase Risk for AD in Late-Onset Alzheimer’s Disease Families. *PLoS ONE*, 7(2), e31039. <https://doi.org/10.1371/journal.pone.0031039>
- Cuddapah, S., Schones, D. E., Cui, K., Roh, T.-Y., Barski, A., Wei, G., Rochman, M., Bustin, M., & Zhao, K. (2011). Genomic Profiling of HMGN1 Reveals an Association with Chromatin at Regulatory Regions. *Molecular and Cellular Biology*, 31(4), 700–709. <https://doi.org/10.1128/MCB.00740-10>
- Cutter, A. R., & Hayes, J. J. (2015). A brief review of nucleosome structure. *FEBS Letters*, 589(20PartA), 2914–2922. <https://doi.org/10.1016/j.febslet.2015.05.016>
- De Strooper, B., Saftig, P., Craessaerts, K., Vanderstichele, H., Guhde, G., Annaert, W., Von Figura, K., & Van Leuven, F. (1998). Deficiency of presenilin-1 inhibits the normal cleavage of amyloid precursor protein. *Nature*, 391(6665), 387–390. <https://doi.org/10.1038/34910>
- Deng, T., Postnikov, Y., Zhang, S., Garrett, L., Becker, L., Rácz, I., Höltner, S. M., Wurst, W., Fuchs, H., Gailus-Durner, V., de Angelis, M. H., & Bustin, M. (2017). Interplay between H1 and HMGN epigenetically regulates OLIG1&2 expression and oligodendrocyte differentiation. *Nucleic Acids Research*, 45(6), 3031–3045. <https://doi.org/10.1093/nar/gkw1222>
- Deng, T., Zhu, Z. I., Zhang, S., Leng, F., Cherukuri, S., Hansen, L., Mariño-Ramírez, L., Meshorer, E., Landsman, D., & Bustin, M. (2013). HMGN1 modulates nucleosome occupancy and DNase I hypersensitivity at the CpG island promoters of embryonic stem cells. *Molecular and Cellular Biology*, 33(16), 3377–3389. <https://doi.org/10.1128/MCB.00435-13>

- DiMeglio, T., Kratochwil, C. F., Vilain, N., Loche, A., Vitobello, A., Yonehara, K., Hrycaj, S. M., Roska, B., Peters, A. H. F. M., Eichmann, A., Wellik, D., Ducret, S., & Rijli, F. M. (2013). Ezh2 orchestrates topographic migration and connectivity of mouse precerebellar neurons. *Science (New York, N.Y.)*, 339(6116), 204–207. <https://doi.org/10.1126/science.1229326>
- Douvaras, P., Rusielewicz, T., Kim, K., Haines, J., Casaccia, P., & Fossati, V. (2016). Epigenetic Modulation of Human Induced Pluripotent Stem Cell Differentiation to Oligodendrocytes. *International Journal of Molecular Sciences*, 17(4), 614. <https://doi.org/10.3390/ijms17040614>
- Eiraku, M., Watanabe, K., Matsuo-Takasaki, M., Kawada, M., Yonemura, S., Matsumura, M., Wataya, T., Nishiyama, A., Muguruma, K., & Sasai, Y. (2008). Self-organized formation of polarized cortical tissues from ESCs and its active manipulation by extrinsic signals. *Cell Stem Cell*, 3(5), 519–532. <https://doi.org/10.1016/j.stem.2008.09.002>
- Fan, Y., Nikitina, T., Zhao, J., Fleury, T. J., Bhattacharyya, R., Bouhassira, E. E., Stein, A., Woodcock, C. L., & Skoultchi, A. I. (2005). Histone H1 Depletion in Mammals Alters Global Chromatin Structure but Causes Specific Changes in Gene Regulation. *Cell*, 123(7), 1199–1212. <https://doi.org/10.1016/j.cell.2005.10.028>
- Farley, S. J., Grishok, A., & Zeldich, E. (2022). Shaking up the silence: Consequences of HMGN1 antagonizing PRC2 in the Down syndrome brain. *Epigenetics & Chromatin*, 15(1), 39. <https://doi.org/10.1186/s13072-022-00471-6>
- Feng, X., Juan, A. H., Wang, H. A., Ko, K. D., Zare, H., & Sartorelli, V. (2016). Polycomb Ezh2 controls the fate of GABAergic neurons in the embryonic cerebellum. *Development (Cambridge, England)*, 143(11), 1971–1980. <https://doi.org/10.1242/dev.132902>
- Feng, Y., Reznik, S. E., & Fricker, L. D. (2002). ProSAAS and prohormone convertase 1 are broadly expressed during mouse development. *Brain Research. Gene Expression Patterns*, 1(2), 135–140. [https://doi.org/10.1016/s1567-133x\(02\)00002-9](https://doi.org/10.1016/s1567-133x(02)00002-9)
- Fernández-Martínez, J. L., Álvarez-Machancoses, Ó., de Andrés-Galiana, E. J., Bea, G., & Kloczkowski, A. (2020). Robust Sampling of Defective Pathways in Alzheimer's Disease. Implications in Drug Repositioning. *International Journal of Molecular Sciences*, 21(10), 3594. <https://doi.org/10.3390/ijms21103594>
- Fernandez-Martinez, J., Vela, E. M., Tora-Ponsioen, M., Ocaña, O. H., Nieto, M. A., & Galceran, J. (2009). Attenuation of Notch signalling by the Down-syndrome-associated kinase DYRK1A. *Journal of Cell Science*, 122(Pt 10), 1574–1583. <https://doi.org/10.1242/jcs.044354>

Fischer, D. F. (2005). Activation of the Notch pathway in Down syndrome: Cross-talk of Notch and APP. *The FASEB Journal*, 19(11), 1451–1458. <https://doi.org/10.1096/fj.04-3395.com>

Fogarty, M., Richardson, W. D., & Kessaris, N. (2005). A subset of oligodendrocytes generated from radial glia in the dorsal spinal cord. *Development (Cambridge, England)*, 132(8), 1951–1959. <https://doi.org/10.1242/dev.01777>

Furukawa, T., Tanji, E., Kuboki, Y., Hatori, T., Yamamoto, M., Shimizu, K., Shibata, N., & Shiratori, K. (2012). Targeting of MAPK-associated molecules identifies SON as a prime target to attenuate the proliferation and tumorigenicity of pancreatic cancer cells. *Molecular Cancer*, 11(1), 88. <https://doi.org/10.1186/1476-4598-11-88>

Goate, A., Chartier-Harlin, M.-C., Mullan, M., Brown, J., Crawford, F., Fidani, L., Giuffra, L., Haynes, A., Irving, N., James, L., Mant, R., Newton, P., Rooke, K., Roques, P., Talbot, C., Pericak-Vance, M., Roses, A., Williamson, R., Rossor, M., ... Hardy, J. (1991). Segregation of a missense mutation in the amyloid precursor protein gene with familial Alzheimer's disease. *Nature*, 349(6311), 704–706. <https://doi.org/10.1038/349704a0>

Golden, J. A., & Hyman, B. T. (1994). Development of the superior temporal neocortex is anomalous in trisomy 21. *Journal of Neuropathology and Experimental Neurology*, 53(5), 513–520. <https://doi.org/10.1097/00005072-199409000-00011>

Gómez-Isla, T., Hollister, R., West, H., Mui, S., Growdon, J. H., Petersen, R. C., Parisi, J. E., & Hyman, B. T. (1997). Neuronal loss correlates with but exceeds neurofibrillary tangles in Alzheimer's disease. *Annals of Neurology*, 41(1), 17–24. <https://doi.org/10.1002/ana.410410106>

Goodwin, G. H., Shooter, K. V., & Johns, E. W. (1975). Interaction of a Non-Histone Chromatin Protein (High-Mobility Group Protein 2) with DNA. *European Journal of Biochemistry*, 54(2), 427–433. <https://doi.org/10.1111/j.1432-1033.1975.tb04153.x>

Götz, J., Chen, F., van Dorpe, J., & Nitsch, R. M. (2001). Formation of Neurofibrillary Tangles in P301L Tau Transgenic Mice Induced by A β 42 Fibrils. *Science*, 293(5534), 1491–1495. <https://doi.org/10.1126/science.1062097>

Gouras, G. K., Tsai, J., Naslund, J., Vincent, B., Edgar, M., Checler, F., Greenfield, J. P., Haroutunian, V., Buxbaum, J. D., Xu, H., Greengard, P., & Relkin, N. R. (2000). Intraneuronal Abeta42 accumulation in human brain. *The American Journal of Pathology*, 156(1), 15–20. [https://doi.org/10.1016/s0002-9440\(10\)64700-1](https://doi.org/10.1016/s0002-9440(10)64700-1)

Graves, B. J., & Petersen, J. M. (1998). Specificity within the ets Family of Transcription Factors. In *Advances in Cancer Research* (Vol. 75, pp. 1–57). Elsevier. [https://doi.org/10.1016/S0065-230X\(08\)60738-1](https://doi.org/10.1016/S0065-230X(08)60738-1)

- Griffin, W. S., Stanley, L. C., Ling, C., White, L., MacLeod, V., Perrot, L. J., White, C. L., & Araoz, C. (1989). Brain interleukin 1 and S-100 immunoreactivity are elevated in Down syndrome and Alzheimer disease. *Proceedings of the National Academy of Sciences of the United States of America*, 86(19), 7611–7615.
<https://doi.org/10.1073/pnas.86.19.7611>
- Gueant, J.-L. (2005). Homocysteine and related genetic polymorphisms in Down's syndrome IQ. *Journal of Neurology, Neurosurgery & Psychiatry*, 76(5), 706–709.
<https://doi.org/10.1136/jnnp.2004.039875>
- Guidi, S., Bonasoni, P., Ceccarelli, C., Santini, D., Gualtieri, F., Ciani, E., & Bartesaghi, R. (2007). Neurogenesis Impairment and Increased Cell Death Reduce Total Neuron Number in the Hippocampal Region of Fetuses with Down Syndrome: Hippocampal Hypocellularity in Down Fetuses. *Brain Pathology*, 18(2), 180–197.
<https://doi.org/10.1111/j.1750-3639.2007.00113.x>
- Guidi, S., Ciani, E., Bonasoni, P., Santini, D., & Bartesaghi, R. (2011). Widespread Proliferation Impairment and Hypocellularity in the Cerebellum of Fetuses with Down Syndrome: Down Syndrome Fetal Cerebellum. *Brain Pathology*, 21(4), 361–373.
<https://doi.org/10.1111/j.1750-3639.2010.00459.x>
- Harada, H., Harada, Y., Niimi, H., Kyo, T., Kimura, A., & Inaba, T. (2004). High incidence of somatic mutations in the AML1/RUNX1 gene in myelodysplastic syndrome and low blast percentage myeloid leukemia with myelodysplasia. *Blood*, 103(6), 2316–2324. <https://doi.org/10.1182/blood-2003-09-3074>
- Hatakeyama, J., Bessho, Y., Katoh, K., Ookawara, S., Fujioka, M., Guillemot, F., & Kageyama, R. (2004). Hes genes regulate size, shape and histogenesis of the nervous system by control of the timing of neural stem cell differentiation. *Development (Cambridge, England)*, 131(22), 5539–5550. <https://doi.org/10.1242/dev.01436>
- He, B., Deng, T., Zhu, I., Furusawa, T., Zhang, S., Tang, W., Postnikov, Y., Ambs, S., Li, C. C., Livak, F., Landsman, D., & Bustin, M. (2018). Binding of HMGN proteins to cell specific enhancers stabilizes cell identity. *Nature Communications*, 9(1), 5240.
<https://doi.org/10.1038/s41467-018-07687-9>
- He, B., Zhu, I., Postnikov, Y., Furusawa, T., Jenkins, L., Nanduri, R., Bustin, M., & Landsman, D. (2022). Multiple epigenetic factors co-localize with HMGN proteins in A-compartment chromatin. *Epigenetics & Chromatin*, 15(1), 23.
<https://doi.org/10.1186/s13072-022-00457-4>
- Head, E., Azizeh, B. Y., Lott, I. T., Tenner, A. J., Cotman, C. W., & Cribbs, D. H. (2001). Complement association with neurons and beta-amyloid deposition in the brains of aged individuals with Down Syndrome. *Neurobiology of Disease*, 8(2), 252–265.
<https://doi.org/10.1006/nbdi.2000.0380>

- Heru Sumarsono, S., Wilson, T. J., Tymms, M. J., Venter, D. J., Corrick, C. M., Kola, R., Lahoud, M. H., Papas, T. S., Seth, A., & Kola, I. (1996). Down's syndrome-like skeletal abnormalities in *Ets2* transgenic mice. *Nature*, 379(6565), 534–537. <https://doi.org/10.1038/379534a0>
- Hibaoui, Y., Grad, I., Letourneau, A., Sailani, M. R., Dahoun, S., Santoni, F. A., Gimelli, S., Guipponi, M., Pelte, M. F., Béna, F., Antonarakis, S. E., & Feki, A. (2014). Modelling and rescuing neurodevelopmental defect of Down syndrome using induced pluripotent stem cells from monozygotic twins discordant for trisomy 21. *EMBO Molecular Medicine*, 6(2), 259–277. <https://doi.org/10.1002/emmm.201302848>
- Hoshino, A., Helwig, M., Rezaei, S., Berridge, C., Eriksen, J. L., & Lindberg, I. (2014). A novel function for proSAAS as an amyloid anti-aggregant in Alzheimer's disease. *Journal of Neurochemistry*, 128(3), 419–430. <https://doi.org/10.1111/jnc.12454>
- Huang, H., Rambaldi, I., Daniels, E., & Featherstone, M. (2003). Expression of the *Wdr9* gene and protein products during mouse development. *Developmental Dynamics*, 227(4), 608–614. <https://doi.org/10.1002/dvdy.10344>
- Huen, M. S. Y., Sy, S. M. H., Leung, K. M., Ching, Y.-P., Tipoe, G. L., Man, C., Dong, S., & Chen, J. (2010). SON is a spliceosome-associated factor required for mitotic progression. *Cell Cycle*, 9(13), 2679–2685. <https://doi.org/10.4161/cc.9.13.12151>
- Ingram, W. J., McCue, K. I., Tran, T. H., Hallahan, A. R., & Wainwright, B. J. (2008). Sonic Hedgehog regulates *Hes1* through a novel mechanism that is independent of canonical Notch pathway signalling. *Oncogene*, 27(10), 1489–1500. <https://doi.org/10.1038/sj.onc.1210767>
- J. Tymms, M., & Kola, I. (1994). Regulation of gene expression by transcription factors *Ets-1* and *Ets-2*. *Molecular Reproduction and Development*, 39(2), 208–214. <https://doi.org/10.1002/mrd.1080390214>
- Jayaraman, G., Srinivas, R., Duggan, C., Ferreira, E., Swaminathan, S., Somasundaram, K., Williams, J., Hauser, C., Kurkinen, M., Dhar, R., Weitzman, S., Buttice, G., & Thimmapaya, B. (1999). P300/cAMP-responsive Element-binding Protein Interactions with *Ets-1* and *Ets-2* in the Transcriptional Activation of the Human Stromelysin Promoter. *Journal of Biological Chemistry*, 274(24), 17342–17352. <https://doi.org/10.1074/jbc.274.24.17342>
- Jiang, J., Jing, Y., Cost, G. J., Chiang, J.-C., Kolpa, H. J., Cotton, A. M., Carone, D. M., Carone, B. R., Shivak, D. A., Guschin, D. Y., Pearl, J. R., Rebar, E. J., Byron, M., Gregory, P. D., Brown, C. J., Urnov, F. D., Hall, L. L., & Lawrence, J. B. (2013). Translating dosage compensation to trisomy 21. *Nature*, 500(7462), 296–300. <https://doi.org/10.1038/nature12394>

- Kagoshima, H., Shigesada, K., Satake, M., Ito, Y., Miyoshi, H., Ohki, M., Pepling, M., & Gergen, P. (1993). The runt domain identifies a new family of heterometric transcriptional regulators. *Trends in Genetics*, 9(10), 338–341. [https://doi.org/10.1016/0168-9525\(93\)90026-E](https://doi.org/10.1016/0168-9525(93)90026-E)
- Kahlem, P., Sultan, M., Herwig, R., Steinfath, M., Balzereit, D., Eppens, B., Saran, N. G., Pletcher, M. T., South, S. T., Stetten, G., Lehrach, H., Reeves, R. H., & Yaspo, M.-L. (2004). Transcript level alterations reflect gene dosage effects across multiple tissues in a mouse model of down syndrome. *Genome Research*, 14(7), 1258–1267. <https://doi.org/10.1101/gr.1951304>
- Kamminga, L. M., Bystrykh, L. V., de Boer, A., Houwer, S., Douma, J., Weersing, E., Dontje, B., & de Haan, G. (2006). The Polycomb group gene *Ezh2* prevents hematopoietic stem cell exhaustion. *Blood*, 107(5), 2170–2179. <https://doi.org/10.1182/blood-2005-09-3585>
- Kessarlis, N., Fogarty, M., Iannarelli, P., Grist, M., Wegner, M., & Richardson, W. D. (2006). Competing waves of oligodendrocytes in the forebrain and postnatal elimination of an embryonic lineage. *Nature Neuroscience*, 9(2), 173–179. <https://doi.org/10.1038/nn1620>
- Kitabayashi, I. (1998). Interaction and functional cooperation of the leukemia-associated factors AML1 and p300 in myeloid cell differentiation. *The EMBO Journal*, 17(11), 2994–3004. <https://doi.org/10.1093/emboj/17.11.2994>
- Klein, J. A., Li, Z., Rampam, S., Cardini, J., Ayoub, A., Shaw, P., Rachubinski, A. L., Espinosa, J. M., Zeldich, E., & Haydar, T. F. (2022). Sonic Hedgehog Pathway Modulation Normalizes Expression of *Olig2* in Rostrally Patterned NPCs With Trisomy 21. *Frontiers in Cellular Neuroscience*, 15, 794675. <https://doi.org/10.3389/fncel.2021.794675>
- Korbel, J. O., Tirosh-Wagner, T., Urban, A. E., Chen, X.-N., Kasowski, M., Dai, L., Grubert, F., Erdman, C., Gao, M. C., Lange, K., Sobel, E. M., Barlow, G. M., Aylsworth, A. S., Carpenter, N. J., Clark, R. D., Cohen, M. Y., Doran, E., Falik-Zaccai, T., Lewin, S. O., ... Korenberg, J. R. (2009). The genetic architecture of Down syndrome phenotypes revealed by high-resolution analysis of human segmental trisomies. *Proceedings of the National Academy of Sciences of the United States of America*, 106(29), 12031–12036. <https://doi.org/10.1073/pnas.0813248106>
- Korenberg, J. R., Chen, X. N., Schipper, R., Sun, Z., Gonsky, R., Gerwehr, S., Carpenter, N., Daumer, C., Dignan, P., & Disteché, C. (1994). Down syndrome phenotypes: The consequences of chromosomal imbalance. *Proceedings of the National Academy of Sciences of the United States of America*, 91(11), 4997–5001. <https://doi.org/10.1073/pnas.91.11.4997>

Korenberg, J. R., Kawashima, H., Pulst, S. M., Ikeuchi, T., Ogasawara, N., Yamamoto, K., Schonberg, S. A., West, R., Allen, L., & Magenis, E. (1990). Molecular definition of a region of chromosome 21 that causes features of the Down syndrome phenotype. *American Journal of Human Genetics*, 47(2), 236–246.

Körner, U., Bustin, M., Scheer, U., & Hock, R. (2003). Developmental role of HMGN proteins in *Xenopus laevis*. *Mechanisms of Development*, 120(10), 1177–1192. <https://doi.org/10.1016/j.mod.2003.07.001>

Kuzmichev, A., Nishioka, K., Erdjument-Bromage, H., Tempst, P., & Reinberg, D. (2002). Histone methyltransferase activity associated with a human multiprotein complex containing the Enhancer of Zeste protein. *Genes & Development*, 16(22), 2893–2905. <https://doi.org/10.1101/gad.1035902>

Lacaud, G. (2002). Runx1 is essential for hematopoietic commitment at the hemangioblast stage of development in vitro. *Blood*, 100(2), 458–466. <https://doi.org/10.1182/blood-2001-12-0321>

Lancaster, M. A., Renner, M., Martin, C.-A., Wenzel, D., Bicknell, L. S., Hurles, M. E., Homfray, T., Penninger, J. M., Jackson, A. P., & Knoblich, J. A. (2013). Cerebral organoids model human brain development and microcephaly. *Nature*, 501(7467), 373–379. <https://doi.org/10.1038/nature12517>

Lane, A. A., Chapuy, B., Lin, C. Y., Tivey, T., Li, H., Townsend, E. C., van Bodegom, D., Day, T. A., Wu, S.-C., Liu, H., Yoda, A., Alexe, G., Schinzel, A. C., Sullivan, T. J., Malinge, S., Taylor, J. E., Stegmaier, K., Jaffe, J. D., Bustin, M., ... Weinstock, D. M. (2014). Triplication of a 21q22 region contributes to B cell transformation through HMGN1 overexpression and loss of histone H3 Lys27 trimethylation. *Nature Genetics*, 46(6), 618–623. <https://doi.org/10.1038/ng.2949>

Lanfranchi, S., Jerman, O., Dal Pont, E., Alberti, A., & Vianello, R. (2010). Executive function in adolescents with Down Syndrome: Executive function in Down Syndrome. *Journal of Intellectual Disability Research*, 54(4), 308–319. <https://doi.org/10.1111/j.1365-2788.2010.01262.x>

Laufer, B. I., Gomez, J. A., Jianu, J. M., & LaSalle, J. M. (2021). Stable DNMT3L overexpression in SH-SY5Y neurons recreates a facet of the genome-wide Down syndrome DNA methylation signature. *Epigenetics & Chromatin*, 14(1), 13. <https://doi.org/10.1186/s13072-021-00387-7>

Lee, T. I., Jenner, R. G., Boyer, L. A., Guenther, M. G., Levine, S. S., Kumar, R. M., Chevalier, B., Johnstone, S. E., Cole, M. F., Isono, K., Koseki, H., Fuchikami, T., Abe, K., Murray, H. L., Zucker, J. P., Yuan, B., Bell, G. W., Herbolsheimer, E., Hannett, N. M., ... Young, R. A. (2006). Control of developmental regulators by Polycomb in human embryonic stem cells. *Cell*, 125(2), 301–313. <https://doi.org/10.1016/j.cell.2006.02.043>

Lejeune, J., Turpin, R., & Gautier, M. (1959). [Mongolism; a chromosomal disease (trisomy)]. *Bulletin de l'Academie Nationale de Medecine*, 143(11–12), 256–265.

Lepagnol-Bestel, A.-M., Zvara, A., Maussion, G., Quignon, F., Ngimbous, B., Ramoz, N., Imbeaud, S., Loe-Mie, Y., Benihoud, K., Agier, N., Salin, P. A., Cardona, A., Khung-Savatovsky, S., Kallunki, P., Delabar, J.-M., Puskas, L. G., Delacroix, H., Aggerbeck, L., Delezoide, A.-L., ... Simonneau, M. (2009). DYRK1A interacts with the REST/NRSF-SWI/SNF chromatin remodelling complex to deregulate gene clusters involved in the neuronal phenotypic traits of Down syndrome. *Human Molecular Genetics*, 18(8), 1405–1414. <https://doi.org/10.1093/hmg/ddp047>

Leverenz, J. B., & Raskind, M. A. (1998). Early amyloid deposition in the medial temporal lobe of young Down syndrome patients: A regional quantitative analysis. *Experimental Neurology*, 150(2), 296–304. <https://doi.org/10.1006/exnr.1997.6777>

Lewis, J., Dickson, D. W., Lin, W. L., Chisholm, L., Corral, A., Jones, G., Yen, S. H., Sahara, N., Skipper, L., Yager, D., Eckman, C., Hardy, J., Hutton, M., & McGowan, E. (2001). Enhanced neurofibrillary degeneration in transgenic mice expressing mutant tau and APP. *Science (New York, N.Y.)*, 293(5534), 1487–1491. <https://doi.org/10.1126/science.1058189>

Li, C., Liu, C., Zhou, B., Hu, C., & Xu, X. (2016). Novel microduplication of CHL1 gene in a patient with autism spectrum disorder: A case report and a brief literature review. *Molecular Cytogenetics*, 9(1), 51. <https://doi.org/10.1186/s13039-016-0261-9>

Li, S., Xu, C., Fu, Y., Lei, P.-J., Yao, Y., Yang, W., Zhang, Y., Washburn, M. P., Florens, L., Jaiswal, M., Wu, M., & Mohan, M. (2018). DYRK1A interacts with histone acetyl transferase p300 and CBP and localizes to enhancers. *Nucleic Acids Research*, 46(21), 11202–11213. <https://doi.org/10.1093/nar/gky754>

Li, Z., Klein, J. A., Rampam, S., Kurzion, R., Patel, Y., Haydar, T. F., & Zeldich, E. (n.d.). Asynchronous excitatory neuron development in an isogenic cortical spheroid model of Down syndrome. *bioRxiv* <https://doi.org/10.1101/2022.04.30.490174>

Lithner, C. U., Lacor, P. N., Zhao, W.-Q., Mustafiz, T., Klein, W. L., Sweatt, J. D., & Hernandez, C. M. (2013). Disruption of neocortical histone H3 homeostasis by soluble A β : Implications for Alzheimer's disease. *Neurobiology of Aging*, 34(9), 2081–2090. <https://doi.org/10.1016/j.neurobiolaging.2012.12.028>

Liu, J., Wu, X., Zhang, H., Pfeifer, G. P., & Lu, Q. (2017). Dynamics of RNA Polymerase II Pausing and Bivalent Histone H3 Methylation during Neuronal Differentiation in Brain Development. *Cell Reports*, 20(6), 1307–1318. <https://doi.org/10.1016/j.celrep.2017.07.046>

- Liu, P.-P., Xu, Y.-J., Dai, S.-K., Du, H.-Z., Wang, Y.-Y., Li, X.-G., Teng, Z.-Q., & Liu, C.-M. (2019). Polycomb Protein EED Regulates Neuronal Differentiation through Targeting SOX11 in Hippocampal Dentate Gyrus. *Stem Cell Reports*, 13(1), 115–131. <https://doi.org/10.1016/j.stemcr.2019.05.010>
- Liu, W., Duan, X., Xu, L., Shang, W., Zhao, J., Wang, L., Li, J.-C., Chen, C.-H., Liu, J.-P., & Tong, C. (2020). Chchd2 regulates mitochondrial morphology by modulating the levels of Opa1. *Cell Death and Differentiation*, 27(6), 2014–2029. <https://doi.org/10.1038/s41418-019-0482-7>
- Loh, Y.-H., Agarwal, S., Park, I.-H., Urbach, A., Huo, H., Heffner, G. C., Kim, K., Miller, J. D., Ng, K., & Daley, G. Q. (2009). Generation of induced pluripotent stem cells from human blood. *Blood*, 113(22), 5476–5479. <https://doi.org/10.1182/blood-2009-02-204800>
- Lott, I. T., & Dierssen, M. (2010). Cognitive deficits and associated neurological complications in individuals with Down's syndrome. *The Lancet. Neurology*, 9(6), 623–633. [https://doi.org/10.1016/S1474-4422\(10\)70112-5](https://doi.org/10.1016/S1474-4422(10)70112-5)
- Lu, H.-E., Yang, Y.-C., Chen, S.-M., Su, H.-L., Huang, P.-C., Tsai, M.-S., Wang, T.-H., Tseng, C.-P., & Hwang, S.-M. (2013). Modeling neurogenesis impairment in Down syndrome with induced pluripotent stem cells from Trisomy 21 amniotic fluid cells. *Experimental Cell Research*, 319(4), 498–505. <https://doi.org/10.1016/j.yexcr.2012.09.017>
- Lyle, R., Gehrig, C., Neergaard-Henrichsen, C., Deutsch, S., & Antonarakis, S. E. (2004). Gene expression from the aneuploid chromosome in a trisomy mouse model of down syndrome. *Genome Research*, 14(7), 1268–1274. <https://doi.org/10.1101/gr.2090904>
- Maclean, G. A., Menne, T. F., Guo, G., Sanchez, D. J., Park, I.-H., Daley, G. Q., & Orkin, S. H. (2012). Altered hematopoiesis in trisomy 21 as revealed through in vitro differentiation of isogenic human pluripotent cells. *Proceedings of the National Academy of Sciences of the United States of America*, 109(43), 17567–17572. <https://doi.org/10.1073/pnas.1215468109>
- Mann, D. M. A., & Esiri, M. M. (1989). The pattern of acquisition of plaques and tangles in the brains of patients under 50 years of age with Down's syndrome. *Journal of the Neurological Sciences*, 89(2–3), 169–179. [https://doi.org/10.1016/0022-510X\(89\)90019-1](https://doi.org/10.1016/0022-510X(89)90019-1)
- Mardian, J. K. W., Paton, A. E., Bunick, G. J., & Olins, D. E. (1980). Nucleosome Cores Have Two Specific Binding Sites for Nonhistone Chromosomal Proteins HMG 14 and HMG 17. *Science*, 209(4464), 1534–1536. <https://doi.org/10.1126/science.7433974>

- Margueron, R., Justin, N., Ohno, K., Sharpe, M. L., Son, J., Drury III, W. J., Voigt, P., Martin, S. R., Taylor, W. R., De Marco, V., Pirrotta, V., Reinberg, D., & Gambin, S. J. (2009). Role of the polycomb protein EED in the propagation of repressive histone marks. *Nature*, 461(7265), 762–767. <https://doi.org/10.1038/nature08398>
- Martin, C., Cao, R., & Zhang, Y. (2006). Substrate Preferences of the EZH2 Histone Methyltransferase Complex. *Journal of Biological Chemistry*, 281(13), 8365–8370. <https://doi.org/10.1074/jbc.M513425200>
- Marzi, S. J., Leung, S. K., Ribarska, T., Hannon, E., Smith, A. R., Pishva, E., Poschmann, J., Moore, K., Troakes, C., Al-Sarraj, S., Beck, S., Newman, S., Lunnon, K., Schalkwyk, L. C., & Mill, J. (2018). A histone acetylome-wide association study of Alzheimer’s disease identifies disease-associated H3K27ac differences in the entorhinal cortex. *Nature Neuroscience*, 21(11), 1618–1627. <https://doi.org/10.1038/s41593-018-0253-7>
- Mattioni, T., Hume, C. R., Konigorski, S., Hayes, P., Osterweil, Z., & Lee, J. S. (1992). A cDNA clone for a novel nuclear protein with DNA binding activity. *Chromosoma*, 101(10), 618–624. <https://doi.org/10.1007/BF00360539>
- McCarron, M., McCallion, P., Reilly, E., & Mulryan, N. (2014). A prospective 14-year longitudinal follow-up of dementia in persons with Down syndrome. *Journal of Intellectual Disability Research: JIDR*, 58(1), 61–70. <https://doi.org/10.1111/jir.12074>
- McKee, A. E., Minet, E., Stern, C., Riahi, S., Stiles, C. D., & Silver, P. A. (2005). A genome-wide in situ hybridization map of RNA-binding proteins reveals anatomically restricted expression in the developing mouse brain. *BMC Developmental Biology*, 5, 14. <https://doi.org/10.1186/1471-213X-5-14>
- Meharena, H. S., Marco, A., Dileep, V., Lockshin, E. R., Akatsu, G. Y., Mullahoo, J., Watson, L. A., Ko, T., Guerin, L. N., Abdurrob, F., Rengarajan, S., Papanastasiou, M., Jaffe, J. D., & Tsai, L.-H. (2022). Down-syndrome-induced senescence disrupts the nuclear architecture of neural progenitors. *Cell Stem Cell*, 29(1), 116-130.e7. <https://doi.org/10.1016/j.stem.2021.12.002>
- Mikkelsen, T. S., Hanna, J., Zhang, X., Ku, M., Wernig, M., Schorderet, P., Bernstein, B. E., Jaenisch, R., Lander, E. S., & Meissner, A. (2008). Dissecting direct reprogramming through integrative genomic analysis. *Nature*, 454(7200), 49–55. <https://doi.org/10.1038/nature07056>
- Miller, J. A., Ding, S.-L., Sunkin, S. M., Smith, K. A., Ng, L., Szafer, A., Ebbert, A., Riley, Z. L., Royall, J. J., Aiona, K., Arnold, J. M., Bennet, C., Bertagnolli, D., Brouner, K., Butler, S., Caldejon, S., Carey, A., Cuhaciyani, C., Dalley, R. A., ... Lein, E. S. (2014). Transcriptional landscape of the prenatal human brain. *Nature*, 508(7495), 199–206. <https://doi.org/10.1038/nature13185>

- Mohamed, O. A., Bustin, M., & Clarke, H. J. (2001). High-Mobility Group Proteins 14 and 17 Maintain the Timing of Early Embryonic Development in the Mouse. *Developmental Biology*, 229(1), 237–249. <https://doi.org/10.1006/dbio.2000.9942>
- Morgan, D. J., Mzhavia, N., Peng, B., Pan, H., Devi, L. A., & Pintar, J. E. (2005). Embryonic gene expression and pro-protein processing of proSAAS during rodent development. *Journal of Neurochemistry*, 93(6), 1454–1462. <https://doi.org/10.1111/j.1471-4159.2005.03138.x>
- Mowery, C. T., Reyes, J. M., Cabal-Hierro, L., Higby, K. J., Karlin, K. L., Wang, J. H., Kimmerling, R. J., Cejas, P., Lim, K., Li, H., Furusawa, T., Long, H. W., Pellman, D., Chapuy, B., Bustin, M., Manalis, S. R., Westbrook, T. F., Lin, C. Y., & Lane, A. A. (2018). Trisomy of a Down Syndrome Critical Region Globally Amplifies Transcription via HMGN1 Overexpression. *Cell Reports*, 25(7), 1898-1911.e5. <https://doi.org/10.1016/j.celrep.2018.10.061>
- Mullighan, C. G., Collins-Underwood, J. R., Phillips, L. A. A., Loudin, M. G., Liu, W., Zhang, J., Ma, J., Coustan-Smith, E., Harvey, R. C., Willman, C. L., Mikhail, F. M., Meyer, J., Carroll, A. J., Williams, R. T., Cheng, J., Heerema, N. A., Basso, G., Pession, A., Pui, C.-H., ... Rabin, K. R. (2009). Rearrangement of CRLF2 in B-progenitor- and Down syndrome-associated acute lymphoblastic leukemia. *Nature Genetics*, 41(11), 1243–1246. <https://doi.org/10.1038/ng.469>
- Nagao, M., Lanjakornsiripan, D., Itoh, Y., Kishi, Y., Ogata, T., & Gotoh, Y. (2014). High Mobility Group Nucleosome-Binding Family Proteins Promote Astrocyte Differentiation of Neural Precursor Cells. *Stem Cells*, 32(11), 2983–2997. <https://doi.org/10.1002/stem.1787>
- Narayan, P. J., Lill, C., Faull, R., Curtis, M. A., & Dragunow, M. (2015). Increased acetyl and total histone levels in post-mortem Alzheimer's disease brain. *Neurobiology of Disease*, 74, 281–294. <https://doi.org/10.1016/j.nbd.2014.11.023>
- Nativio, R., Lan, Y., Donahue, G., Sidoli, S., Berson, A., Srinivasan, A. R., Shcherbakova, O., Amlie-Wolf, A., Nie, J., Cui, X., He, C., Wang, L.-S., Garcia, B. A., Trojanowski, J. Q., Bonini, N. M., & Berger, S. L. (2020). An integrated multi-omics approach identifies epigenetic alterations associated with Alzheimer's disease. *Nature Genetics*, 52(10), 1024–1035. <https://doi.org/10.1038/s41588-020-0696-0>
- North, T. E., Stacy, T., Matheny, C. J., Speck, N. A., & de Bruijn, M. F. T. R. (2004). Runx1 Is Expressed in Adult Mouse Hematopoietic Stem Cells and Differentiating Myeloid and Lymphoid Cells, But Not in Maturing Erythroid Cells. *Stem Cells*, 22(2), 158–168. <https://doi.org/10.1634/stemcells.22-2-158>
- Nuytten, M., Beke, L., Van Eynde, A., Ceulemans, H., Beullens, M., Van Hummelen, P., Fuks, F., & Bollen, M. (2008). The transcriptional repressor NIPPI1 is an essential player

in EZH2-mediated gene silencing. *Oncogene*, 27(10), 1449–1460.
<https://doi.org/10.1038/sj.onc.1210774>

Nye, J. S., Kopan, R., & Axel, R. (1994). An activated Notch suppresses neurogenesis and myogenesis but not gliogenesis in mammalian cells. *Development* (Cambridge, England), 120(9), 2421–2430. <https://doi.org/10.1242/dev.120.9.2421>

Oakford, P. C., James, S. R., Qadi, A., West, A. C., Ray, S. N., Bert, A. G., Cockerill, P. N., & Holloway, A. F. (2010). Transcriptional and epigenetic regulation of the GM-CSF promoter by RUNX1. *Leukemia Research*, 34(9), 1203–1213.
<https://doi.org/10.1016/j.leukres.2010.03.029>

Olmos-Serrano, J. L., Kang, H. J., Tyler, W. A., Silbereis, J. C., Cheng, F., Zhu, Y., Pletikos, M., Jankovic-Rapan, L., Cramer, N. P., Galdzicki, Z., Goodliffe, J., Peters, A., Sethares, C., Delalle, I., Golden, J. A., Haydar, T. F., & Sestan, N. (2016). Down Syndrome Developmental Brain Transcriptome Reveals Defective Oligodendrocyte Differentiation and Myelination. *Neuron*, 89(6), 1208–1222.
<https://doi.org/10.1016/j.neuron.2016.01.042>

Ovchinnikov, D. A., Korn, O., Virshup, I., Wells, C. A., & Wolvetang, E. J. (2018). The Impact of APP on Alzheimer-like Pathogenesis and Gene Expression in Down Syndrome iPSC-Derived Neurons. *Stem Cell Reports*, 11(1), 32–42.
<https://doi.org/10.1016/j.stemcr.2018.05.004>

Paddison, P. J., Caudy, A. A., Bernstein, E., Hannon, G. J., & Conklin, D. S. (2002). Short hairpin RNAs (shRNAs) induce sequence-specific silencing in mammalian cells. *Genes & Development*, 16(8), 948–958. <https://doi.org/10.1101/gad.981002>

Palmer, C. R., Liu, C. S., Romanow, W. J., Lee, M.-H., & Chun, J. (2021). Altered cell and RNA isoform diversity in aging Down syndrome brains. *Proceedings of the National Academy of Sciences of the United States of America*, 118(47), e2114326118.
<https://doi.org/10.1073/pnas.2114326118>

Pan, M.-R., Hsu, M.-C., Chen, L.-T., & Hung, W.-C. (2018). Orchestration of H3K27 methylation: Mechanisms and therapeutic implication. *Cellular and Molecular Life Sciences*, 75(2), 209–223. <https://doi.org/10.1007/s00018-017-2596-8>

Pandya, N. J., Wang, C., Costa, V., Lopatta, P., Meier, S., Zampeta, F. I., Punt, A. M., Mientjes, E., Grossen, P., Distler, T., Tzouros, M., Martí, Y., Banfai, B., Patsch, C., Rasmussen, S., Hoener, M., Berrera, M., Kremer, T., Dunkley, T., ... Jagasia, R. (2021). Secreted retrovirus-like GAG-domain-containing protein PEG10 is regulated by UBE3A and is involved in Angelman syndrome pathophysiology. *Cell Reports Medicine*, 2(8), 100360. <https://doi.org/10.1016/j.xcrm.2021.100360>

Paranjape, S. M., Krumm, A., & Kadonaga, J. T. (1995). HMG17 is a chromatin-specific transcriptional coactivator that increases the efficiency of transcription initiation. *Genes & Development*, 9(16), 1978–1991. <https://doi.org/10.1101/gad.9.16.1978>

Park, I.-H., Arora, N., Huo, H., Maherali, N., Ahfeldt, T., Shimamura, A., Lensch, M. W., Cowan, C., Hochedlinger, K., & Daley, G. Q. (2008). Disease-specific induced pluripotent stem cells. *Cell*, 134(5), 877–886. <https://doi.org/10.1016/j.cell.2008.07.041>

Paşca, A. M., Sloan, S. A., Clarke, L. E., Tian, Y., Makinson, C. D., Huber, N., Kim, C. H., Park, J.-Y., O'Rourke, N. A., Nguyen, K. D., Smith, S. J., Huguenard, J. R., Geschwind, D. H., Barres, B. A., & Paşca, S. P. (2015). Functional cortical neurons and astrocytes from human pluripotent stem cells in 3D culture. *Nature Methods*, 12(7), 671–678. <https://doi.org/10.1038/nmeth.3415>

Pereira, J. D., Sansom, S. N., Smith, J., Dobenecker, M.-W., Tarakhovsky, A., & Livesey, F. J. (2010). Ezh2, the histone methyltransferase of PRC2, regulates the balance between self-renewal and differentiation in the cerebral cortex. *Proceedings of the National Academy of Sciences of the United States of America*, 107(36), 15957–15962. <https://doi.org/10.1073/pnas.1002530107>

Perluigi, M., & Butterfield, D. A. (2012). Oxidative Stress and Down Syndrome: A Route toward Alzheimer-Like Dementia. *Current Gerontology and Geriatrics Research*, 2012, 724904. <https://doi.org/10.1155/2012/724904>

Persico, G., Casciaro, F., Amatori, S., Rusin, M., Cantatore, F., Perna, A., Auber, L. A., Fanelli, M., & Giorgio, M. (2022). Histone H3 Lysine 4 and 27 Trimethylation Landscape of Human Alzheimer's Disease. *Cells*, 11(4), 734. <https://doi.org/10.3390/cells11040734>

Petit, T. L., LeBoutillier, J. C., Alfano, D. P., & Becker, L. E. (1984). Synaptic development in the human fetus: A morphometric analysis of normal and Down's syndrome neocortex. *Experimental Neurology*, 83(1), 13–23. [https://doi.org/10.1016/0014-4886\(84\)90041-4](https://doi.org/10.1016/0014-4886(84)90041-4)

Pinter, J. D., Brown, W. E., Eliez, S., Schmitt, J. E., Capone, G. T., & Reiss, A. L. (2001). Amygdala and hippocampal volumes in children with Down syndrome: A high-resolution MRI study. *Neurology*, 56(7), 972–974. <https://doi.org/10.1212/WNL.56.7.972>

Pinter, J. D., Eliez, S., Schmitt, J. E., Capone, G. T., & Reiss, A. L. (2001). Neuroanatomy of Down's Syndrome: A High-Resolution MRI Study. *American Journal of Psychiatry*, 158(10), 1659–1665. <https://doi.org/10.1176/appi.ajp.158.10.1659>

Pinto, B., Morelli, G., Rastogi, M., Savardi, A., Fumagalli, A., Petretto, A., Bartolucci, M., Varea, E., Catelani, T., Contestabile, A., Perlini, L. E., & Cancedda, L. (2020). Rescuing Over-activated Microglia Restores Cognitive Performance in Juvenile Animals

of the Dp(16) Mouse Model of Down Syndrome. *Neuron*, 108(5), 887-904.e12.
<https://doi.org/10.1016/j.neuron.2020.09.010>

Pipino, C., Mukherjee, S., David, A. L., Blundell, M. P., Shaw, S. W., Sung, P., Shangaris, P., Waters, J. J., Ellershaw, D., Cavazzana, M., Mostoslavsky, G., Pandolfi, A., Pierro, A., Guillot, P. V., Thrasher, A. J., & De Coppi, P. (2014). Trisomy 21 mid-trimester amniotic fluid induced pluripotent stem cells maintain genetic signatures during reprogramming: Implications for disease modeling and cryobanking. *Cellular Reprogramming*, 16(5), 331–344. <https://doi.org/10.1089/cell.2013.0091>

Plath, K., Fang, J., Mlynarczyk-Evans, S. K., Cao, R., Worringer, K. A., Wang, H., de la Cruz, C. C., Otte, A. P., Panning, B., & Zhang, Y. (2003). Role of Histone H3 Lysine 27 Methylation in X Inactivation. *Science*, 300(5616), 131–135.
<https://doi.org/10.1126/science.1084274>

Poepsel, S., Kasinath, V., & Nogales, E. (2018). Cryo-EM structures of PRC2 simultaneously engaged with two functionally distinct nucleosomes. *Nature Structural & Molecular Biology*, 25(2), 154–162. <https://doi.org/10.1038/s41594-018-0023-y>

Prasher, V. P., Farrer, M. J., Kessler, A. M., Fisher, E. M., West, R. J., Barber, P. C., & Butler, A. C. (1998). Molecular mapping of Alzheimer-type dementia in Down's syndrome. *Annals of Neurology*, 43(3), 380–383. <https://doi.org/10.1002/ana.410430316>

Prymakowska-Bosak, M., Hock, R., Catez, F., Lim, J.-H., Birger, Y., Shirakawa, H., Lee, K., & Bustin, M. (2002). Mitotic Phosphorylation of Chromosomal Protein HMGN1 Inhibits Nuclear Import and Promotes Interaction with 14.3.3 Proteins. *Molecular and Cellular Biology*, 22(19), 6809–6819. <https://doi.org/10.1128/MCB.22.19.6809-6819.2002>

Prymakowska-Bosak, M., Misteli, T., Herrera, J. E., Shirakawa, H., Birger, Y., Garfield, S., & Bustin, M. (2001). Mitotic Phosphorylation Prevents the Binding of HMGN Proteins to Chromatin. *Molecular and Cellular Biology*, 21(15), 5169–5178.
<https://doi.org/10.1128/MCB.21.15.5169-5178.2001>

Rabin, K. R., & Whitlock, J. A. (2009). Malignancy in children with trisomy 21. *The Oncologist*, 14(2), 164–173. <https://doi.org/10.1634/theoncologist.2008-0217>

Rao, J. S., Keleshian, V. L., Klein, S., & Rapoport, S. I. (2012). Epigenetic modifications in frontal cortex from Alzheimer's disease and bipolar disorder patients. *Translational Psychiatry*, 2(7), e132–e132. <https://doi.org/10.1038/tp.2012.55>

Reed-Inderbitzin, E., Moreno-Miralles, I., Vanden-Eynden, S. K., Xie, J., Lutterbach, B., Durst-Goodwin, K. L., Luce, K. S., Irvin, B. J., Cleary, M. L., Brandt, S. J., & Hiebert, S. W. (2006). RUNX1 associates with histone deacetylases and SUV39H1 to repress transcription. *Oncogene*, 25(42), 5777–5786. <https://doi.org/10.1038/sj.onc.1209591>

- Reiche, L., Küry, P., & Göttle, P. (2019). Aberrant Oligodendrogenesis in Down Syndrome: Shift in Gliogenesis? *Cells*, 8(12), 1591. <https://doi.org/10.3390/cells8121591>
- Ridsdale, J. A., Hendzel, M. J., Delcuve, G. P., & Davie, J. R. (1990). Histone acetylation alters the capacity of the H1 histones to condense transcriptionally active/competent chromatin. *The Journal of Biological Chemistry*, 265(9), 5150–5156.
- Rodríguez-Ortiz, A., Montoya-Villegas, J. C., García-Vallejo, F., & Mina-Paz, Y. (2021). Spatial and Temporal Expression of High-Mobility-Group Nucleosome-Binding (HMGN) Genes in Brain Areas Associated with Cognition in Individuals with Down Syndrome. *Genes*, 12(12), 2000. <https://doi.org/10.3390/genes12122000>
- Ronan, A., Fagan, K., Christie, L., Conroy, J., Nowak, N. J., & Turner, G. (2007). Familial 4.3 Mb duplication of 21q22 sheds new light on the Down syndrome critical region. *Journal of Medical Genetics*, 44(7), 448–451. <https://doi.org/10.1136/jmg.2006.047373>
- Rouillard, A. D., Gundersen, G. W., Fernandez, N. F., Wang, Z., Monteiro, C. D., McDermott, M. G., & Ma'ayan, A. (2016). The harmonizome: A collection of processed datasets gathered to serve and mine knowledge about genes and proteins. *Database: The Journal of Biological Databases and Curation*, 2016, baw100. <https://doi.org/10.1093/database/baw100>
- Routh, A., Sandin, S., & Rhodes, D. (2008). Nucleosome repeat length and linker histone stoichiometry determine chromatin fiber structure. *Proceedings of the National Academy of Sciences of the United States of America*, 105(26), 8872–8877. <https://doi.org/10.1073/pnas.0802336105>
- Royston, M. C., McKenzie, J. E., Gentleman, S. M., Sheng, J. G., Mann, D. M., Griffin, W. S., & Mrazek, R. E. (1999). Overexpression of s100beta in Down's syndrome: Correlation with patient age and with beta-amyloid deposition. *Neuropathology and Applied Neurobiology*, 25(5), 387–393. <https://doi.org/10.1046/j.1365-2990.1999.00196.x>
- Rumble, B., Retallack, R., Hilbich, C., Simms, G., Multhaup, G., Martins, R., Hockey, A., Montgomery, P., Beyreuther, K., & Masters, C. L. (1989). Amyloid A4 Protein and Its Precursor in Down's Syndrome and Alzheimer's Disease. *New England Journal of Medicine*, 320(22), 1446–1452. <https://doi.org/10.1056/NEJM198906013202203>
- Scheuner, D., Eckman, C., Jensen, M., Song, X., Citron, M., Suzuki, N., Bird, T. D., Hardy, J., Hutton, M., Kukull, W., Larson, E., Levy-Lahad, L., Viitanen, M., Peskind, E., Poorkaj, P., Schellenberg, G., Tanzi, R., Wasco, W., Lannfelt, L., ... Younkin, S. (1996). Secreted amyloid β -protein similar to that in the senile plaques of Alzheimer's disease is increased in vivo by the presenilin 1 and 2 and APP mutations linked to familial

- Alzheimer's disease. *Nature Medicine*, 2(8), 864–870. <https://doi.org/10.1038/nm0896-864>
- Schnittger, S., Dicker, F., Kern, W., Wendland, N., Sundermann, J., Alpermann, T., Haferlach, C., & Haferlach, T. (2011). RUNX1 mutations are frequent in de novo AML with noncomplex karyotype and confer an unfavorable prognosis. *Blood*, 117(8), 2348–2357. <https://doi.org/10.1182/blood-2009-11-255976>
- Schupf, N., Kapell, D., Nightingale, B., Rodriguez, A., Tycko, B., & Mayeux, R. (1998). Earlier onset of Alzheimer's disease in men with Down syndrome. *Neurology*, 50(4), 991–995. <https://doi.org/10.1212/WNL.50.4.991>
- Seidl, R., Bidmon, B., Bajo, M., Yoo, P. C., Cairns, N., LaCasse, E. C., & Lubec, G. (2001). Evidence for apoptosis in the fetal Down syndrome brain. *Journal of Child Neurology*, 16(6), 438–442. <https://doi.org/10.1177/088307380101600610>
- Seol, S., Kwon, J., & Kang, H. J. (2023). Cell type characterization of spatiotemporal gene co-expression modules in Down syndrome brain. *iScience*, 26(1), 105884. <https://doi.org/10.1016/j.isci.2022.105884>
- Seth, A., Watson, D. K., Blair, D. G., & Papas, T. S. (1989). C-ets-2 protooncogene has mitogenic and oncogenic activity. *Proceedings of the National Academy of Sciences U.S.A.*, 86(20), 7833–7837. <https://doi.org/10.1073/pnas.86.20.7833>
- Sevilla, L., Aperlo, C., Dulic, V., Chambard, J. C., Boutonnet, C., Pasquier, O., Pognonec, P., & Boulukos, K. E. (1999). The Ets2 Transcription Factor Inhibits Apoptosis Induced by Colony-Stimulating Factor 1 Deprivation of Macrophages through a Bcl-x L -Dependent Mechanism. *Molecular and Cellular Biology*, 19(4), 2624–2634. <https://doi.org/10.1128/MCB.19.4.2624>
- Shaytan, A. K., Armeev, G. A., Goncarenco, A., Zhurkin, V. B., Landsman, D., & Panchenko, A. R. (2016). Coupling between Histone Conformations and DNA Geometry in Nucleosomes on a Microsecond Timescale: Atomistic Insights into Nucleosome Functions. *Journal of Molecular Biology*, 428(1), 221–237. <https://doi.org/10.1016/j.jmb.2015.12.004>
- Shen, X., Liu, Y., Hsu, Y.-J., Fujiwara, Y., Kim, J., Mao, X., Yuan, G.-C., & Orkin, S. H. (2008). EZH1 Mediates Methylation on Histone H3 Lysine 27 and Complements EZH2 in Maintaining Stem Cell Identity and Executing Pluripotency. *Molecular Cell*, 32(4), 491–502. <https://doi.org/10.1016/j.molcel.2008.10.016>
- Sher, F., Rößler, R., Brouwer, N., Balasubramaniyan, V., Boddeke, E., & Copray, S. (2008). Differentiation of Neural Stem Cells into Oligodendrocytes: Involvement of the Polycomb Group Protein Ezh2. *Stem Cells*, 26(11), 2875–2883. <https://doi.org/10.1634/stemcells.2008-0121>

Shi, Y., Kirwan, P., & Livesey, F. J. (2012). Directed differentiation of human pluripotent stem cells to cerebral cortex neurons and neural networks. *Nature Protocols*, 7(10), 1836–1846. <https://doi.org/10.1038/nprot.2012.116>

Shi, Y., Kirwan, P., Smith, J., MacLean, G., Orkin, S. H., & Livesey, F. J. (2012). A human stem cell model of early Alzheimer's disease pathology in Down syndrome. *Science Translational Medicine*, 4(124), 124ra29. <https://doi.org/10.1126/scitranslmed.3003771>

Shi, Y., Kirwan, P., Smith, J., Robinson, H. P. C., & Livesey, F. J. (2012). Human cerebral cortex development from pluripotent stem cells to functional excitatory synapses. *Nature Neuroscience*, 15(3), 477–486, S1. <https://doi.org/10.1038/nn.3041>

Sinet, P. M., Théophile, D., Rahmani, Z., Chettouh, Z., Blouin, J. L., Prieur, M., Noel, B., & Delabar, J. M. (1994). Mapping of the Down syndrome phenotype on chromosome 21 at the molecular level. *Biomedicine & Pharmacotherapy = Biomedecine & Pharmacotherapie*, 48(5–6), 247–252. [https://doi.org/10.1016/0753-3322\(94\)90140-6](https://doi.org/10.1016/0753-3322(94)90140-6)

Song, L., Yuan, X., Jones, Z., Griffin, K., Zhou, Y., Ma, T., & Li, Y. (2019). Assembly of Human Stem Cell-Derived Cortical Spheroids and Vascular Spheroids to Model 3-D Brain-like Tissues. *Scientific Reports*, 9(1), 5977. <https://doi.org/10.1038/s41598-019-42439-9>

Startin, C. M., Hamburg, S., Hithersay, R., Davies, A., Rodger, E., Aggarwal, N., Al-Janabi, T., & Strydom, A. (2016). The LonDownS adult cognitive assessment to study cognitive abilities and decline in Down syndrome. *Wellcome Open Research*, 1, 11. <https://doi.org/10.12688/wellcomeopenres.9961.1>

Stoltzner, S. E., Grenfell, T. J., Mori, C., Wisniewski, K. E., Wisniewski, T. M., Selkoe, D. J., & Lemere, C. A. (2000). Temporal Accrual of Complement Proteins in Amyloid Plaques in Down's Syndrome with Alzheimer's Disease. *The American Journal of Pathology*, 156(2), 489–499. [https://doi.org/10.1016/S0002-9440\(10\)64753-0](https://doi.org/10.1016/S0002-9440(10)64753-0)

Sugaya, K. (2008). Mechanism of glial differentiation of neural progenitor cells by amyloid precursor protein. *Neuro-Degenerative Diseases*, 5(3–4), 170–172. <https://doi.org/10.1159/000113693>

Sun, H.-J., Xu, X., Wang, X.-L., Wei, L., Li, F., Lu, J., & Huang, B.-Q. (2006). Transcription Factors Ets2 and Sp1 Act Synergistically with Histone Acetyltransferase p300 in Activating Human Interleukin-12 p40 Promoter. *Acta Biochimica et Biophysica Sinica*, 38(3), 194–200. <https://doi.org/10.1111/j.1745-7270.2006.00147.x>

Takahashi, K., Tanabe, K., Ohnuki, M., Narita, M., Ichisaka, T., Tomoda, K., & Yamanaka, S. (2007). Induction of Pluripotent Stem Cells from Adult Human Fibroblasts by Defined Factors. *Cell*, 131(5), 861–872. <https://doi.org/10.1016/j.cell.2007.11.019>

Takahashi, K., & Yamanaka, S. (2006). Induction of Pluripotent Stem Cells from Mouse Embryonic and Adult Fibroblast Cultures by Defined Factors. *Cell*, 126(4), 663–676. <https://doi.org/10.1016/j.cell.2006.07.024>

Takashima, S., Ieshima, A., Nakamura, H., & Becker, L. E. (1989). Dendrites, dementia and the Down syndrome. *Brain & Development*, 11(2), 131–133. [https://doi.org/10.1016/s0387-7604\(89\)80082-8](https://doi.org/10.1016/s0387-7604(89)80082-8)

Tang, X.-Y., Xu, L., Wang, J., Hong, Y., Wang, Y., Zhu, Q., Wang, D., Zhang, X.-Y., Liu, C.-Y., Fang, K.-H., Han, X., Wang, S., Wang, X., Xu, M., Bhattacharyya, A., Guo, X., Lin, M., & Liu, Y. (2021). DSCAM/PAK1 pathway suppression reverses neurogenesis deficits in iPSC-derived cerebral organoids from patients with Down syndrome. *The Journal of Clinical Investigation*, 131(12), 135763. <https://doi.org/10.1172/JCI135763>

Tarui, T., Im, K., Madan, N., Madankumar, R., Skotko, B. G., Schwartz, A., Sharr, C., Ralston, S. J., Kitano, R., Akiyama, S., Yun, H. J., Grant, E., & Bianchi, D. W. (2020). Quantitative MRI Analyses of Regional Brain Growth in Living Fetuses with Down Syndrome. *Cerebral Cortex*, 30(1), 382–390. <https://doi.org/10.1093/cercor/bhz094>

Teller, J. K., Russo, C., Debusk, L. M., Angelini, G., Zaccheo, D., Dagna-Bricarelli, F., Scartezzini, P., Bertolini, S., Mann, D. M. A., Tabaton, M., & Gambetti, P. (1996). Presence of soluble amyloid β -peptide precedes amyloid plaque formation in Down's syndrome. *Nature Medicine*, 2(1), 93–95. <https://doi.org/10.1038/nm0196-93>

Toskas, K., Yaghmaeian-Salmani, B., Skiteva, O., Paslawski, W., Gillberg, L., Skara, V., Antoniou, I., Södersten, E., Svenningsson, P., Chergui, K., Ringnér, M., Perlmann, T., & Holmberg, J. (2022). PRC2-mediated repression is essential to maintain identity and function of differentiated dopaminergic and serotonergic neurons. *Science Advances*, 8(34), eabo1543. <https://doi.org/10.1126/sciadv.abo1543>

Trieschmann, L., Martin, B., & Bustin, M. (1998). The chromatin unfolding domain of chromosomal protein HMG-14 targets the N-terminal tail of histone H3 in nucleosomes. *Proceedings of the National Academy of Sciences of the United States of America*, 95(10), 5468–5473. <https://doi.org/10.1073/pnas.95.10.5468>

Trieschmann, L., Postnikov, Y. V., Rickers, A., & Bustin, M. (1995). Modular structure of chromosomal proteins HMG-14 and HMG-17: Definition of a transcriptional enhancement domain distinct from the nucleosomal binding domain. *Molecular and Cellular Biology*, 15(12), 6663–6669. <https://doi.org/10.1128/MCB.15.12.6663>

Ueda, T., Catez, F., Gerlitz, G., & Bustin, M. (2008). Delineation of the Protein Module That Anchors HMGN Proteins to Nucleosomes in the Chromatin of Living Cells. *Molecular and Cellular Biology*, 28(9), 2872–2883. <https://doi.org/10.1128/MCB.02181-07>

Ueda, T., Postnikov, Y. V., & Bustin, M. (2006). Distinct domains in high mobility group N variants modulate specific chromatin modifications. *The Journal of Biological Chemistry*, 281(15), 10182–10187. <https://doi.org/10.1074/jbc.M600821200>

Utagawa, E. C., Moreno, D. G., Schafernak, K. T., Arva, N. C., Malek-Ahmadi, M. H., Mufson, E. J., & Perez, S. E. (2022). Neurogenesis and neuronal differentiation in the postnatal frontal cortex in Down syndrome. *Acta Neuropathologica Communications*, 10(1), 86. <https://doi.org/10.1186/s40478-022-01385-w>

Vicari, S., Bellucci, S., & Carlesimo, G. A. (2005). Visual and spatial long-term memory: Differential pattern of impairments in Williams and Down syndromes. *Developmental Medicine & Child Neurology*, 47(5), 305–311. <https://doi.org/10.1017/S0012162205000599>

vonSchimmelmänn, M., Feinberg, P. A., Sullivan, J. M., Ku, S. M., Badimon, A., Duff, M. K., Wang, Z., Lachmann, A., Dewell, S., Ma'ayan, A., Han, M.-H., Tarakhovsky, A., & Schaefer, A. (2016). Polycomb repressive complex 2 (PRC2) silences genes responsible for neurodegeneration. *Nature Neuroscience*, 19(10), 1321–1330. <https://doi.org/10.1038/nn.4360>

Wada, M., Ren, C.-H., Koyama, S., Arawaka, S., Kawakatsu, S., Kimura, H., Nagasawa, H., Kawanami, T., Kurita, K., Daimon, M., Hirano, A., & Kato, T. (2004). A human granin-like neuroendocrine peptide precursor (proSAAS) immunoreactivity in tau inclusions of Alzheimer's disease and parkinsonism-dementia complex on Guam. *Neuroscience Letters*, 356(1), 49–52. <https://doi.org/10.1016/j.neulet.2003.11.028>

Wang, S., Sdrulla, A., Johnson, J. E., Yokota, Y., & Barres, B. A. (2001). A role for the helix-loop-helix protein Id2 in the control of oligodendrocyte development. *Neuron*, 29(3), 603–614. [https://doi.org/10.1016/s0896-6273\(01\)00237-9](https://doi.org/10.1016/s0896-6273(01)00237-9)

Wang, W., Cho, H., Kim, D., Park, Y., Moon, J. H., Lim, S. J., Yoon, S. M., McCane, M., Aicher, S. A., Kim, S., Emery, B., Lee, J. W., Lee, S., Park, Y., & Lee, S.-K. (2020). PRC2 Acts as a Critical Timer That Drives Oligodendrocyte Fate over Astrocyte Identity by Repressing the Notch Pathway. *Cell Reports*, 32(11), 108147. <https://doi.org/10.1016/j.celrep.2020.108147>

Watson, D. K., Robinson, L., Hodge, D. R., Kola, I., Papas, T. S., & Seth, A. (1997). FLI1 and EWS-FLI1 function as ternary complex factors and ELK1 and SAP1a function as ternary and quaternary complex factors on the Egr1 promoter serum response elements. *Oncogene*, 14(2), 213–221. <https://doi.org/10.1038/sj.onc.1200839>

Wei, F., Yang, D., Tewary, P., Li, Y., Li, S., Chen, X., Howard, O. M. Z., Bustin, M., & Oppenheim, J. J. (2014). The Alarmin HMG1 contributes to antitumor immunity and is a potent immunoadjuvant. *Cancer Research*, 74(21), 5989–5998. <https://doi.org/10.1158/0008-5472.CAN-13-2042>

Wei, Y., Vellanki, R. N., Coyaud, É., Ignatchenko, V., Li, L., Krieger, J. R., Taylor, P., Tong, J., Pham, N.-A., Liu, G., Raught, B., Wouters, B. G., Kislinger, T., Tsao, M. S., & Moran, M. F. (2015). CHCHD2 Is Coamplified with EGFR in NSCLC and Regulates Mitochondrial Function and Cell Migration. *Molecular Cancer Research*, 13(7), 1119–1129. <https://doi.org/10.1158/1541-7786.MCR-14-0165-T>

Weick, J. P., Held, D. L., Bonadurer, G. F., Doers, M. E., Liu, Y., Maguire, C., Clark, A., Knackert, J. A., Molinarolo, K., Musser, M., Yao, L., Yin, Y., Lu, J., Zhang, X., Zhang, S.-C., & Bhattacharyya, A. (2013). Deficits in human trisomy 21 iPSCs and neurons. *Proceedings of the National Academy of Sciences of the United States of America*, 110(24), 9962–9967. <https://doi.org/10.1073/pnas.1216575110>

Wilcock, D. M., & Griffin, W. S. T. (2013). Down's syndrome, neuroinflammation, and Alzheimer neuropathogenesis. *Journal of Neuroinflammation*, 10, 84. <https://doi.org/10.1186/1742-2094-10-84>

Willcockson, M. A., Heaton, S. E., Weiss, C. N., Bartholdy, B. A., Botbol, Y., Mishra, L. N., Sidhwani, D. S., Wilson, T. J., Pinto, H. B., Maron, M. I., Skalina, K. A., Toro, L. N., Zhao, J., Lee, C.-H., Hou, H., Yusufova, N., Meydan, C., Osunsade, A., David, Y., ... Skoultchi, A. I. (2021). H1 histones control the epigenetic landscape by local chromatin compaction. *Nature*, 589(7841), 293–298. <https://doi.org/10.1038/s41586-020-3032-z>

Winter, T. C., Ostrovsky, A. A., Komarniski, C. A., & Uhrich, S. B. (2000). Cerebellar and frontal lobe hypoplasia in fetuses with trisomy 21: Usefulness as combined US markers. *Radiology*, 214(2), 533–538. <https://doi.org/10.1148/radiology.214.2.r00fe40533>

Wisniewski, K. E., & Schmidt-Sidor, B. (1989). Postnatal delay of myelin formation in brains from Down syndrome infants and children. *Clinical Neuropathology*, 8(2), 55–62.

Wisniewski, K. E., Wisniewski, H. M., & Wen, G. Y. (1985). Occurrence of neuropathological changes and dementia of Alzheimer's disease in Down's syndrome. *Annals of Neurology*, 17(3), 278–282. <https://doi.org/10.1002/ana.410170310>

Wisniewski, K., Howe, J., Williams, D. G., & Wisniewski, H. M. (1978). Precocious aging and dementia in patients with Down's syndrome. *Biological Psychiatry*, 13(5), 619–627.

Wolvetang, E. J. (2003). ETS2 overexpression in transgenic models and in Down syndrome predisposes to apoptosis via the p53 pathway. *Human Molecular Genetics*, 12(3), 247–255. <https://doi.org/10.1093/hmg/ddg015>

Wolvetang, E. W., Bradfield, O. M., Tymms, M., Zavarsek, S., Hatzistavrou, T., Kola, I., & Hertzog, P. J. (2003). The chromosome 21 transcription factor ETS2 transactivates the β -APP promoter: Implications for Down syndrome. *Biochimica et Biophysica Acta*

(BBA) - Gene Structure and Expression, 1628(2), 105–110.
[https://doi.org/10.1016/S0167-4781\(03\)00121-0](https://doi.org/10.1016/S0167-4781(03)00121-0)

Xu, C., Bian, C., Yang, W., Galka, M., Ouyang, H., Chen, C., Qiu, W., Liu, H., Jones, A. E., MacKenzie, F., Pan, P., Li, S. S.-C., Wang, H., & Min, J. (2010). Binding of different histone marks differentially regulates the activity and specificity of polycomb repressive complex 2 (PRC2). *Proceedings of the National Academy of Sciences*, 107(45), 19266–19271. <https://doi.org/10.1073/pnas.1008937107>

Yang, E. J., Ahn, Y. S., & Chung, K. C. (2001). Protein Kinase Dyrk1 Activates cAMP Response Element-binding Protein during Neuronal Differentiation in Hippocampal Progenitor Cells. *Journal of Biological Chemistry*, 276(43), 39819–39824.
<https://doi.org/10.1074/jbc.M104091200>

Yu, J., Vodyanik, M. A., Smuga-Otto, K., Antosiewicz-Bourget, J., Frane, J. L., Tian, S., Nie, J., Jonsdottir, G. A., Ruotti, V., Stewart, R., Slukvin, I. I., & Thomson, J. A. (2007). Induced pluripotent stem cell lines derived from human somatic cells. *Science (New York, N.Y.)*, 318(5858), 1917–1920. <https://doi.org/10.1126/science.1151526>

Zhang, K., Schrag, M., Crofton, A., Trivedi, R., Vinters, H., & Kirsch, W. (2012). Targeted proteomics for quantification of histone acetylation in Alzheimer's disease. *Proteomics*, 12(8), 1261–1268. <https://doi.org/10.1002/pmic.201200010>

Zhang, S., Postnikov, Y., Lobanov, A., Furusawa, T., Deng, T., & Bustin, M. (2022). H3K27ac nucleosomes facilitate HMGN localization at regulatory sites to modulate chromatin binding of transcription factors. *Communications Biology*, 5(1), 159.
<https://doi.org/10.1038/s42003-022-03099-0>

Zhao, L., Li, J., Ma, Y., Wang, J., Pan, W., Gao, K., Zhang, Z., Lu, T., Ruan, Y., Yue, W., Zhao, S., Wang, L., & Zhang, D. (2015). Ezh2 is involved in radial neuronal migration through regulating Reelin expression in cerebral cortex. *Scientific Reports*, 5(1), 15484. <https://doi.org/10.1038/srep15484>

Zhu, L., Gomez-Duran, A., Saretzki, G., Jin, S., Tilgner, K., Melguizo-Sanchis, D., Anyfantis, G., Al-Aama, J., Vallier, L., Chinnery, P., Lako, M., & Armstrong, L. (2016). The mitochondrial protein CHCHD2 primes the differentiation potential of human induced pluripotent stem cells to neuroectodermal lineages. *The Journal of Cell Biology*, 215(2), 187–202. <https://doi.org/10.1083/jcb.201601061>

CURRICULUM VITAE

